MOLECULAR PROPERTIES, BIOACTIVITIES AND GUT MICROBIAL METABOLISM OF EXOPOLYSACCHARIDES FROM *CORDYCEPS* CS-HK1 MYCELIAL FERMENTATION

GU FANGTING

PhD

The Hong Kong Polytechnic University

2025

The Hong Kong Polytechnic University

Department of Food Science and Nutrition

Molecular properties, bioactivities and gut microbial metabolism of exopolysaccharides from *Cordyceps* Cs-HK1 mycelial fermentation

GU Fangting

A thesis submitted in partial fulfilment of the requirements for the degree of Doctor of Philosophy

August 2025

CERTIFICATION OF ORIGONALITY

I hereby declare that this thesis is my own work and that, to the best of my knowledge and belief, it reproduces no material previously published or written, nor material that has been accepted for the award of any other degree or diploma, except where due acknowledgement has been made in the text.

_____ (Signed)

GU Fangting (Student name)

Abstract

Cordyceps sinensis is a valuable Chinese medicinal fungus with a wide range of physiological activities. Polysaccharides are a major class of active constituents of *C. sinensis*, which have shown numerous bioactivities such as antioxidant, anti-inflammation, immunomodulation and hypoglycemic activities. Since natural *C. sinensis* is very rare and expensive, mycelial fermentation has become a more viable process for production of the fungal biomass and polysaccharides. Cs-HK1 is a *C. sinensis* fungus and capable of producing exopolysaccharide (EPS) in mycelial liquid fermentation. This research aims to investigate the prebiotic activities and potential health benefits on intestinal health through *in vitro* fecal fermentation of EPS isolated from Cs-HK1 mycelial fermentation liquid. Furthermore, the physicochemical properties and structural characteristics of separated and purified EPS fractions were analyzed to examine the structure-activity relationship. The following are the most significant research results and findings:

In the first part of this research, a Cs-HK1 EPS, EPS-LM was assessed together with LBPS isolated from a well-known medicinal plant *Lycium barbarum* L. and the subsequent influences on human gut microbiota through simulated gastrointestinal systems were investigated. EPS-LM, an EPS isolated from mycelial culture of a medicinal fungus *C. sinensis* Cs-HK1, was characterized as a heteropolysaccharide consisting of Man(108):Gal(52.7):Glc(29.2) (molar ratio) with an average molecular weight (MW)

5.513×10^6 Da. LBPS was isolated from a well-known medicinal plant (*Lycium barbarum* L.) which was also characterized as a heteropolysaccharide (1.236×10^5 Da). Both polysaccharides were highly resistant to saliva, gastric and small-intestine digestion with negligible MW reduction and release of reducing sugars but were quickly degraded to lower MW during *in vitro* human fecal fermentation. They were consumed as a carbon source by the gut bacteria to produce short-chain fatty acids (SCFAs). In comparison, the carbohydrate content of EPS-LM was more completely consumed than LBPS and there were also notable differences in consumption of specific monosaccharides and production of specific SCFAs, propionic and butyric acid, and relative abundance of gut bacterial populations between EPS-LM and LBPS group. The results suggested that metabolic outcomes and modulating effects of EPS-LM and LBPS on the gut microbiota were highly dependent on their molecular composition.

The second part of the research was to the prebiotic properties and the protective effects of EPS and human fecal fermentation products on gut barrier. Two EPS fractions with different MW and composition, EPS-LM (4.5×10^6 Da) and EPS-HM (9.4×10^7 Da) were fractionated through ethanol precipitation. The results revealed that the EPS fractions were highly resistant to digestive enzymes and gastric acid in a simulated human gastrointestinal tract but the EPS fractions were highly fermentable in human fecal culture, serving as a carbon source for the gut microbiota. Over 48 hours of fecal fermentation, EPS fractions were significantly degraded and utilized by the intestinal microbiota, resulting in

a notable increase in production of SCFAs including acetic, propionic and butyric acid. The consumption rates of carbohydrates and the production levels of SCFAs varied slightly between the two EPS fractions. The fecal fermentation of EPS fractions increased the abundance of *Actinobacteria*, *Bacteroidetes* and *Faecalibacterium*, which are associated with improved gut health and metabolic function. In lipopolysaccharide (LPS)-stimulated Caco-2/Raw264.7 co-culture model, the fecal fermentation products of the EPS fractions exhibited a potential protective effect against inflammatory damage of gut barrier function, by inhibiting the proinflammatory cytokines, maintaining the trans-epithelial resistance (TEER) and upregulating the tight junction (TJ) proteins. Therefore, these findings suggest that EPS fractions may serve as promising therapeutic agents for enhancing gut barrier function and improving gut health through the modulation of gut microbiota.

In the third part of the research, a neutral polysaccharide, EPS-LM-n was isolated from the low-MW Cs-HK1 EPS and further purified through anion-exchange and gel permeation chromatography. EPS-LM-n had a weight-average MW of 4.17×10^5 Da, a monosaccharide composition of Man:Glc:Gal 1:0.49:0.21 molar ratio, and a backbone structure of →2)-α-Manp-(1→ with branches →4)-α-Glc*p*-(1→, →3)-α-Gal*p*-(1→. EPS-LM-n showed potential hypoglycemic activities by inhibiting α-amylase and α-glucosidase (IC_{50} values of 0.64 and 0.74 mg/mL, respectively) and significant antioxidant, and radical scavenging activities by several chemical assays. Furthermore, EPS-LM-n suppressed the ROS level and H_2O_2-induced cell damage and apoptosis in human vascular endothelial cell EA.hy926

culture. The results and findings collectively indicate that EPS-LM-n isolated from the Cs-HK1 EPS may serve as a potential candidate for dietary and therapeutic management of hyperglycemia and oxidative stress-related metabolic and cardiovascular diseases.

In summary, the results from this research project are helpful to establish the structure and prebiotic function relationship for EPS from the Cs-HK1 mycelial fermentation. The Cs-HK1 EPS can regulate gut microbiota and alleviate intestinal damage by regulating intestinal flora, thereby maintaining intestinal health. These findings provide a theoretical basis for the future development of the Cs-HK1 EPS as a novel prebiotic food ingredient and for the creation of functional food products specifically designed to enhance human health.

List of publications

Journal papers

1. **Gu, F. T**., Li, J. H., Zhao, Z. C., Zhu, Y. Y., Huang, L. X., & Wu, J. Y (2026). Structural characteristics and bioactivities of an exopolysaccharide from mycelial fermentation of a medicinal fungus Cs-HK1. *Carbohydrate Polymers. Carbohydrate Polymers,* 373, 124582.
2. **Gu, F. T**., Zhao, Z. C., Zhu, Y. Y., Huang, L. X., Li, J. H., Liu, X. W., & Wu, J. Y (2025). Human fecal fermentation of high/low-molecular weight exopolysaccharides from a medicinal fungus Cs-HK1 and anti-inflammatory protection on gut barrier function. *International Journal of Biological Macromolecules,*145481.
3. **Gu, F. T**., Li, J. H., Zhao, Z. C., Zhu, Y. Y., Huang, L. X., & Wu, J. Y (2025). Metabolic outcomes of *Cordyceps* fungus and Goji plant polysaccharides during *in vitro* human fecal fermentation. *Carbohydrate Polymers,* 350, 123019.
4. Li, J. H., **Gu, F. T**., Yang, Y., Zhao, Z. C., Zhu, Y. Y., Huang, L. X., Chen, S. G., & Wu, J. Y (2024), Simulated human digestion and fermentation of a high-molecular weight polysaccharide from Lentinula edodes mushroom and protective effects on intestinal barrier. *Carbohydrate Polymers*, 343, 122478.

5. Huang, L. X., **Gu, F. T**., Zhu, Y. Y., Zhao, Z. C., & Wu, J. Y. (2024). Bifidogenic properties of polysaccharides isolated from mushroom Lentinula edodes and enhanced immunostimulatory activities through Bifidobacterial fermentation. *Food Bioscience*, 62 (2024), Article 105121.
6. Zhao, Z. C., **Gu, F. T**., Li, J. H., Zhu, Y. Y., Huang, L. X., & Wu, J. Y. (2024). Fractionation, characterization, and assessment of nutritional and immunostimulatory protein-rich polysaccharide-protein complexes isolated from Lentinula edodes mushroom. *International Journal of Biological Macromolecules,* 237, 124216.
7. Zhu, Y. Y., Dong, Y. H., **Gu, F. T**., Zhao, Z. C., Huang, L. X., Cheng, W. Y.[#], & Wu, J. Y[#]. (2024). Anti-Inflammatory Effects of *Cordyceps* Cs-HK1 Fungus Exopolysaccharide on Lipopolysaccharide-Stimulated Macrophages via the TLR4/MyD88/NF-κB Pathway. *Nutrients*, 16(22), 3885.
8. Li, J. H., Zhu, Y. Y., **Gu, F. T**., & Wu, J. Y. (2023). Efficient isolation of immunostimulatory polysaccharides from Lentinula edodes by autoclaving-ultrasonication extraction and fractional precipitation. *International Journal of Biological Macromolecules,* 237, 124216.

Conference presentations and posters (International)

1. **Gu, F. T.**, Zhao, Z. C., & Wu, J. Y. Simulated digestion and gut microbial fermentation of *Cordyceps sinensis* polysaccharides and effects on intestinal barrier. PolyU Research Student Conference (PRSC 2024), Hong Kong, China, 2024.
2. **Gu, F. T.**, Zhao, Z. C., & Wu, J. Y. Simulated human digestion and fermentation of different fractions of *Cordyceps sinensis* polysaccharides and protective effects on intestinal barrier. 1st FSN Research Postgraduate Symposium, Hong Kong, China, 2024.
3. **Gu, F. T.**, Li, J. H., Yang, Y., Zhao, Z. C. & Wu, J. Y. Simulated digestion and gut microbial fermentation of *Cordyceps sinensis* polysaccharides and effects on intestinal barrier. 21st Annual Meeting of CIFST, Chongqing, China, 2024.
4. **Gu, F. T.**, Li, J. H., Zhao, Z. C. & Wu, J. Y Simulated digestion and gut microbial fermentation of *cordyceps sinensis* polysaccharides and effects on intestinal barrier. 10th International Conference on Food Chemistry &Technology (FCT-2024), Valencia, Spain, 2024.
5. **Gu, F. T.**, Li, J. H., Zhao, Z. C. & Wu, J. Y. Human fecal fermentation of high/low-molecular weight exopolysaccharides from a medicinal fungus Cs-HK1 and anti-inflammatory protection on gut barrier function. International Conference on Polysaccharides for Nutraceuticals and Future Foods (ICPNFF-2025), Hong Kong, China, 2025.

6. **Gu, F. T**. & Wu, J. Y. Structural characterization and antioxidant activity of exopolysaccharide from mycelial fermentation of a medicinal fungus Cs-HK1. 2nd FSN Research Postgraduate Symposium, Hong Kong, China, 2025.

Acknowledgements

I would like to thank my chief supervisor, Prof. Jian-yong Wu and co-supervisor Prof. Amber Jiachi Chiou, for all their guidance. Professional advice and encouragement throughout this project as well as their comments on this thesis and all the publications.

I would also like to thank the Department of Food Science and Nutrition and the Department of Applied Biology and Chemical Technology of The Hong Kong Polytechnic University, all the technicians and staff, and my lab mates in Prof. JY Wu's group for their valuable suggestions and technical support in the past years.

I would like to express my gratitude to my family members and friends for their support and encouragement throughout this long journey. Their belief in my abilities has provided me with the motivation to persevere during challenging times. Whether it was through their words of encouragement, their willingness to listen, or their understanding when I needed time to focus on my work, their presence has been invaluable. I am truly thankful for their love and support, which has played a significant role in my accomplishments.

Table of Contents

List of Figures

(B) acetic acid, (C) propionic acid, (D) butyric acid. Blank: no additional carbohydrate source; FOS (fructo-oligosaccharide): a probiotic reference; EPS-LM and EPS-HM: the experimental group.

Figure 3-5. α-Diversity analysis of fecal microbial communities throughout *in vitro* fecal fermentation for 0 (Initial group) and 48 h of different carbohydrate sources and carbohydrate blank with different indexes including (A) Chao1, (B) Shannon, (C) Simpson, statistically significant differences between the methods were determined using Tukey's multiple comparison test, with $p<0.05$; β-diversity analysis of fecal microbial communities using (D) principal component analysis (PCA) of fecal microbial communities based on the relative abundances of OTUs at a 97% similarity level and (E) multivariate analysis of variance from matrix scores based on Bray-Curtis method at the genus level. Blank: no additional carbohydrate source; FOS (fructo-oligosaccharide): a probiotic reference; EPS-LM and EPS-HM: the experimental group.

Figure 3-6. Comparisons of different groups on gut microbial composition for 0 (Initial group) and 48 h fermentation. Bacterial taxonomic profiling at the (A) phylum level and (B) genus level; Bacterial analysis based on (C) heatmap at genus level; Species difference of gut microbiota based on (D) Linear discriminant analysis (LDA) score and (E) LEfSe diagram. Blank: no additional carbohydrate source; FOS (fructo-oligosaccharide): a probiotic reference; EPS-LM and EPS-HM: the experimental group.

List of Tables

List of Abbreviations and Symbols

EPS-LM Low molecular weight fraction of exopolysaccharides from Cs-HK1

EPS-HM High molecular weight fraction of exopolysaccharides from Cs-HK1

LBPS *Lycium barbarum* polysaccharides

USEP40-1 Ultrasonic extraction of polysaccharide from cordyceps cephalosporium mycelia

HWE Hot water extraction

LVP *Lentinus velutinus* polysaccharide

POPPS-a Purified proteoglycan of the fruiting bodies of *Pleurotus ostreatus*

EnAPS Enzyme-assisted extraction from *Agaricus bisporus*

EPS Exopolysaccharides

GC Gas chromatography

FID Flame ionization detector

HPGPC High performance gel permeation chromatograph

HPLC High performance liquid chromatography

LPS lipopolysaccharides

MW Molecular weight

NMR Nuclear magnetic resonance

NO Nitric oxide

Chapter 1 Introduction

There are approximately 15,000 species of macrofungi, distributed across China, Japan, South Korea and other parts of the world. Currently, over 2,000 species of edible fungi are edible. The use of fungi as food has a long history in China, with over 1,000 edible fungi species documented (Shao, Si, Zhang, Tu, & Zhang, 2020). As a unique natural resource, fungi are diverse and delicious, rich in polysaccharides, proteins, amino acids and vitamins, most of which had physiological activities and health effects on the human body. These bioactive components have made edible fungi a valuable source of natural active ingredients. In addition, fungi are attracting attention not only as food but also for their medicinal properties. Polysaccharides are one of the most important active components of fungi. Fungal polysaccharides exhibit a variety of biological activities and have broad application prospects (Qi Guo, Liang, Xiao, & Ge, 2023).

Polysaccharides are a class of macromolecular carbohydrates with a variety of functional properties, which are widely distributed in nature but easily form complexes with other macromolecules (Junqiao Wang, Hu, Nie, Yu, & Xie, 2016; Y. Yu, Shen, Song, & Xie, 2018) and synthesized naturally by microorganisms (Xie et al., 2016). These complex carbohydrates are composed of monosaccharide units linked by glycosidic bonds. Their structural diversity is vast with variations in monosaccharide composition, linkage types, branching degree and molecular weight, all of which contribute to their biological

activities. These activities include anti-tumor, anti-inflammatory, antioxidant, anti-angiogenic and immunomodulatory activities (Q. Zhang et al., 2024). Polysaccharides also exhibit prebiotic properties, selectively stimulating the growth and activity of beneficial gut microorganisms, which in turn contribute to the health of the host. This prebiotic activity is mainly attributed to non-digestible polysaccharides that reach the colon intact and are fermented by the gut microbiota, resulting in the production of SCFAs and other metabolites that have systemic health effects.

C. sinensis (**Figure 1-1**), also known as *Ophiocordyceps sinensis* and traditionally referred to as "Dong-Chong-Xia-Cao" in Chinese, is a valued medicinal fungus, renowned for its health benefits and therapeutic properties. Found on the Qinghai Tibetan Plateau at altitudes above 2000 meters, *C. sinensis* has a unique life cycle where the fungus parasitizes ghost moth larvae, eventually consuming and replacing its host tissue. It has been proved that *C. sinensis* has good health benefits for the body, such as anti-tumor, anti-cancer and immunomodulatory effects (Jiaping Chen et al., 2006; D.-T. Wu et al., 2014). These biological activities were due to its diverse active ingredients, including polysaccharides, nucleosides, cordycepic acid, amino acids, active peptides and sterols. *C. sinensis* polysaccharides, one of its primary active ingredients, account for 3% to 8% of the raw material's dry weight.

Figure 1-1. Nature of wild *Cordyceps sinensis*.

The polysaccharides extracted from *C. sinensis* have been extensively studied and found to exhibit significant biological activities. These polysaccharides displayed potent antioxidant properties and combating oxidative stress (Nguyen et al., 2021). Additionally, these polysaccharides have been shown to exert prebiotic effects, enhancing the growth of beneficial gut microbes and contributing to a balanced gut microbiota (Mao et al., 2020). Their immunomodulatory activity is also noticeable; they can modulate the immune system by activating immune cells (such as TNF-α and IL-10) (T. Hu, Jiang, Huang, & Sun, 2016). Furthermore, *C. sinensis* polysaccharides have demonstrated anti-tumor potential by inhibiting the proliferation of cancer cells (N.-F. Ji et al., 2011). The diverse activities of these polysaccharides showed their potential as functional food ingredients and therapeutic agents.

Based on the above background of bioactivities of *C. sinensis* polysaccharides, a systematic understanding of their structure-function relationship remains limited, especially for exopolysaccharides EPS derived from *C. sinensis* mycelial fermentation culture. Specifically, it was unclear how the molecular properties of Cs-HK1 EPS influence their digestive stability, fermentation behavior, and subsequent bioactivities. Furthermore, the precise structural characterization of its bioactive component and its direct health benefits beyond gut fermentation were unknown. Therefore, this thesis hypothesized that the monosaccharide composition and molecular weight MW of Cs-HK1 EPS are critical factors for gut microbiota fermentation, which in turn reflected their prebiotic and anti-

inflammatory activities. We further hypothesized that the bioactive component of EPS-LM fraction is a novel polysaccharide with unique structure and potential hypoglycemic and antioxidant activities.

1.1 Natural polysaccharides from fungus sources

Fungal polysaccharides are complex carbohydrates derived from various fungi and play an important role in ecology and industry. Macrofungi are fungi with complex morphology and structure, large fruiting bodies and visible to the naked eye and pluckable (Chang & Wasser, 2018). Most of them belong to the phylum *Basidiomycetes*, such as mushrooms. Besides, a small number belong to the phylum *Ascomycotina*, such as *Cordyceps*. Macrofungi are important sources of food and medicine for humans, such as *Auricularia auricula*, *Lentinula edodes* (shiitake mushroom), *Antrodia cinnamomea*, *Ganoderma lucidum* (Reishi mushroom) and *Flammulina velutipes* (enoki mushroom). There are more than 2,000 edible macrofungi species in the world. China has also recorded thousands of edible fungi species (C. Li & Xu, 2022). Macrofungi can produce a variety of metabolites, such as nucleotides, amino acids, terpenes and polysaccharides, which have important medicinal and edible values.

Fungal polysaccharides are high molecular weight polymers and composed of more than 10 monosaccharides linked by glycosidic bonds. They are isolated from fungal fruiting bodies, mycelium and fermentation broth. They are a type of active polysaccharides that

can control cell division, differentiation and regulate cell growth and aging. It is well known that fungal polysaccharides have diverse biological functions, such as antioxidant activities, anti-inflammatory activities, immunomodulatory effects and anti-tumor activities (C. Chen et al., 2014; Niego et al., 2021; Schepetkin & Quinn, 2006). Common fungal polysaccharides include *Lentinula edodes* (Lentinan) polysaccharides, *Ganoderma lucidum* polysaccharides, Pachyman polysaccharides, Coriolan polysaccharides, Tremella polysaccharides, *Grifola frondosa* polysaccharides and *Cordyceps* polysaccharides.

1.2 Extraction, Fractionation and purification of polysaccharides

Fungal polysaccharides can be divided into into exopolysaccharides (EPS) and endopolysaccharides. EPS are released outside fungal cells and can be found in liquid cultures or surrounding liquids. To extract these exopolysaccharides, the liquid culture is typically separated from the fungal biomass. This extraction of exopolysaccharides is relatively simple since it does not necessitate the disruption of cells (Ferraboschi, Ciceri, & Grisenti, 2021; Larrañaga-Ordaz et al., 2022). For the extraction of endopolysaccharides, the fungal mycelium or fruiting body are firstly collected and then disrupted by chemical or mechanical methods, which can destroy the cell wall. Many fungi contain lipid substances, which will need to be removed using solvents such as ether, petroleum ether and ethanol before extraction. This step can also remove some pigments. Common polysaccharide extraction methods include hot water extraction (Y. Wang, Jia, Ren, Li, &

Zhang, 2018), acid or alkaline extraction (Yi, Xu, Wang, Huang, & Wang, 2020), ultrasonic-assisted extraction (Ke, 2015), microwave-assisted extraction (Gil-Ramírez, Smiderle, Morales, Iacomini, & Soler-Rivas, 2019), enzyme-assisted extraction (G. Yu et al., 2019) and so on, which is summarized in **Table 3-1**.

Crude polysaccharides obtained by various extraction methods often contain pigments, proteins and some small molecule impurities. Therefore, in order to avoid the influence of impurities on the purity, properties and biological activity of polysaccharides, it is necessary to remove impurities and further purify the crude polysaccharides.

1.2.1 Extraction of exopolysaccharides

The methodology for extracting exopolysaccharides EPS from fungi depends on the source species, the structural characterization and the targeted purity for the end-use application (Elsehemy et al., 2020). For instance, lentinan, which is derived from the shiitake mushroom (*Lentinus edodes*), is initially precipitated with ethanol, subsequently dissolved in acetic acid and finally purified through chromatographic techniques (Venkatachalam, Arumugam, & Doble, 2021).

Generally, fermentation is used for the production of EPS. The extraction of EPS usually involves in several simple methods. EPS are firstly separated from the liquid culture medium by removing the fungal mycelium and cells through filtration or centrifugation and then the supernatant is collected (Stoica, Moscovici, Lakatos, & Cioca,

2023). The EPS in the supernatant are then precipitated with an organic solvent (such as acetone, ethanol, propanpol, isopropanol) under low temperature (Elisashvili, Kachlishvili, & Wasser, 2009). After precipitation, crude EPS are collected by centrifugation or filtration. This process is more efficient and cost-effective than extracting polysaccharides from solid fungal matrices or yeast cell structures. The crude EPS are then processed into a powder form by vaccum drying or freeze drying, followed by dialysis to remove impurities (da Silva Fonseca et al., 2020). Subsequent purification steps may include ion exchange chromatography and gel permeation chromatography to purify EPS to the desired purity (Osińska-Jaroszuk et al., 2015).

1.2.2 Decolorization

Soluble pigments are often precipitated during the extraction of polysaccharides. It is often necessary to decolorize polysaccharides with darker color. At present, the common decolorization methods include ion exchange method, activated carbon method and hydrogen peroxide (H_2O_2) method.

Activated carbon adsorption method is suitable for the adsorption of water-soluble pigments because it has the advantages of low cost, strong adsorption capacity and no effect on the structure of polysaccharides. However, the activated carbon method removes pigments by adsorption using Van der Waals forces, which has poor selectivity and high loss rate of polysaccharides. The H_2O_2 decolorization method is suitable for pigments

containing aromatic rings, double bonds and hydroxyl groups. Different decolorization methods may have different effects on the properties of polysaccharides. Rosa et. al (da Rosa, Bresolin, Ugalde, & Kuhn, 2024) used fixed-bed column with activated carbon to purify the shiitake for 24 h and finally the yield of purified exopolysaccharide was 921.43 μg/ml in the end. The results also showed that after activated carbon purification, purified exopolysaccharide has a high antioxidant activity.

Macroporous resin method uses van der Waals force to adsorb pigments for purification, which has the characteristics of large adsorption capacity, simple operation and does not change the structure of polysaccharides. Hu et. al (Z. Hu et al., 2019) optimized the purification conditions of microporous resin method for purifying crude polysaccharides from *Carex meyeriana* Kunth. The results showed that AB-8 macroporous resin was the most suitable material and the polysaccharide content significantly increased from 37% to 78%.

1.2.3 Deproteinization

Currently, the traditional deproteinization methods include the Sevag method, trifluoroacetic acid (TCA), enzymatic hydrolysis and combined methods. The Sevag method is currently the most widely used method because of its mild and convenient conditions, but it uses a large number of organic reagents in the process and often requires multiple deproteinization, resulting in a high loss of polysaccharides. The TCA method

utilizes the denaturation of proteins under acidic conditions and the generation of insoluble salts to achieve the separation effect. This method has the advantages of high efficiency and low loss of polysaccharides. Enzymatic methods often use papain to hydrolyze proteins to remove them. Enzymatic digestion is characterized by high specificity, but it often takes a long time. In addition, the combined use of multiple methods has been widely used due to the advantages of high protein removal and low loss of polysaccharides. Zeng et al. (Zeng et al., 2019) evaluated the effects of enzymatic hydrolysis, TCA, and salting out on the polysaccharides of *Ganoderma lucidum*. The results showed that enzyme digestion, TCA and salting out could effectively remove proteins and had no significant effect on the molecular weight of polysaccharides, but these methods resulted in different degrees of glycosidic bond loss. In addition, the *in vitro* antioxidant activity results showed that the enzymatically purified *Ganoderma lucidum* polysaccharides had the strongest antioxidant activity.

1.2.4 Fractionated purification

Subsequent isolation and purification of polysaccharides are important for accurate structural analysis of polysaccharides and research on their biological activities. In recent years, the separation and purification of polysaccharides are the most complicated and time-consuming operations in the preparation process. In order to obtain purified polysaccharide components with uniform molecular weight and degree of polymerization,

it is often necessary to classify and purify the crude polysaccharide obtained. Currently, commonly used classification methods include precipitation, anion exchange chromatography, gel chromatography and ultrafiltration.

The precipitation method takes advantage of the different solubility of polysaccharides having different molecular weights in organic solvents and then adjusts the concentration of the solvent to achieve the separation of polysaccharides. This method is easy to operate and can separate polysaccharides according to molecular weight. However, the homogeneity of the polysaccharide fractions obtained by this method is not high enough, and it is only suitable for preliminary separation. Long et al. (Long et al., 2020) obtained five polysaccharides from *shiitake* mushrooms by the method of graded precipitation and studied the physicochemical properties and bile acid binding capacity of the obtained polysaccharide fractions. The results showed that the yields, molecular weights, monosaccharide compositions, surface morphologies, neutral sugars, glyoxylates and sulfates of the precipitated polysaccharides were significantly different at different ethanol concentrations.

Ion exchange chromatography is currently the most widely used purification method. The principle is to use a charged filler as a substrate and take advantage of the differences in the binding capacity of different charged polysaccharides and the substrate, so as to achieve the separation. Anion-exchange cellulose and cation-exchange cellulose are commonly used substrates. The adsorption capacity of cellulose on polysaccharides is

related to the structure of polysaccharides. Polysaccharides with more acidic groups, large molecular weight and fewer branched chains usually have stronger adsorption capacity. For the fractionation of acidic, neutral and mucopolysaccharides, cation-exchanged cellulose has unique advantages.

Gel chromatography is the separation of polysaccharides by molecular sieve, according to the relationship between the molecular size of the polysaccharide to be separated and the pore size of the gel. It is commonly used in further purification after preliminary purification of crude polysaccharide to avoid the gel blockage and affect the separation effect. Polyamide gels, dextran gels (Sephadex) and agarose gels (Sepharose) are usually used in this method (Y. Bai et al., 2017). This method is characterized by simple and rapid operation, but not suitable for the separation of viscous polysaccharides and the small volume of sample is small.

Ultrafiltration membrane separation refers to the method to purify large molecules by utilizing the selectivity of the membrane with pressure. In addition, by choosing different molecular weight ultrafiltration membranes, polysaccharides with uniform molecular weight can be selected. Zhang et. al (L. Zhang & Wang, 2016) prepared polysaccharides from *Tremella fuciformis* by ultrafiltration-assisted extraction. The results showed that polysaccharides recovery and purity of ultrafiltration separation were 81.8% and 85.6%, which were much higher than ethanol precipitation.

In addition, metal ion precipitation, quaternary ammonium precipitation and electrophoresis are also chosen in the purification of polysaccharides. Actually, it is difficult to obtain pure polysaccharides by only one method, and necessary to combine two or more methods according to the characteristics of polysaccharides to obtain high-purity components.

1.3 Structural characterization of polysaccharides

The structure of polysaccharides determines their unique biological activities and the structural analysis of polysaccharides is the basis for analyzing their structural relationships, which is of great significance for the investigation of their biological activities. The structure of polysaccharides is complex. It is known that polysaccharide macromolecules are characterized by a wide distribution of molecular weights, multiple monosaccharides, complex glycosidic bonding and variations in the conformation of the sugar chain, which mainly include the composition and proportion of molecular weights, monosaccharide composition and the type of glycosidic bonds. The structure of polysaccharides is characterized using analytical methods by various types of chemical and instrumental analysis methods.

1.3.1 Purity and molecular weight

Polysaccharides are polymer compounds. Their purity is the basis for the study of the structural characteristics of polysaccharides and a prerequisite for the study of their

chemical properties. The purity of polysaccharides is different from the concept of conventional compounds and usually refers to the average distribution of similar chain lengths. The main methods to determine the purity of polysaccharides include high performance gel permeation chromatography (HPGPC), specific optical rotation, electrophoresis, ultraviolet spectrophotometry and thin-layer chromatography. The molecular weight of polysaccharides is closely related to the properties of polysaccharides. The determination of molecular weight is the basis for the study of polysaccharide properties and an important index for quality control. The molecular weight of polysaccharides can be expressed by the methods of weight average molecular weight (Mw), number average molecular weight (Mn) and viscosity average molecular weight (Mn). The molecular mass of polysaccharides includes gel chromatography, viscosity, mass spectrometry, ultrafiltration, osmolarity and light scattering. In recent years, HPGPC has been widely used for the determination of polysaccharide purity and molecular weight because of its simple operation, short analyzing time and good reproducibility. The Mw distribution of fungal polysaccharides is very wide, as shown in **Table 3-1**. Its differences are mainly attributed to different sources and experimental methods.

1.3.2 Monosaccharide composition

Monosaccharides are the basis of polysaccharides. Polysaccharides with different monosaccharides will show great differences in their properties, structures and biological

activities. The analysis of the composition of monosaccharides generally requires the hydrolysis of glycosidic bonds of polysaccharides. Then, the products of hydrolysis are subjected to a series of reactions and finally measured by various analytical methods. At present, the hydrolysis methods commonly include enzymatic hydrolysis, acid hydrolysis and oxidative hydrolysis. The composition of monosaccharides can be determined by high performance liquid chromatography (HPLC) (J. Yan et al., 2016; X. Zhang et al., 2021), high performance capillary electrophoresis (HPCE) (X. L. Ma, Song, Zhang, Huan, & Li, 2017; X. Yang, Zhao, & Lv, 2007), gas chromatography (GC) (Black, Heiss, & Azadi, 2019) and so on. However, each method has its own advantages and disadvantages, as well as its scope of application. A combination of methods should be considered to accurately determine the composition of monosaccharides. **Table 1-1** summarized the monosaccharide composition of some fungal polysaccharides.

Table 1-1. Sources, extraction and purification from different fungal polysaccharides.

Polysaccharide	Fungi sources	Extraction method	Purification methods	Monosaccharide composition	Molecular weight (Da)	Refs
EPS	*Cordyceps sinensis* Cs-HK1	Mycelial fermentation	-	Man:Glc:Gal=2:6:1	1.4×10^7	(L.-Q. Li et al., 2020)
USEP40-1	Cordyceps cephalosporium mycelia	Ultrasonic extraction	Sevag method and Sephadex G-100	Man:Glc:Gal:Rha:Ara=11:5:8:2:2	6.1×10^4	(J. Xiao et al., 2012)
HWE	Lentinula edodes	Hot water extraction	-	Glc:Gal:Man=3.5:1.5:1	2.8×10^6	(J. H. Li, Zhu, Gu, & Wu, 2023)
LVP	*Lentinus velutinus*	Hot water extraction	DEAE-FF and Sephadex G-100	Glc	3.3×10^5	(Udchumpisai & Bangyeekhun, 2020)
POPPS-a	*Pleurotus ostreatus*	Hot water extraction	DEAE-cellulose and Sepharose CL-6B	Ara:Man:Gal:Glc:GalA=1:0.9:1.7:5:0.6	3.3×10^4	(Xia, Fan, Zhu, & Tong, 2011)
EnAPS	*Agaricus bisporus*	Enzyme-assisted extraction	Sevag method and DEAE-52	Rha:Fuc:Xyl:Man:Gal:Glc=1:3.6:2.8:55.3:9:10.2	-	(S. Li et al., 2018)

Note: "-" means not determined.

1.3.3 Determination of glycosidic bond types and connections

After determining the monosaccharide composition of the polysaccharide, the type of linkage between the monosaccharides also needs to be determined. Currently, the methods of glycosidic bond determination mainly include methylation, infrared spectroscopy and nuclear magnetic resonance (NMR).

1.3.3.1 Methylation analysis

The basic procedure of methylation analysis is to methylate the hydroxyl groups on all monosaccharide residues in polysaccharides. After a series of reactions to generate products of sugar alcohol acetylation (PMAAs), high-resolution glycosyl ion flow peaks were obtained by GC-MS and results can be analyzed by the information on the connecting sites of each monosaccharide residue in the polysaccharide molecule, the proportion of the branching sites and the non-reduced terminal units by comparing it to the mass spectrometry library. However, due to the complexity and difficulty of polysaccharide structure, there is not yet a set of methylation methods that are universally applicable to different types of polysaccharide structures is usually necessary to optimize the methylation test according to the specific polysaccharide properties to achieve better analysis and identification results.

Polysaccharides can be classified into neutral polysaccharides and acidic polysaccharides according to their glyoxalate content. The methylation of acidic

polysaccharides is more difficult than that of neutral polysaccharides, mainly due to several reasons. Most acidic polysaccharides contain carboxyl groups or sulfate, which makes it difficult to be dissolved in dimethyl sulfoxide solvents. Thus, many hydroxyl groups cannot participate in the methylation reaction, so the degree of methylation is relatively low. Another reason is that polysaccharides containing glyoxalate are prone to side reactions such as elimination reaction during methylation analysis. It is difficult to clearly determine the connecting sites of glyoxalate and sulfate in the structure of the sugar chain, thus it is difficult to determine its specific structure. For these problems of acidic polysaccharides in the methylation process, the current solutions mainly include promoting the solubility of polysaccharides in dimethyl sulfoxide by heating and extending the dissolution time or adding some reducing agents. In addition, reducing the carboxyl group of the glyoxalate for several times to obtain neutral polysaccharides before the subsequent analysis is also a good option.

1.3.3.2 NMR analysis

Nuclear magnetic resonance (NMR) spectroscopy usually analyses the heterogeneous configurations of glycosidic residues and plays an important role in the structural study of polysaccharides (H.-Y.-Y. Yao, Wang, Yin, Nie, & Xie, 2021).

^{1}H-NMR can be used to determine the conformation of polysaccharide glycosidic bonds. The chemical shift of the heterocaptoproton (H-1) is usually greater than δ 4.95 ppm

for α-type pyranose and less than δ 4.95 ppm for β-type pyranose. For ^{13}C-NMR, the α-type conformation occurs in the range of δ 95-103 ppm, while the β-type heterocaptoproton occurs in the range of δ 101 ppm or higher. In addition, the signals in the low-field range of ^{1}H-NMR and ^{13}C-NMR can be used to determine how many monosaccharides are contained in the polysaccharides. However, due to the complexity of the polysaccharide structure, there is a serious signal overlap in 1D-NMR, and 1D-NMR alone is not sufficient for a comprehensive analysis of the polysaccharide structure. Therefore, it is necessary to use 2D-NMR to attribute the overlapping signals in 1D-NMR to determine the order of the sugar residues and obtain the complete structural information. Currently, the used 2D-NMR techniques include homonuclear shift correlation (COSY, TOCSY, NOESY), heteronuclear multiple bond correlation (HMBC), heteronuclear multiple quantum correlation (HMQC) and heteronuclear single quantum correlation (HSQC). The development of 2D-NMR has greatly facilitated the progress of the structural analysis of polysaccharides and it can provide the linkage order of the glycan residues as well as confirm the C, H chemical shift attribution. The development of 2D-NMR technology has greatly facilitated the structural analysis of polysaccharides, which can provide the connection order of each sugar residue and confirm the attribution of C and H chemical shifts.

1.4 Bioactivities of polysaccharides

Macrofungal polysaccharides have a variety of biological activities, including antioxidant activities, anti-inflammation, hypoglycemic activities, anti-tumor activities, regulating the gut microbiota and other activities, shown in **Table 1-2**. These biological activities make macrofungal polysaccharides widely used in the fields of medicine and health products.

1.4.1 Regulating the activity of intestinal flora

Intestinal flora refers to the structurally diverse microbial communities living in the human intestinal tract, which participate in the metabolic, immune and protective functions of the host and play an important role in human health. Studies have shown that intestinal flora has a close relationship with the nervous and cardiovascular system. When the microbiota is dysregulated, neurological disorders, obesity, diabetes and liver diseases appear (X. An et al., 2019; Dabke, Hendrick, & Devkota, 2019; X. Hu, Wang, & Jin, 2016; Patterson et al., 2016; Quigley, 2017). Restoring intestinal microecological balance by regulating intestinal flora has become one of the effective methods to improve human health and prevent and treat diseases. Most dietary polysaccharides are not broken down by the digestive system are important energy source substances for intestinal flora. It has been widely studied for the prebiotic effects of polysaccharides in regulating the intestinal flora, improving the intestinal barrier and enhancing immunity.

Renata Nowak et. al (Nowak, Nowacka-Jechalke, Juda, & Malm, 2018) investigated the digestibility of polysaccharides of 53 wild-growing mushrooms and found that mushroom polysaccharides do not break down in the stomach and small intestine and reach the colon in *in vitro* model. In addition, many literatures have suggested that fungal polysaccharides have a prebiotic-like effect and can regulate intestinal flora. For example, *Ganoderma lucidum* polysaccharides can increase the abundance of *Bifidobacteriaceae* and *Lactobacillaceae* and reduce the abundance of *Lachnospiraceae* and *Enterobacteriaceae* (K. Yang et al., 2020). Khan et al. (Khan et al., 2018) studied the effect of *Ganoderma lucidum* polysaccharide and *Poria cocos* polysaccharide on the intestinal flora of mice and found that both fungal polysaccharides have anti-obesity effects and can also increase the abundance of beneficial bacteria such as *Bifidobacterium* and *Lactobacillus*. *Bifidobacterium* and *Lactobacillus* are recognized as beneficial bacteria and probiotics in the intestine. This shows that these two fungal polysaccharides can increase the abundance of beneficial bacteria and promote anti-obesity.

1.4.2 Anti-inflammatory activity

Inflammation is the body's protective response to harmful stimuli, characterized by signs such as redness, swelling, heat, pain and functional disruption. While typically a beneficial defence mechanism, inflammation can sometimes cause damage, including autoimmunity or harm to transparent tissues.

Extensive research has highlighted the anti-inflammatory properties of polysaccharides from various sources. Specifically, *Morchella esculenta* polysaccharide (EMP-1) and its sulfated derivative (SEMP-1) have shown promising protective effects against PM2.5-induced cytotoxicity in rat alveolar macrophage NR8383 cells. The results included reduction in cell death, apoptosis and pro-inflammatory cytokines production (TNF-α and IL-1β), along with diminished reactive oxygen species (ROS) formation (W. Li et al., 2019). Furthermore, SEMP-1 has been observed to downregulate inducible nitric oxide synthase (iNOS) and cyclooxygenase-2 (COX-2) expression, and mitigate the activation of the NF-κB pathway in the presence of PM2.5. Additionally, acetylated polysaccharides extracted from *Morchella angusticeps*, specifically PEMP and Ac-PMEP1–3, have been reported to enhance cell proliferation and NO and TNF-α production in RAW264.7 macrophages, even in the absence of lipopolysaccharide. Ac-PMEP3, in particular, has demonstrated an ability to improve cell viability and NO production, potentially through mechanisms involving NF-κB signalling and the MAPK pathway (Y. Yang et al., 2019). *Trametes orientalis* polysaccharide, TOP-2 has been discovered to reduce lung injury in mice, with alleviating pulmonary edema, reducing inflammatory cell infiltrates and restoring macrophage levels in bronchoalveolar lavage fluid. TOP-2 also has been shown to decrease various inflammatory and oxidative stress markers in BALF, such as total protein, albumin, CRP, MPO, LDH, AKP, ASM, TNF-α, IL-1β, and IL-6.

Additionally, TOP-2 treatment has been associated with the upregulation of Nrf2 expression tissue (Y. Zheng, Fan, Chen, & Liu, 2019).

1.4.3 Hypoglycemic activities

Generally, the mechanisms of action of hypoglycemic substances are mainly divided into two categories. One is to reduce the absorption of glucose, and the other is to regulate carbohydrate metabolism and insulin synthesis. Studies have shown that a variety of fungal polysaccharides from *Ganoderma lucidum* (Meng et al., 2011), black *Ganoderma lucidum* (Yi Chen, Xie, & Gong, 2007), *Coriolus versicolor* (Hsu, Hsu, Lin, Cheng, & Yang, 2013), *Grifola frondosa* (Lei et al., 2012) and *Pleurotus sajor-caju* (Pramanik, Chakraborty, Mondal, & Islam, 2007) have hypoglycemic activities. Studies have found that two water soluble polysaccharides RVP-1 and RVP-2 from *Russula virescens* polysaccharides had the potential to inhibit α-glucosidase and α-amylase activities and showed a dose-manner. At 3.2 mg/mL, RVP-1 had a better inhibitory effect on α-glucosidase (77.59%) and RVP-2 had a better inhibitory effect on α-amylase (77.59%) (Y.-M. Li, Zhong, Chen, & Luo, 2021).

1.4.4 Antioxidant activities

Free radicals are produced by the body through oxidative reactions in the process of maintaining normal life activities. Under normal physiological conditions, they can be scavenged by the body's defense mechanism. But when the increase of free radicals in the

body disrupts the redox balance, it will cause damage to the body. In addition, aging and other disease processes are associated with an excess of free radicals, including superoxide anion ($O2^{\cdot -}$), hydrogen peroxide (H_2O_2) and nitric oxide (NO). Therefore, the search for safe and efficient natural antioxidants has become a hot research topic in biomedical fields.

In recent years, the antioxidant activity of polysaccharides *in vitro* and *in vivo* has been widely proved. Su and Li (Su & Li, 2020) extracted four Auricularia polysaccharides by enzymatic extraction and purified by dialysis. The results showed that Auricularia polysaccharides have good antioxidant activity, especially A.polytricha polysaccharides. In addition, the antioxidant activity of polysaccharides is also related to the activity of antioxidant enzymes (Y. Yu et al., 2018). Guo et al. (Yuanheng Guo et al., 2016) isolated three polysaccharide grades, CDP-A, CDP-B and CDP-C, from *Cistanchia cistanches*. The results of the *in vitro* antioxidant activity showed that CDP-C, which contained a higher proportion of galacturonic acid, had the highest activity. Furthermore, in *in vivo* studies, CDP-C improved the alterations of alcohol-induced chronic liver damage in model animals, including serum parameters (alanine transaminase, acid phosphatase and triglycerides) and liver parameters (malondialdehyde, superoxide dismutase). These results suggest that the hepatoprotective activity of CDP-C against alcohol-induced chronic liver injury, which may be due to the fact that CDP-C reduces malondialdehyde and triglyceride levels and regulates the activities of related enzymes and that the activity of CDP-C may be related to galacturonic acid.

In addition, there are also four common chemical methods used to measure the antioxidant activity of polysaccharides, including hydroxyl radical, superoxide anion radical , 2,2′-Azino-bis (3-ethylbenzthiazoline-6-sulfonic acid) method and 2,2-diphenyl-1-picrylhydrazyl method.

The hydroxyl radical (OH•) is formed from the precursor molecules superoxide (O_2•−) and hydrogen peroxide (H_2O_2). Due to its high reactivity, the OH• is one of the most reactive radical species, capable of interacting with virtually all types of compounds. Consequently, substances that demonstrate scavenging activity against OH• are considered antioxidants (Gulcin, 2020; Magalhães, Segundo, Reis, & Lima, 2008). The superoxide anion radical (O_2•−) arises when molecular dioxygen (O_2) undergoes a one-electron reduction. O_2•− is a byproduct of various cellular metabolic activities (Halliwell, 2006), its scavenging by antioxidants, such as polysaccharides, is often studied to infer potential antioxidant effects within living systems (Gulcin, 2020; Magalhães et al., 2008). The ABTS•+ radical cation is generated by oxidizing the ABTS reagent, typically using potassium persulfate, which results in a distinctive blue coloration (Gulcin, 2020; Magalhães et al., 2008). Due to the water-solubility of both the ABTS reagent and many polysaccharides, this assay is well-suited for evaluating the antioxidant activity of polysaccharides. The decrease in color intensity, signifying the reduction of ABTS•+ radicals, is quantified spectrophotometrically at a wavelength of 734 nm (Ahmadi, Rezadoost, Alilou, Stuppner, & Farimani, 2022; Ning et al., 2021; Z.-W. Wang, Zhang,

Qiao, Cai, & Yan, 2021; X. Xiao et al., 2022). This reduction is indicative of the antioxidant's capacity to donate hydrogen atoms or electrons. The DPPH• assay is commonly used for preliminary antioxidant activity assessments due to the high stability of the DPPH radical, which stems from electron delocalization throughout the molecule (Gulcin, 2020; Magalhães et al., 2008). The DPPH• assay is favored for its simplicity, affordability, and rapid results, and remains useful for testing antioxidants, including polysaccharides and oligosaccharides, that are amenable to solubilization in organic media. Studies have shown that polysaccharides extracted from Pleurotus *citrinipileatus* (ERPS) have antioxidant and hepatoprotective effects (Xinchao Liu et al., 2019). Animal experiments have shown that ERPS can reduce the levels of multiple indicators in serum and enhance the activity of antioxidant enzymes in the liver.

1.4.5 Other activities

In addition to the above activities, fungal polysaccharides also have anti-tumor, anti-aging, anti-fatigue activities, and immune function regulation functions. Xu et al. (Xu, Yang, Ning, & Zhang, 2015) found that a heteropolysaccharide L2 extracted from shiitake mushrooms can enhance the immune response of elderly mice and affect the composition of intestinal microbiota, reversing the age-changed intestinal microbiota structure, such as the reduction of the ratio of *Firmicutes*/*Bacteroides*.

1.5 Relationships of structures and properties to bioactivities of polysaccharides

The ability of polysaccharides to exert specific functional activities depends mainly on their physicochemical properties and structural characteristics. Polysaccharides with different structural characteristics have significant differences in their functional activities (X. Ji et al., 2017). It has been reported that the molecular weight distribution of polysaccharides, the monosaccharide composition, the type of glycosidic bond and the linkage between the main chain and the side chain all affect their functional activities, as summarized in **Table 1-2**.

Polysaccharides with higher molecular weights are more likely to exert their chain conformation in solution and thus may exhibit stronger biological activities, such as antitumor and immune activities (J. Li, Fan, & Ding, 2011). However, it has also been reported that the bioactivity of polysaccharides and their molecular weights show opposite trends (Qu et al., 2020). Therefore, the molecular weight of polysaccharides is not simply positively or negatively related to their biological activities but should be combined with their structural characteristics and molecular space conformation. Monosaccharide compositions and ratio are one of the important factors affecting the activity of polysaccharides. Lo et al. measured 10 kinds of polysaccharides extracted from culture broth filtrates of *Lentinula edodes* and found that as the ratio of Man and Rha increased, the antioxidant capacity gradually increased. While as the ratio of Ara and Glc increased,

the antioxidant capacity gradually decreased. For the glycosidic bond configuration, polysaccharides with (1→3) glycosidic bond configuration show stronger biological activity, such as mushroom polysaccharide β-(1→3)-glucan, which can play a good anti-tumor effect (Yangyang Zhang, Li, Wang, Zhang, & Cheung, 2011). In addition, for polysaccharides with branching structure, the branched structure and degree of branching are closely related to their functional activities, and the activity of polysaccharides with too high or too low a proportion of branched chains may be affected, which needs to be analyzed in the light of the specific structural properties (J. Chen & Seviour, 2007). In addition, polysaccharides undergo targeted chemical modifications, such as some conventional chemical modifications including selenization, acetylation, carboxymethylation, and sulfate esterification in the study, also show some degree of improvement in biological activity.

Table 1-2. Structural characterization and bioactivities from fungal polysaccharides.

Source	Fractions	Structural features	Bioactivities	Refs
Ganoderma lucidum	GLP-1b	1.7×10^4 Da; Man:Glc:Gal:Fuc=1:1:9.5:3.9; →6)-α-D-Galp-(1→6)-α-D-Galp-(1→	Immunomodulatory activity: activation of the NF-κB and MAPK signaling pathways;NO and pro-inflammatory cytokines (IL-1β, IL-6, and TNF-α) increased;*Lactobacillus* and *Alistipes* enriched	(Z.-W. Wu et al., 2025)
Auricularia auricula	dME-2	2.1×10^5Da; Man:Xyl:Gal:Glc=218.2:29.7:1:1; →3)-α-Manp-(1→	Anti-inflammatory activity: the mRNA levels of IL-1β, INF-γ and TNF-α decreased	(J. Liang et al., 2023)
Hericium coralloides	EPS	413 and 1578 Da; Glc;	Antioxidant activity: EC_{50} of DPPH, FRAP and ABTS was 4.12, 17.0, and 2.83 mg/mL	(Tabibzadeh et al., 2024)
Auricularia auricula	AAP-3-1	3.2×10^5Da; Man:Glc=1.4:1	Antioxidant activity: intracellular ROS, SOD, GSH–Px and CAT inhibited; the MDA content decreased	(L. Qian et al., 2020)
Grifola frondosa	GFP	Fuc:GlcN:Gal:Glc:Man=6.25:1:15.75:217:9.5; mainly β-glucan	Anti-inflammatory activity: the colon length restored; IL-10 increased; IL-6 and TNF-α decreased	(X. Liu et al., 2023)
Cordyceps cicadae	SPP	7.2×10^5Da;Glc:Man:Gal:Xyl=9.4:4.8:1.7:1; → 3)-Glcp-(1 → main backbone and →6)-Manp-(1→,→3,4)-Glcp-(1→ and →4,6)-Glcp-(1 → branch chain	Hypoglycemic Activity: glucose consumption increased; lower the blood glucose; the spleen index decreased; the expression of IRS-1, PI3K, Akt, and GLUT4 enhanced	(Y. Wang et al., 2023)
Dictyophora indusiata	$DIP1_p$	7.2×10^5Da;Glc:Man:Gal:Xyl=9.4:4.8:1.7:1; → 3)-Glcp-(1 → main backbone and →6)-Manp-(1→,→3,4)-Glcp-(1→ and →4,6)-Glcp-(1 → branch chain	Regulating gut microbiota: acetic acid and propionic acid increased; *Proteobacteria* decreased; *Blautia* and *Roseburia* increased	(L. Wang et al., 2025)

1.6 Exopolysaccharides from medicinal fungus *C. sinensis*

The polysaccharides extracted from *Cordyceps* have been extensively studied and found to exhibit significant biological activities. They display potent antioxidant properties, combating oxidative stress. Furthermore, these polysaccharides have been shown to have prebiotic effects, enhancing the growth of beneficial gut microbes and contributing to a balanced gut microbiota. Their immunomodulatory activity is also noteworthy; they can modulate the immune system by activating immune cells, leading to a more robust defense against pathogens and diseases. The diverse activities of these polysaccharides emphasize their potential as functional food ingredients and therapeutic agents.

Current studies have uncovered the connection between the structural attributes of *C. sinensis* polysaccharides and their bioactivities. Yan et al. (J.-K. Yan, Wang, Li, & Wu, 2011) conducted a comparative analysis of the structural and pharmacological differences between polysaccharides extracted from *C. sinensis* using hot water and alkaline methods. Both types are α-D-glucans and have comparable molecular weight, measuring 1180 kDa for hot water extraction and 1150 kDa for alkaline water extraction) and a (1→4)-linked α-D-glucopyranosyl backbone, the hot water-extracted polysaccharide featured a branching pattern of (1→6)-linked α-D-glucopyranosyl units, whereas the alkaline water-extracted polysaccharide was a linear glucan. Notably, the alkaline water-extracted polysaccharide exhibited more pronounced anti-cancer and immunostimulatory effects

than its hot water-extracted counterpart. The polysaccharide CS-81002 was found to enhance the phagocytic activity of mouse peritoneal macrophages, with this effect diminishing progressively upon acid hydrolysis-induced reduction in molecular weight until it ceased entirely (Gong et al., 1990). Conversely, Li et al. (L. Q. Li, A. X. Song, W. T. Wong, & J. Y. Wu, 2021b) demonstrated that the low-molecular-weight polysaccharide LM-EPS produced by *Bifidobacteria*-mediated degradation of EPS in fermentation broth boasted a more potent anti-inflammatory effect than its higher-MW precursor, EPS. Collectively, these studies underscore a strong correlation between the structural configuration of *C. sinensis* polysaccharides and their pharmacological properties. Variations in monosaccharide composition, molecular weight, and structural arrangement appear to be pivotal in influencing pharmacological efficacy. Extracellular polysaccharides (EPS) from *C. sinensis* cultures have shown significant potential in inhibiting melanoma growth in the lungs and liver of mice, suggesting their promise as an adjunct therapy for cancer (X. Yang et al., 2007).

1.7 Objectives and significance

1.7.1 Objectives

This research project is aimed to investigate the prebiotic and protective effects for gut health of Cs-HK1 EPS. Besides, potential hypoglycemic, antioxidant activities and structures of EPS-LM-n from Cs-HK1 mycelial fermentation were also evaluated.

Different EPS-fractions were used in this project are from *C. sinensis* fungus Cs-HK1 mycelial fermentation. EPS-HM was isolated from the Cs-HK1 mycelial fermentation medium by the step of ethanol precipitation at 40% of ethanol. The supernatant was then added with ethanol to extracted EPS-LM (final concentration of ethanol was 80%, v/v). EPS-LM-n was further purified by DEAE-52 and Superdex 200 pg column. The whole isolation and purification process was briefly described in **Figure 1-2**. EPS-LM and Goji LBPS (a plant source polysaccharide) was used in Chapter 2 to investigate the digestion resistance, fermentability, SCFA production and prebiotic effects of EPS-LM and LBPS on human gut microbiota, establishing foundational differences based on *in vitro* fecal fermentation. EPS-HM and EPS-LM fraction were used in Chapter 3 to explore the impact of Cs-HK1 EPS fractions on fermentation profiles and demonstrated the anti-inflammatory and barrier-protective effects of their fermentation products in a co-culture model. EPS-LM-n was used in Chapter 4 to investigate the neutral EPS, EPS-LM-n and evaluate its hypoglycemic activities, including α-amylase and α-glucosidase inhibitory activities and antioxidant activities.

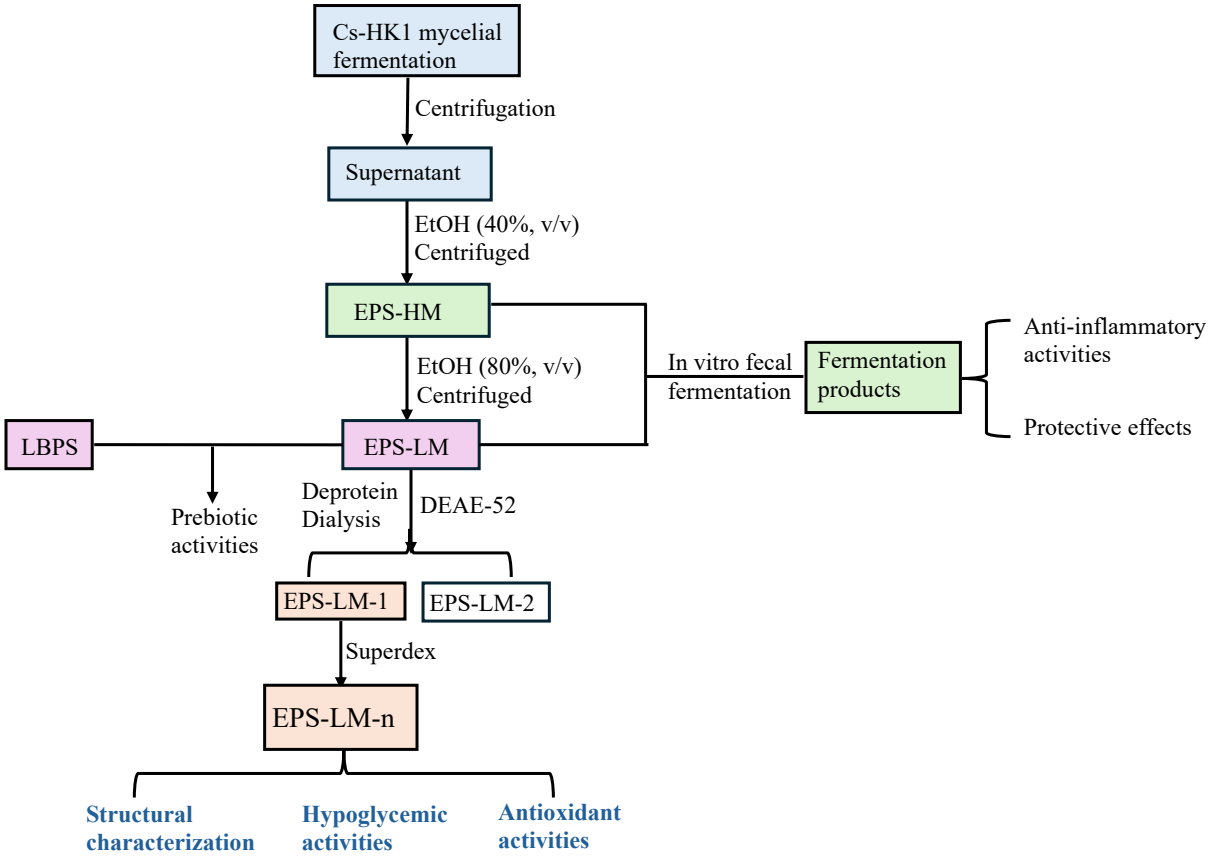

Figure 1-2. Outline of the project.

These will be achieved through the following studies:

1) To evaluate the potential prebiotic effects of EPS-LM and LBPS in *in vitro* fecal fermentation. An upper gastrointestinal digestion and *in vitro* fecal fermentation was utilized. During the whole process, physicochemical properties and gut microbiota profiles were measured. The experiments included total carbohydrate, molecular weight, monosaccharide composition, pH value, SCFAs production and the composition and diversity of gut microbiota.

2) To evaluate the protective and anti-inflammatory effects of metabolites from high/low-MW Cs-HK1 EPS on gut barrier function. LPS-induced Caco-2/RAW264.7 co-culture model was utilized to test the anti-inflammatory activities of EPS-LM and EPS-HM fecal fermentation products.

3) To purify and structurally characterize EPS-LM-n. Analysis of the physiochemical properties, including chemical component, monosaccharide composition, MW distribution, linkages, and possible structures were analyzed. To evaluate the *in vitro* hypoglycemic and antioxidant activities of EPS-LM-n, including α-amylase, α-glucosidase inhibitory activities, hydroxyl, ABTS, DPPH radical scavenging and FRAP ability and protective functions of H_2O_2-induced EA. hy926 cells.

1.7.2 Significance

Cs-HK1, a fungal species isolated from the fruiting body of natural *C. sinensis*, has demonstrated a substantial yield of EPS during liquid fermentation. While various bioactivities of *C. sinensis* EPS have been reported, such as anti-inflammatory and immunomodulatory effects. This research will provide a comprehensive structure-activity framework for Cs-HK1 EPS, highlighting the specific effects derived from Cs-HK1. It will demonstrate the connection between polysaccharide fermentation and the integrity of the gut barrier. Additionally, the research will identify different fractions of Cs-HK1 EPS, exhibiting multifunctional potential, including prebiotic, gut-protective, hypoglycemic and

antioxidant properties. Ultimately, this work will support the development of polysaccharide-based interventions aimed at enhancing gut and metabolic health.

Chapter 2 Metabolic outcomes of Cs-HK1 exopolysaccharide during *in vitro* human fecal fermentation: Compared with Goji plant polysaccharides

2.1 Introduction

Human gut microbiota refers to the huge number and diverse array of microorganisms that inhabit the human intestine, most of which are bacteria existing in the colon. A balanced microbiota is crucial to the host health by contributing to digestion, metabolism, immune function, and other physiological functions, while the dysbiosis of gut microbiota is implicated in metabolic disorders and chronic diseases (Fan & Pedersen, 2021; Mancin, Wu, & Paoli, 2023). For example, the comparison of the microbiota between obese and lean human subjects has shown that the relative abundance of *Firmicutes* increased and *Bacteroidetes* decreased (Nakamura & Omaye, 2012). The increased ratio of *Firmicutes* to *Bacteroidetes* is most likely to contribute to the weight gain (Turnbaugh et al., 2009). A beneficial outcome from fermentative metabolism of non-digestible polysaccharides in the gut microbiota is the production of SCFAs including acetic, propionic and butyric acid. Of the three SCFAs, acetic acid is usually the produced at the highest level through anaerobic metabolism of pyruvate via the acetyl-coenzyme A (acetyl-CoA) or the Wood-Ljungdahl pathway (A. Koh, De Vadder, Kovatcheva-Datchary, & Bäckhed, 2016). Propionic acid, which may have a significant impact on the energy homeostasis, is produced by conversion of succinate to methylmalonyl-CoA via the succinate pathway. Butyric acid is formed by the condensation of two molecules of acetyl CoA followed by reduction to butyryl-CoA (Ana Nogal, Ana M. Valdes, & Cristina Menni, 2021). In addition, diet is among the most

important factors that can influence the microbial composition of gut microbiota (Singh et al., 2017).

Polysaccharides are major constituents of edible and medicinal plants and fungi, many of which have special bioactivities and health benefits such as anti-inflammatory, antioxidant, antitumor, anti-fatigue and immunomodulatory (H. Liu, Liu, Xie, & Chen, 2023; Tudu & Samanta, 2023). Cs-HK1 is a medicinal fungus species isolated from the Chinese caterpillar fungus *C. sinensis* (= *Ophiocordyceps sinensis*) and capable of producing exopolysaccharides (EPS) in mycelial culture (P. H. Leung, Q. X. Zhang, & J. Y. Wu, 2006). In our previous studies, the EPS isolated from the Cs-HK1 mycelial culture, which was composed mainly of mannose, glucose and galactose has shown notable prebiotic properties (A.-X. Song, Mao, Siu, Tai, & Wu, 2019) and significant anti-inflammatory activities (L.-Q. Li et al., 2020). Other studies have also shown the structural characteristics of polysaccharides isolated from different *C. sinensis* species are significant factors affecting the bioactivities such as immunostimulatory effects *(Junqiao Wang et al., 2017)* and amelioration of liver diseases (H. Tang et al., 2017). Similarly, *Lycium barbarum* L. generally known as Goji is a well-known medicinal plant for its fruit called the Wolfberry or Goji berry and has been widely used as a heath food and a herbal medicine (D. Qian, Zhao, Yang, & Huang, 2017). Polysaccharides from *L. barbarum* L. (LBPS) are among the major bioactive constituents of Goji berry with a broad spectrum of health and therapeutic benefits, such as antioxidant, anti-tumor, anti-diabetic, immunomodulatory effects (R.-H. Ma et al., 2023). LBPS typically have a high molecular weight (ranging from 2.1×10^3 to 6.5×10^6 Da) and a branched structure, composed of several monosaccharides

including glucose, mannose, rhamnose, galactose and galacturonic acid (D.-T. Wu et al., 2018).

Most of the bioactive polysaccharides are resistant to human digestive enzymes and mainly decomposed by the bacteria in the large intestine. Therefore, their health benefits are most probably linked with their fermentative metabolism in the gut microbiota. In other words, the polysaccharides may function as prebiotics to promote a healthy balance of gut microbiota (Q. Song et al., 2021). The non-digestible polysaccharides that enter the large intestine can be consumed as the carbon source by the gut bacteria and through fermentation and produce SCFAs. Recently, LBPS have been shown prebiotic functions which are closely related to their structural characteristics such as molecular weight and monosaccharide composition (Feng et al., 2022). The results from previous studies indicate that the biological activities and potential therapeutic effects of polysaccharides are closely related to their chemical composition and structural characteristics.

Based on the above literature review and technical background, it is hypothesized that these medicinal fungal and plant polysaccharides may modulate the gut microbiota by serving as fermentable substrates for certain populations of the gut bacteria and may also derive metabolites such as SCFAs which have beneficial effects on the host. Further studies on such relationships are of significance for understanding their health benefits and also for their effective utilization to improve human health. As an effort toward this goal, this study was performed on the prebiotic properties and metabolism outcomes of Cs-HK1 EPS and LPBS during *in vitro* fermentation by human fecal microbiota. A Cs-HK1 EPS fraction, EPS-LM, and an LBPS were chosen in this study as the representative polysaccharide with different structural characteristics from two most popular and valuable medicinal fungus

and plant. Moreover, as LBPS or Goji polysaccharides have been extensively studied for their health benefits including the prebiotic functions with respect to the structural characteristics, the LBPS can be a good reference for the relatively new and rare EPS-LM. By comparing the modulatory effects of these polysaccharides on fecal microbiota during *in vitro* human fecal fermentation, this study aims to elucidate the specific changes induced in microbial populations and metabolic outcomes. Changes in molecular weight, monosaccharide composition and SCFAs were detected during *in vitro* human fecal fermentation to evaluate the consumption and metabolism of EPS-LM and LBPS. The composition and diversity of fecal microbiota were assessed using 16S rRNA gene analysis.

2.2 Materials and methods

2.2.1 Materials and reagents

Lycium barbarum L. polysaccharide (LBPS) in the form of solid powder was purchased from Xi'an Shengqing Biotechnology Co., Ltd. Dextran molecular weight standards (1–670 kDa) were obtained from International Laboratory USA (San Bruno, CA, USA). Pepsin (3000 U/g) and trypsin (250 U/g), along with bile salts and Fructooligosaccharide (FOS), were purchased from Solarbio (Beijing, China). Gastric lipase (100,000 U/g) and pancreatin (250 U/mg) were acquired from Yuanye (Shanghai, China). Monosaccharide standards (Mannose, rhamnose, glucuronic acid, galacturonic acid, glucose, galactose, xylose, arabinose and fucose) of analytical grade, trifluoroacetic acid (TFA), acetonitrile (ACN, HPLC grade), and methanol (MeOH) were from Sigma-Aldrich (St. Louis, MO, USA).

2.2.2 Isolation and purification of EPS-LM fraction and LBPS

As reported previously (A.-X. Song et al., 2019), the Cs-HK1 fungus was routinely preserved in mycelial culture on solid Potato Dextrose Agar, and the mycelial fermentation of Cs-HK1 was performed in shake flasks filled with a liquid medium consisting of 40 g/L glucose, 5 g/L peptone, 1 g/L KH_2PO_4, 0.5 g/L $MgSO_4 \cdot 7H_2O$, and 10 g/L yeast extract. After flasks were shaken at 250 rpm at 20 °C for 7 days and fermentation liquid was then centrifuged (Beckman Coulter Avanti-JXN26 with JA-10 rotor, Krefeld, Germany) at 9,000 rpm for 30 minutes at 4 °C. The supernatant was collected and subject to a two-step ethanol precipitation. In the first step, ethanol was gradually added to the supernatant medium to achieve a final concentration of 40% (v/v) under continuous stirring, and then left undisturbed at 4 °C for 40 minutes. The solid was then separated from the liquid mixture. In the second step, absolute ethanol was added to the liquid to reach a final ethanol concentration of 80% (v/v) and left at 4 °C overnight. The precipitate was recovered by centrifugation, freeze-dried (LABCONCO, FreeZone 2.5 Liter, PRAMA, USA) and deproteinized for future use. The raw LBPS received from the commercial supplier was further purified by ethanol precipitation before use. The LBPS powder was dissolved in 40% (v/v) of absolute ethanol for overnight at 4 °C. The precipitate was recovered by centrifugation and lyophilized as the final LBPS to be used in the following experiments.

2.2.3 FT-IR and NMR analysis

Fourier transform infrared (FT-IR) spectroscopy of the polysaccharide samples was performed with a FT-IR spectrometer (Nexus 670, Thermo Nicolet Co., Cambridge, UK) in the wavenumber range of 400-4000 cm^{-1}. The polysaccharide samples (EPS-LM and LBPS at 1 mg) were ground with 100 mg KBr and pressed into tablets for the analysis.

Nuclear magnetic resonance (NMR) analysis of EPS-LM and LBPS was performed on a 600 MHz NMR spectrometer (Bruker AVANCE-III 600MHZ, Switzerland) at 25 °C. Each of the polysaccharide samples (~50 mg each) was dissolved in D_2O and lyophilized; the procedure was repeated twice and the final sample was dissolved in 0.6 mL of D_2O. The ^{1}H and ^{13}C NMR spectrum were measured on the NMR instrument. In addition, the micromorphology of polysaccharides was imaged by a Field Emission Scanning Electron Microscope (Brno, Czech Republic).

2.2.4 Simulated gastrointestinal digestion *in vitro*

Polysaccharide samples of EPS-LM and LBPS (5 mg/mL) were digested in simulated oral-gastric-small intestinal digestion model, incubated with shaking at 37 °C in a water bath as reported previously with minor modifications (Brodkorb et al., 2019; G. Ma, Xu, Du, Kimatu, et al., 2022; Q. Yuan et al., 2020). For oral digestion, polysaccharide samples were combined with an equal volume of simulated saliva (2 mM NaCl, 13 mM KCl, 5 mM KH_2PO_4, 3.5 mM Urea) with pH 6.8. Aliquots of 2 mL were collected at 0, and 20 min and quickly heated at 100 °C for 5 min to stop the reaction. For gastric digestion, the samples after oral digestion were each mixed with an equal volume of simulated gastric juice (53 mM NaCl, 15 mM KCl, 1 M $CaCl_2 \cdot 2H_2O$, 7 mM $NaHCO_3$, 1 M (10 mL) CH_3COONa,

25,000 U gastric lipase, 700 U pepsin) at pH 3. Aliquots of 2 mL were collected after 0.5, 1 and 2 h and then heated at 100 °C for 5 min to stop the reaction. For intestinal digestion, the remaining samples were adjusted to 7.0 and mixed with an equal volume of simulated intestinal juice (92 mM NaCl, 9 mM KCl, 2 mM $CaCl_2 \cdot 2H_2O$, 7% 4000 U pancreatin, 4% bile salt, and 130 mg of 250 U/mg trypsin). Samples were taken at 0.5, 1, 2 and 4 h and then heated at 100 °C for 5 min to stop the reaction. Reducing sugars were analyzed by DNS method during the digestion as described in a later section.

2.2.5 *In vitro* fecal fermentation

The *in vitro* fecal fermentation followed the procedure from a previous report with minor modifications (Johnson et al., 2015; Mao et al., 2020). Fructooligosaccharides (FOS), a well-established prebiotic fiber, was included as a positive control and carbohydrate-free culture as a blank control for comparison with EPS-LM and LPBS. The EPS-LM, LBPS or FOS as the carbon source was added into three culture tubes (with 25 mg carbon source in each tube) for triplicate experiments and mixed with 4 mL of a liquid medium. The liquid medium consisted of 2 g/L peptone water, 2 g/L yeast extract, 0.1 g/L NaCl, 40 mg/L K_2HPO_4, 40 mg/L KH_2PO_4, 10 mg/L $MgSO_4 \cdot 7H_2O$, 10 mg/L $CaCl_2 \cdot 6H_2O$, 2 g/L $NaHCO_3$, 0.5 g/L L-cysteine, 0.5 g/L bile salts, 10 μL/L vitamin K, 2 mL/L Tween 80, 1 mg/L resazurin and 5 mg/L hemin at pH 6.8 (a neutral pH in the distal large intestine) adjusted with 1M HCl. For inoculation, stool feces were collected from three healthy donors (males, ages: 20-26 years, body weight range: 66-70 kg, height range: 174-180 cm, body mass index (in kg/m^2) range: 21-22.5) who had maintained a minimum of three months of standard dietary habits, exhibiting no signs of gastrointestinal disorders, chronic disorders and refraining from antibiotic use. The use of fecal cultures from individual donors is a

common and widely accepted approach for studies on the colonic microbiota and allows for direct comparison of the treatment effects among different donors. The feces collected from each donor were suspended in phosphate-buffered saline (PBS) at 1:10 (w/v) ratio and filtered through four layers of cheesecloth and the filtrate was added to the culture tubes (1 mL in each).

The fecal inoculum preparation and inoculation into the culture tubes were all carried out and completed within 2 h in an anaerobic chamber (Ruskinn Anaerobic Workstation Concept 400, Baker, Sanford, ME, USA) which was supplied with gas mixture of 10% H_2, 10% CO_2, and 80% N_2. gas. At selected time points of 0, 6, 12, 24, and 48 hours, fecal culture tubes were taken and pH value of each tube was measured with a PHS-3C pH meter (Sanxin Shanghai, China). Each tube was transferred several aliquots for further analysis. These aliquots were preserved at –80 °C. Fermentation samples were defrosted at room temperature and centrifuged (Hitachi CT15RE, Tokyo, Japan) for 12,000 rpm for 10 minutes at 4 °C. Supernatants were collected for chemical analysis and precipitates for microbial analysis, respectively.

2.2.6 Analysis of reducing sugars and total carbohydrate content

Reducing sugars (C_R) in the digested and fermentation samples were analyzed by DNS method during digestion (Miller, 1959), and by measurement of absorbance at 550 nm using glucose as the reference. Anthrone test was used to determine the total carbohydrate content of polysaccharides during fecal fermentation, which was then measured at 620 nm with glucose as the reference (Chen, Wang, Nie, & Marcone, 2013; Leung, Zhao, Ho, & Wu, 2009).

2.2.7 Determination of molecular weight

To determine the MW of raw EPS-LM and LBPS and their fermented samples, high-pressure gel permeation chromatography (HPGPC) was employed using a previously reported method (Siu, Chen, & Wu, 2014). The HPGPC system was comprised of a Waters 1515 isocratic pump, a 2414 refractive index detector, and three columns in series, Ultrahydrogel 120, 250, and 2000 (7.8 mm × 300 mm) (Waters Co., Milford, MA, USA), operating at 50 °C with water as the mobile phase. Prior to injection, sample solutions were filtered by 0.22 μm membrane and 100 μL of solution was prepared. Dextran standards ranging from 1.0-670 kDa were used for the standard curve.

2.2.8 Analysis of monosaccharide composition

The concentration of monosaccharides in the supernatant of fecal fermentation samples was analyzed by 1-phenyl-3-methyl-5-pyrazolone (PMP)-HPLC as reported previously (L.-Q. Li et al., 2020). Unfermented and fermented samples of EPS-LM and LBPS was dissolved in TFA with finial concentration of 2 M at 100 °C for 4 hours. Subsequent to hydrolysis, the solution was dried by evaporation under vacuum and then derivatized in 450 μL PMP solution (0.5 M in methanol) and an equal volume of 0.3 M NaOH at 70 °C for 30 min. The reaction was terminated by the addition of 450 μL of 0.3 M HCl to neutralize the mixture. Chloroform extraction was performed thrice to purify the solution. The samples were subsequently analyzed by HPLC in an Agilent 1260 system with an ZORBAX Eclipse XDB-C18 column (5 μm, 4.6 mm × 250 mm, Santa Clara, CA, USA). Mannose, rhamnose, glucuronic acid, galacturonic acid, glucose, galactose, xylose, arabinose and fucose were used as the standards.

2.2.9 Analysis of SCFAs

SCFAs in the fecal fermentation supernatant were analyzed by gas chromatography and flame ionization detection (GC-FID) using an Agilent 7980B GC instrument and a fused silica capillary column (Agilent Technologies Inc., Santa Clara, CA, USA) (Song et al., 2019). The sample supernatant was filled in a vial at 400 μL and filtered through 0.22-μm membrane followed with pH adjustment to 2-3 with 1 M HCl and addition of an internal standard (2-ethylbutyric acid). Nitrogen gas was applied at a flow rate of 0.6 ml/min. For the GC-FID analysis, the initial oven temperature was set at 80 °C for 2 minutes and gradually increased to 180 °C at a rate of 6 °C/min for 4 minutes. During the analysis, the injection volume was 1 μL and the temperature was controlled at 200 °C, while the detector temperature was maintained at 220 °C. External standards of acetic acid, propionic acid, and butyric acid (Aladdin, Shanghai, China) were as external standards.

2.2.10 DNA extraction and sequencing analysis

The fermentation samples (1 mL, 0 h and 48 h) collected from Section 2.2.5 were extracted using TIANamp Stool DNA Kit (Tiangen, Beijing, China) according to the manufacturer's instructions. DNA concentration was determined using Nanodrop One UV-Vis Spectrophotometer (ThermoFisher, Massachusetts, USA).

To amplify the V3-V4 region of the 16S rRNA gene, PCR was performed using the extracted DNA. The primers used were 341F (CCTACGGGNGGCWGCAG) and 785R (GACTACHVGGGTATCTAATCC) (Klindworth et al., 2013). High-throughput sequencing analysis of the 16S rRNA gene was performed using the Illumina NovaSeq PE250 platform by a commercial service provider, Novogene (Beijing, China).

2.2.11 Bioinformatics

The raw reads obtained were merged, demultiplexed and quality-filtered with QIIME 2.0, and the resulting reads were clustered into Operational Taxonomic Units (OTUs) with 97% distance-based similarity using the Greengenes (version 13_8) database (McDonald et al., 2012). All the subsequent analysis were based on OTUs table. α-diversity metrics calculated using Mothur and β-diversity metrics calculated using the Bray-Curtis dissimilarity (Lozupone & Knight, 2005). The relative abundance at the phylum and genus levels was calculated to generate the compositional bar plots. The Firmicutes-to-Bacteroidetes (F/B) ratio was calculated from the relative abundance data.

2.2.12 Statistical analysis

All the experiments were performed in triplicate or more repeats. The data were analyzed using a combination of software packages, including SPSS (version 26.0; IBM Inc., Chicago, IL, USA), GraphPad Prism 9 for Mac OS X (GraphPad Software, Inc., La Jolla, CA, US) and RStudio software. Descriptive statistics were calculated for all numerical variables, with results expressed as mean ± standard deviation. A one-way analysis of variance (ANOVA) was employed to evaluate statistical significance, followed by Tukey's pairwise comparisons with a significance level set at $p < 0.05$.

2.3 Results and discussion

2.3.1 Properties of EPS-LM and LBPS

According to the results of Anthrone test, the total carbohydrate content was 71.5% for EPS-LM and 94.7% for LBPS. **Table 2-1** showed the molecular weights (MWs) and

monosaccharide composition of EPS-LM and LBPS. EPS-LM had an average molecular weight of EPS-LM was 5.513×10^6 Da, which were consistent with our previous report (L.-Q. Li, A.-X. Song, W.-T. Wong, & J.-Y. Wu, 2021). LBPS had a lower average molecular weight of 1.236×10^5 Da, which was consistent with previously reported molecular weights of LBPS between 2.1×10^3 and 6.5×10^6 Da (D.-T. Wu et al., 2018). EPS-LM mainly consisted of Man, Rha, Glc and Gal with different molar ratios (108:1:29.2:52.7) with mannose being the most abundant. LBPS was mainly composed of Man, Gal A, Glc and Gal (molar ratio: 1:1.34:313.8:5.24) (without fucose) with a high glucose abundance, which was consistent with previous studies (W. Huang et al., 2023; J. Xu et al., 2021). These results showed that EPS-LM and LBPS have differences in molecular properties and chemical composition.

The FT-IR spectrum of EPS-LM and LBPS was shown in **Figure 2-1**. Overall, both EPS-LM and LBPS had typical bands of carbohydrates, which was from 500-3900 cm^{-1}. The absorption peak near 3400 cm^{-1} was caused by the -OH, $-NH_2$, or -NH- stretching vibration in the molecular structure (G. Chen et al., 2021). The weak absorption peaks at 2900 and 1408 cm^{-1} were individually attributed to C-H stretching vibration, including CH, CH_2 and CH_3 (L. Zhang et al., 2018) and C-O stretching vibration (H.-L. Tang, Chen, Wang, & Sun, 2015). The absorption peak at around 1644 cm^{-1} were due to the bound water or carbonyl stretching (H. Yang et al., 2018), such as uronic acids existing in LBPS (P. He, Zhang, Zhang, Linhardt, & Sun, 2016), the peak around 1053 cm^{-1} were C-O stretching of pyranosides (S. Yuan et al., 2023). From the FT-IR, only slight differences between EPS-LM and LBPS could be observed as follows. The region of 1544 cm^{-1} of EPS-LM corresponds to the symmetric stretching vibration of carboxylate group. The peaks near

929 cm^{-1} and 851 cm^{-1} indicated the presence of α-configuration. Besides, the peaks of EPS-LM around 1244 cm^{-1} may attribute to the Rha and peaks of LBPS near 1708 cm^{-1} may be due to Gal A (Xuwei Liu, Renard, Bureau, & Le Bourvellec, 2021). LBPS showed a stronger absorption peaks at 893 cm^{-1} indicated strong *β*-glycosidic bond chain linkage in their sugar units (Dou, Chen, & Fu, 2019). In addition, the absorption peak of LBPS at around 764 cm^{-1} was indicative of the α-isomers of pyranose (H.-L. Tang et al., 2015).

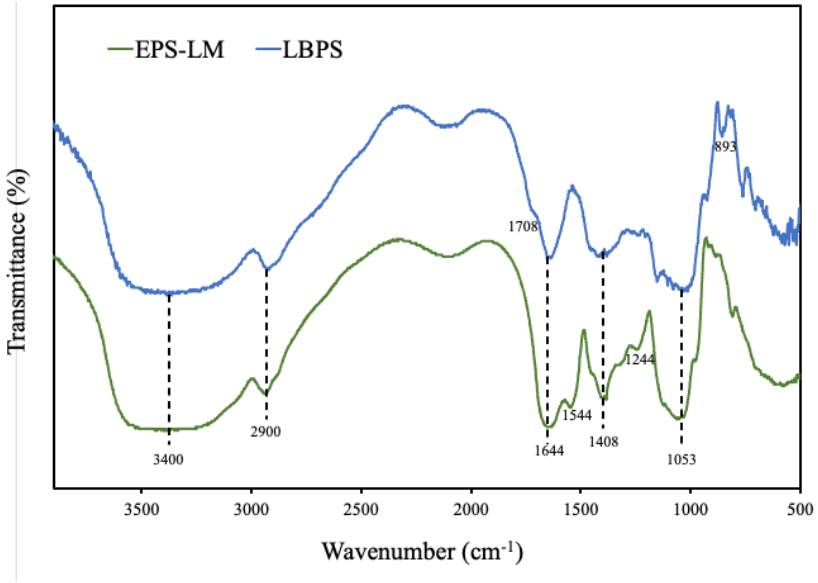

Figure 2-1. FT-IR spectra of EPS-LM and LBPS.

The preliminary results of ^{1}H NMR and ^{13}C NMR analysis of EPS-LM were presented in **Figure 2-2** to reveal the major structural characteristics of EPS-LM and LBPS. The ^{1}H NMR spectra provided the primary information of the glycosidic bond configurations (**Figure 2-2A**). Specifically, the signal at 4.70 ppm was identified as the chemical shifts of HOD and the anomeric protons (H-1) of EPS-LM resonated in the range of δ 4.4–5.5 ppm, indicating the presence of both α- and β-configurations for the anomeric carbons (Zhu et al., 2016). Signals at δ 4.75, 4.90 and 4.97 ppm were assigned to anomeric protons of β-mannopyranose (Elena N. Makarova, Shakhmatov, & Belyy, 2018). Weak signals around

δ 5.21 ppm were attributed to α-rhamnpyranose (Elena N Makarova & Shakhmatov, 2021). Signals at δ 4.94, 5.02 and 5.15 ppm corresponded to α-glucopyranose (Huo et al., 2022) while signals at δ 5.07 and 5.06 ppm were attributed to α-galactopyranose (Elena N Makarova & Shakhmatov, 2021). The ^{13}C NMR spectra further complemented these findings, with chemical shifts in the regions of δ 95–103 ppm and δ 103–110 ppm further confirming the existence of α and β configurations of the anomeric carbons. The predominant peaks in the range of δ 95–103 ppm suggest that the α-configuration is the main glycosidic bond form in EPS-LM, which was consistent with the FT-IR analysis. Signals between δ 103-107 ppm were attributed to β-mannopyranose (Elena N. Makarova et al., 2018), while major signals between δ 99 and 102.4 ppm were assigned to α-glucopyranose (Huo et al., 2022). Signals between δ 96 and 99 ppm corresponded to α-galactopyranose (Elena N. Makarova et al., 2018). The predominant peaks suggested that both α- and β-configurations were the main glycosidic bond forms in EPS-LM, consistent with the ^{1}H NMR analysis. In summary, EPS-LM was a highly complex heteropolysaccharide consisting mainly of Man, Glc and Gal with mixed linkage structures.

The ^{1}H NMR spectrum of LBPS (**Figure 2-2C**) revealed several distinct anomeric proton signals, indicative of various sugar residues including anomeric protons of glucose (Huo et al., 2022), galacturonic acid and galactose units (D. Liu et al., 2022; Elena N. Makarova et al., 2018), and the H2–H6 protons of these sugar residues (H.-L. Tang et al., 2015). On the ^{13}C NMR spectrum (**Figure 2-2D**), the anomeric peaks between δ 95.95 and 104.17 ppm are indicative of both α (δ 95–103 ppm) and β (δ 104–105 ppm) anomeric configuration of pyranose, in line with that of FT-IR spectrum. The anomeric carbon signal

of Glc at ~δ 100 ppm suggests α-glucan structure, consistent with the results reported by Duan et al (Duan et al., 2001) and Zhao et al (C. Zhao, He, Li, & Cui, 1996).

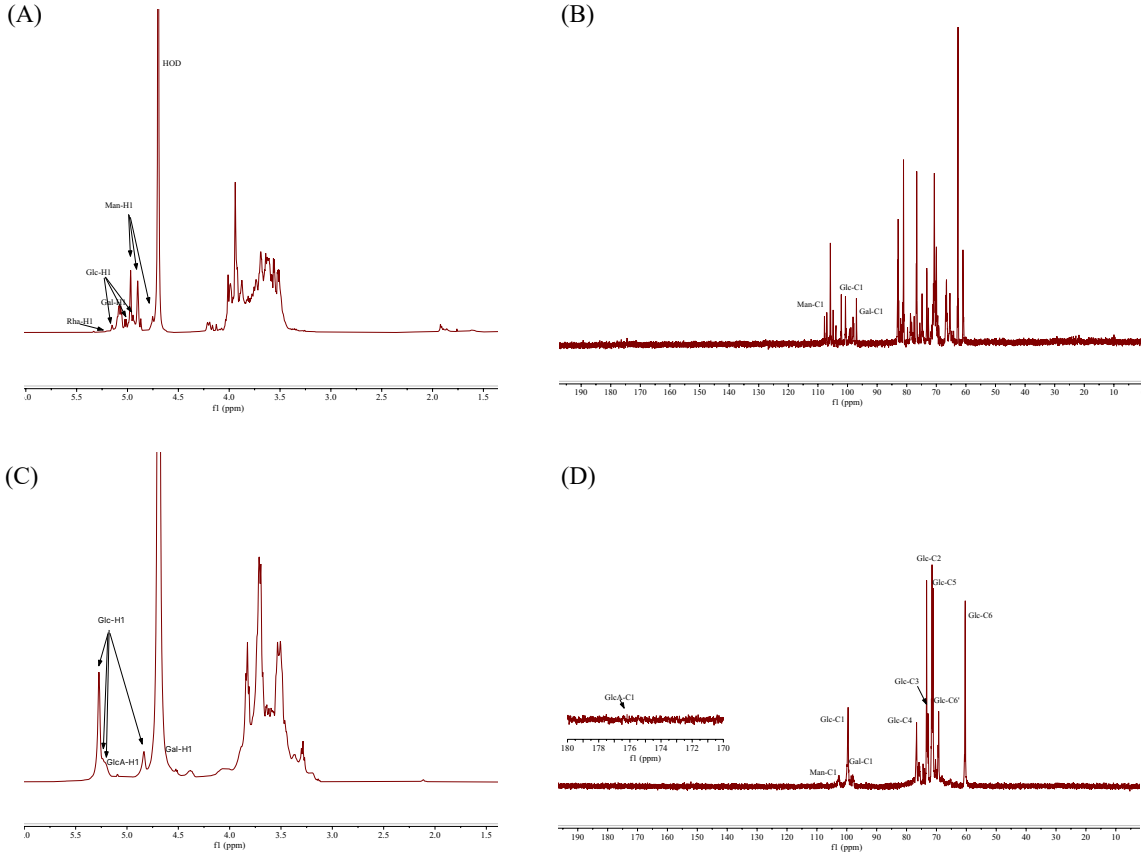

Figure 2-2. ^{1}H NMR (A) and ^{13}C NMR (B) spectrum of EPS-LM; ^{1}H NMR (C) and ^{13}C NMR (D) spectrum of LBPS. Experiments were performed in D_2O at 25 °C (chemical shifts are expressed in δ ppm).

2.3.2. Changes of EPS-LM and LBPS during simulated upper GI digestion

To detect the possible degradation of EPS-LM and LPBS passing through the gastrointestinal tract (GIT), the polysaccharides were exposed to human saliva, simulated gastric and small intestinal digestion. As shown in **Table 2-1**, there was no significant increase in the concentration of reducing sugars or decrease in molecular weight in any of

three simulated digestive sections, implying that EPS-LM and LBPS were highly resistant to the digestive enzymes and gastric acid in the upper GIT and can reach the large intestine and subject to the fermentation by gut microbiota.

Table 2-1. Production of reducing sugars (C_R) and changes of molecular weight during *in vitro* simulated gastrointestinal digestion of EPS-LM and LBPS.

	EPS-LM		LBPS	
	C_R (mg/mL)	MW ($\times 10^6$ Da)	C_R (mg/mL)	MW ($\times 10^5$ Da)
Saliva				
0 min	0.301±0.001[a]	5.513±0.231[a]	0.411±0.002[a]	1.236±0.414[a]
20 min	0.298±0.002[a]	5.534±0.421[a]	0.407±0.003[a]	1.243±0.463[a]
Gastric				
0.5 h	0.243±0.001[a]	5.443±0.234[a]	0.304±0.002[a]	1.198±0.243[a]
1 h	0.241±0.003[a]	5.397±0.273[a]	0.305±0.003[a]	1.154±0.563[a]
2 h	0.238±0.003[a]	5.385±0.352[a]	0.298±0.005[a]	1.096±0.245[a]
Small intestinal				
0.5 h	0.201±0.001[a]	5.318±0.146[a]	0.242±0.001[a]	1.062±0.632[a]
1 h	0.197±0.002[a]	5.292±0.432[a]	0.239±0.004[a]	1.042±0.256[a]
2 h	0.198±0.001[a]	5.336±0.457[a]	0.241±0.005[a]	1.047±0.351[a]
4 h	0.196±0.003[a]	5.323±0.234[a]	0.238±0.003[a]	1.018±0.235[a]

Values are expressed as mean ± SD, $n = 3$.

2.3.3. Consumption of EPS-LM and LBPS carbohydrate during fecal fermentation

Table 2-2 shows the total carbohydrate contents at selected time points over 48 hours of fecal fermentation inoculated with feces from three donors. **Figure 2-3** shows the trends of total carbohydrate consumption derived from the data shown in **Table 2-2**. In most cases, the total carbohydrate contents of EPS-LM and LBPS decreased rapidly in the initial 12 h

with carbohydrate consumption of ~70% for EPS-LM and 50% for LBPS. Additionally, during 48-hour period, the total carbohydrate content in the fermentation medium of EPS-LM group was lower than that of LBPS group (**Table 2-2**). However, the total carbohydrate consumption with ESP-LM was faster than LBPS (**Figure 2-3**) and the total carbohydrate of EPS-LM was more completely used while that of LPBS was mainly consumed in the initial 4 or 8 h and over 20-40% remained unconsumed at the end. Among the three donor groups, the total carbohydrate consumption of EPS-LM showed a closely similar trend while that of LBPS showed notable variation. Furthermore, EPS-LM and LBPS consumption rate in Donor 1 was slightly faster than in Donor 2 and 3 during the fecal fermentation. It is possible that the gut microbiota in Donor 1 was more abundant with carbohydrate-active enzymes for degrading the polysaccharides. As reported previously, an oat β-glucan was utilized by gut bacteria, leading to an increase in Bacteroidetes levels (J. Bai et al., 2021) and *Bacteroidetes* can encode 137.1 carbohydrate-active enzymes per genome on average (T. Zhang, Yang, Liang, Jiao, & Zhao, 2018). Additionally, *Ruminococcus bromii* can stimulate the cleavage of resistant starch, especially resistant starch type 3 (Ze, Duncan, Louis, & Flint, 2012). In summary, EPS-LM and LBPS was consumed and utilized by the fermentation of fecal microbiota.

Table 2-2. Total carbohydrate content changes in liquid medium with EPS-LM and LBPS during fermentation (mg/mL of liquid medium).

	Donor1		Donor2		Donor3	
Time (h)	EPS-LM	LBPS	EPS-LM	LBPS	EPS-LM	LBPS
0	1.19±0.03^{d}	4.74±0.06^{f}	1.23±0.05^{f}	4.72±0.07^{e}	1.21±0.01^{e}	4.71±0.03^{e}
4	0.43±0.03^{c}	3.49±0.07^{e}	0.72±0.07^{e}	2.35±0.05^{cd}	0.74±0.07^{d}	4.15±0.11^{d}
8	0.18±0.02^{b}	1.53±0.06^{d}	0.52±0.02^{d}	2.47±0.20^{d}	0.54±0.07^{c}	3.67±0.14^{c}
12	0.09±0.01^{a}	1.20±0.03^{c}	0.42±0.05^{c}	2.20±0.05^{bc}	0.36±0.01^{b}	2.38±0.11^{b}
24	0.10±0.02^{a}	1.01±0.04^{b}	0.21±0.02^{b}	2.09±0.14^{b}	0.31±0.02^{b}	2.54±0.15^{b}
48	0.06±0.01^{a}	0.80±0.02^{a}	0.09±0.01^{a}	1.41±0.08^{a}	0.11±0.02^{a}	1.94±0.05^{a}

Note: Different letters a-f indicate significant differences between different total carbohydrate content of EPS-LM or LBPS during fermentation. Data with same letters are insignificant (p>0.05).

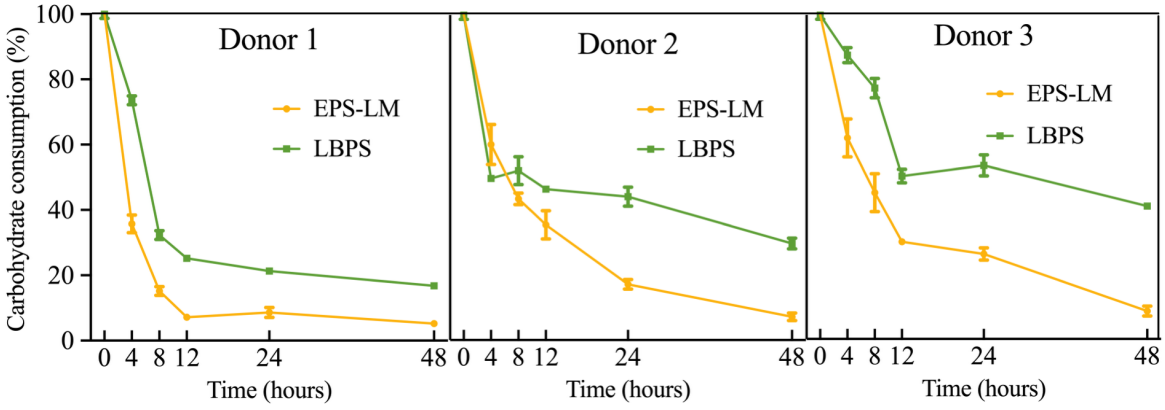

Figure 2-3. Total carbohydrate consumption during fecal fermentation in the liquid medium fed with EPS-LM and LBPS (each date value is expressed as mean ± SD, n = 3, normalized to 100% at 0 h).

2.3.4. Molecular weight reduction of EPS-LM and LBPS during fermentation

Table 2-3 and **Figure 2-4** shows the major MW peaks of EPS-LM and LBPS before fermentation and the liquid medium after 48 hours of fecal fermentation. Before fermentation the GPC spectra showed a few major peaks at relatively shorter retention time (<40 min), corresponding to high MW 5513.1 kDa for EPS-LM and 123.6 kDa for LBPS. As the fermentation time increased, more peaks appeared at longer retention time, indicating the decrease of molecular weight and generation of lower MW fractions. After 48 h fermentation, the MW of fermented EPS-LM was sharply decreased to lower molecular weight. The similar changes occurred to LBPS, from one a single high-MW peak to three low-MW and small peaks. The changes in MW of polysaccharides during fecal fermentation were consistent with those reported previously (G. Ma, Xu, Du, Kimatu, et al., 2022; Y. Ma, Jiang, & Zeng, 2021), indicating the degradation of polysaccharides by fecal fermentation.

Table 2-3. Molecular weight distributions of EPS-LM and LBPS during *in vitro* human fecal fermentation.

Inoculum	Donor	Fermentation time	RT (min)	MW (kDa)	Peak area (%)
EPS-LM	None	0	23.42	5513.1	61.05
			30.27	338.2	38.95
	D1	48	33.22	2.8	63.34
			39.82	0.87	26.05
			43.8	0.43	10.75
	D2	48	33.35	2.2	71.36
			40.3	0.77	28.72
	D3	48	33.17	3.2	68.67
			41.23	0.65	24.18
			43.28	0.42	7.29
LBPS	None	0	31.4	123.6	100
	D1	48	34.96	2.8	52.97
			40.72	0.74	31.25
			46.5	0.23	15.92
	D2	48	32.08	4.1	45.23
			38.8	1.1	38.98
			42.62	0.57	15.94
	D3	48	32.8	2.6	55.04
			40.55	0.86	23.99
			43.85	0.35	12.08

Note: D1, D2, D3 represent Donors 1, 2 and 3.

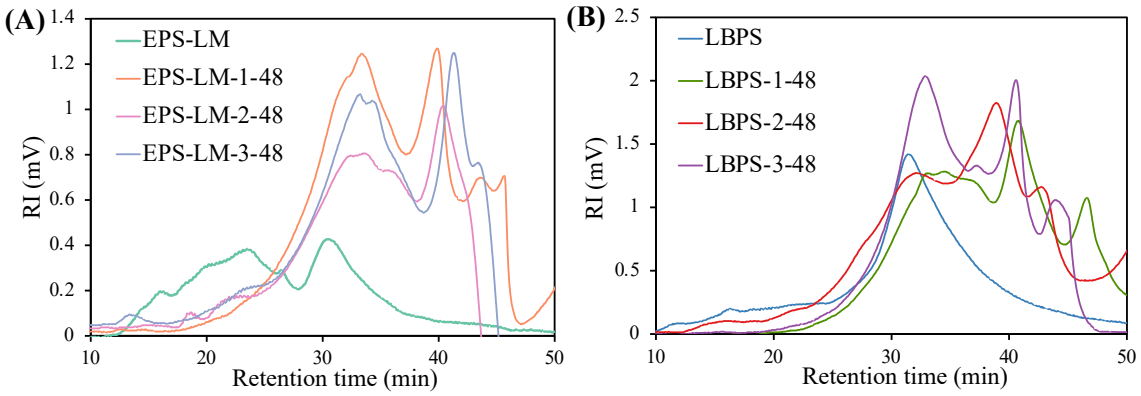

Figure 2-4. Original GPC profiles of EPS-LM (A) and LBPS (B) before and after 48 h fermentation of three donors. 1, 2, 3 mean Donor 1, 2, 3, respectively.

2.3.5. Changes in monosaccharide constituents of EPS-LM and LPBS during fecal fermentation

Figure 2-5 and **Table 2-4** shows the concentration changes of total and individual monosaccharides respectively in the fecal fermentation medium with EPS-LM and LBPS (original HPLC profiles shown in **Figure 2-6**). For all three donors, all the consistent monosaccharides decreased with time over the fermentation period. As seen from **Figure 2-5**, the total monosaccharide decrease with EPS-LM was faster than LBPS (especially within first 4 h), which matched closely with the total carbohydrate consumption (**Figure 2-3**), implying that EPS-LM was more well utilized by the gut bacteria. Among the different constituent monosaccharides of EPS-LM (**Table 2-4**), Man was consumed the most according to its large concentration decrease, from ~1400 μg/mL to ~12.88 μg/mL for Donor1, 31.58 μg/mL for Donor 2 and 48.33 μg/mL for Donor 3, respectively. As for LBPS, Glc was the most significantly consumed and utilized monosaccharide. For both

polysaccharides, the most abundant monosaccharides, Man in EPS-LM and Glc in LBPS, were consumed most significantly. Taken together, these data implied that the consumption of specific monosaccharides by gut bacteria may vary with different polysaccharides.

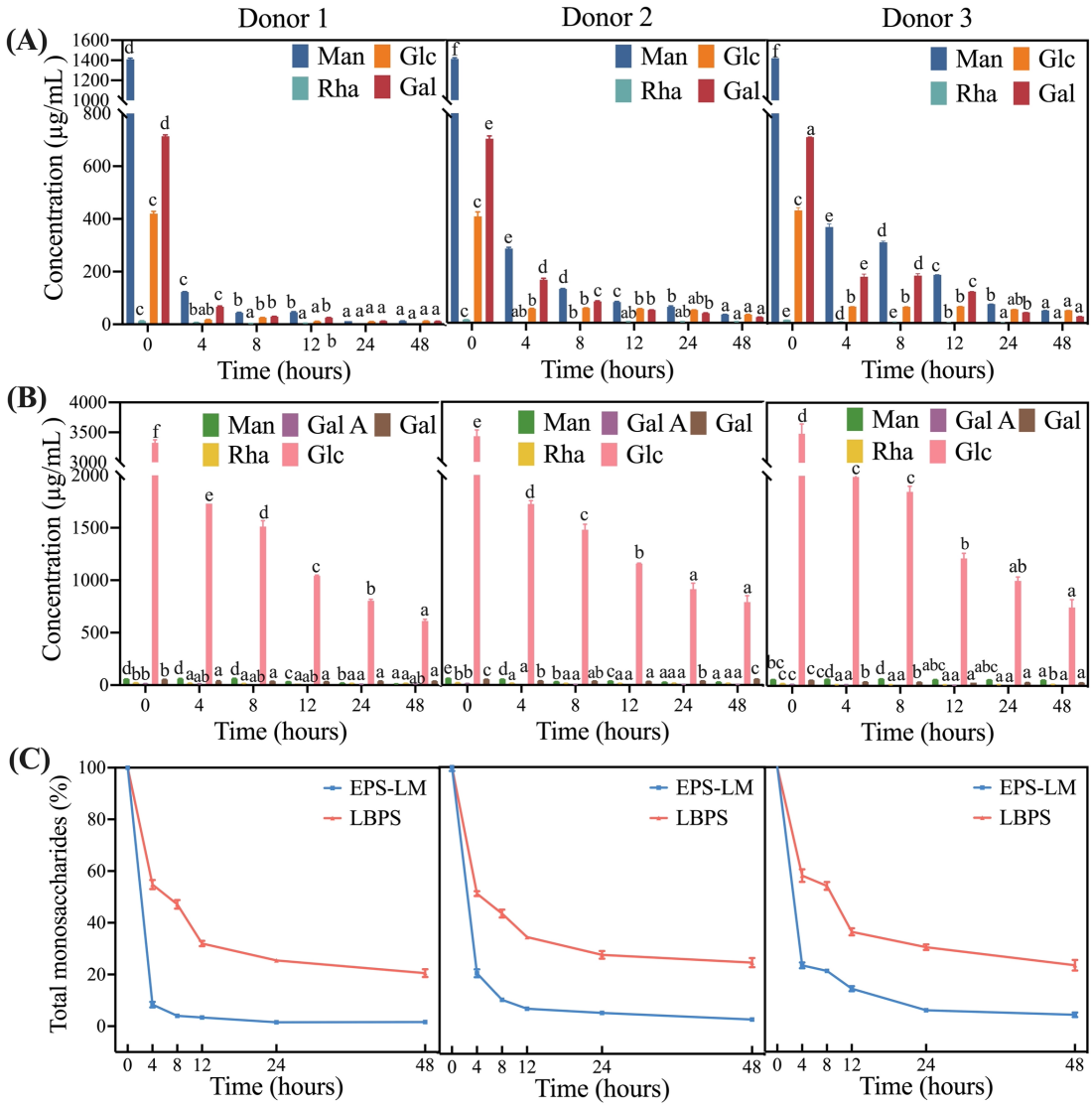

Figure 2-5. Concentration changes (μg/mL) of monosaccharides in the fermentation liquid during *in vitro* fermentation with (A) EPS-LM and (B) LBPS and the changes in (C) total concentration of monosaccharides of EPS-LM and LBPS (each date value is expressed as mean ± SD, n = 3, normalized to 100% at 0 h).

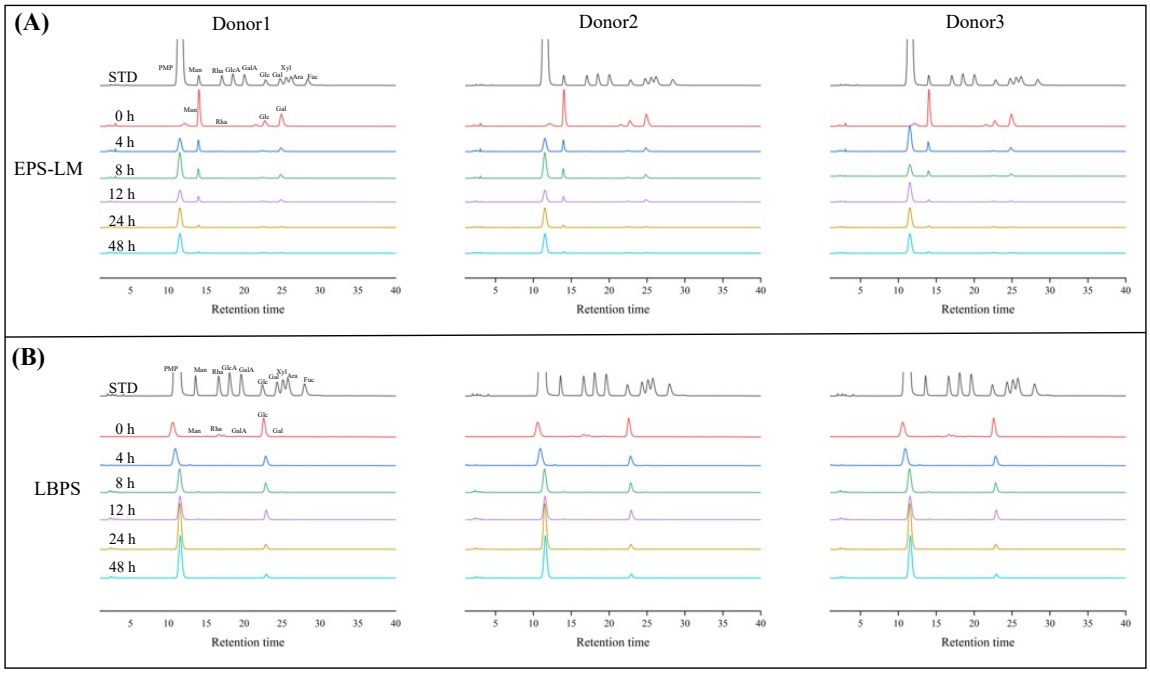

Figure 2-6. HPLC profiles of monosaccharides of EPS-LM (A) and LBPS (B) before and after 48 h fermentation of three donor.

Table 2-4. Concentration changes of monosaccharides in fermentation liquid with EPS-LM and LBPS during *in vitro* fermentations (μg/mL).

	Time (h)	EPS-LM				LBPS				
		Man	Rha	Glc	Gal	Man	Rha	GalA	Glc	Gal
D1	0	1409.90±11.72^{d}	11.63±0.65^{c}	419.94±8.71^{c}	713.59±5.50^{d}	57.64±1.69^{d}	23.22±0.59^{b}	13.76±1.05^{b}	3325.45±49.74^{f}	52.76±2.47^{b}
	4	122.60±1.48^{c}	6.26±0.61^{b}	17.17±1.18^{ab}	66.59±2.96^{c}	59.83±4.02^{d}	17.25±2.72^{a}	10.27±3.20^{ab}	1756.76±28.16^{e}	36.48±6.51^{a}
	8	43.88±1.58^{b}	3.01±0.13^{a}	25.63±0.32^{b}	29.36±0.84^{b}	61.46±4.02^{d}	15.16±0.40^{a}	11.15±0.32^{ab}	1512.24±55.03^{d}	36.59±1.14^{a}
	12	45.88±2.30^{b}	3.70±0.28^{a}	11.23±0.63^{a}	24.99±1.06^{b}	33.62±0.68^{c}	14.79±0.30^{a}	11.15±0.25^{ab}	1042.32±6.46^{c}	32.97±0.9^{a}
	24	12.19±0.14^{a}	3.62±0.08^{a}	10.37±0.20^{a}	12.57±0.16^{a}	19.80±1.29^{b}	16.25±0.82^{a}	8.62±0.26^{a}	803.68±14.52^{b}	35.99±3.94^{a}
	48	12.88±0.44^{a}	3.66±0.13^{a}	12.89±0.48^{a}	11.78±0.56^{a}	12.01±0.24^{a}	17.97±0.68^{a}	10.54±0.54^{ab}	611.18±17.19^{a}	37.93±0.48^{a}
D2	0	1413.95±11.19^{f}	12.07±0.15^{c}	406.01±17.64^{c}	702.79±10.55^{e}	63.91±1.56^{e}	22.44±0.65^{b}	13.63±1.29^{b}	3427.09±106.3^{e}	54.05±1.36^{c}
	4	283.11±4.92^{e}	4.58±0.15^{ab}	53.60±1.50^{b}	164.30±5.57^{d}	56.18±0.99^{d}	16.97±1.68^{a}	6.57±0.52^{a}	1723.19±32.48^{d}	39.97±0.82^{b}
	8	129.23±1.52^{d}	4.65±0.09^{b}	56.84±0.34^{b}	81.71±2.21^{c}	31.53±0.81^{b}	15.79±0.43^{a}	5.86±0.13^{a}	1478.57±51.64^{c}	37.36±1.94^{ab}
	12	79.10±2.53^{c}	4.31±0.08^{ab}	53.38±0.67^{b}	48.90±0.46^{b}	38.26±1.16^{c}	14.77±1.02^{a}	5.12±0.16^{a}	1155.4±4.7^{b}	33.98±1.71^{a}
	24	61.13±3.33^{b}	4.32±0.19^{ab}	49.22±0.43^{ab}	36.45±1.40^{b}	26.98±0.56^{a}	16.58±2.47^{a}	5.58±0.47^{a}	913.17±56.37^{a}	39.66±0.48^{b}
	48	31.58±0.80^{a}	4.22±0.16^{a}	31.10±1.14^{a}	21.71±0.65^{a}	28.21±1.09^{a}	16.66±1.01^{a}	6.13±0.25^{a}	789.04±61.78^{a}	56.63±1.06^{c}
D3	0	1423.17±13.01^{f}	11.96±0.24^{e}	430.25±10.49^{c}	709.37±1.64^{a}	60.51±1.46^{bc}	22.24±0.92^{c}	14.41±0.81^{c}	3483.92±163.83^{d}	52.59±1.06^{c}
	4	366.33±11.69^{e}	5.78±0.15^{d}	62.68±0.85^{b}	176.57±10.11^{e}	63.04±0.47^{cd}	11.68±0.65^{a}	11.86±0.31^{a}	1989.31±88.5^{c}	36.26±1.12^{b}
	8	308.36±4.27^{d}	4.34±0.12^{c}	61.99±0.79^{b}	180.95±6.98^{d}	66.02±2.07^{d}	11.55±0.7^{a}	5.77±0.19^{a}	1847.73±54.19^{c}	34.5±0.92^{b}
	12	183.90±0.93^{c}	3.44±0.18^{b}	63.45±1.01^{b}	119.90±0.71^{c}	59.38±1.66^{abc}	10.85±0.17^{a}	6±0.07^{a}	1214.52±48.72^{b}	30.69±0.26^{a}
	24	72.64±0.63^{b}	2.33±0.13^{a}	52.36±0.57^{ab}	40.81±0.65^{b}	57.92±1.37^{abc}	11.98±0.25^{a}	5.35±0.22^{a}	1000.02±37.44^{ab}	30.63±1.21^{a}
	48	48.23±0.89^{a}	2.05±0.05^{a}	48.65±0.60^{a}	25.26±0.91^{a}	55.89±0.32^{a}	14.55±0.44^{b}	5.86±0.1^{a}	746.29±75.59^{a}	28.93±0.41^{a}

Note: D1, D2, D3 represent Donor1, 2, 3; data values expressed as mean ± SD, n = 3 and different letters a-f indicate significant differences.

2.3.6. Medium pH reduction and SCFA production

Acid production arising from fermentative metabolism of carbohydrates by gut bacteria can be easily detected by measurement of pH change in the fermentation liquid. **Figure 2-7A** presented the pH changes in the fecal fermentation liquid supplemented with EPS-LM, LBPS and FOS after 0, 4, 8, 12, 24 and 48 h fermentation. For all three donors, the pH level showed a rapid decrease in the first 4-8 h and a slow or no change in the remaining period, which were consistent with the trends of total carbohydrate and total monosaccharide (**Figure 2-3 and Figure 2-5**). Among the three carbohydrate groups, the FOS group showed the most significant pH drop, followed by the LBPS group and then the EPS-LM group, which may be correlated with molecular weight. Lower molecular weight polysaccharides can be more readily utilized by gut microbiota to produce more acids (Q.-Y. Li et al., 2022). Besides, as a putative prebiotic oligosaccharide, FOS was well fermented by the gut bacteria to produce SCFAs. In addition, the initial pH of each group in Donor 2 and Donor 3 was similar, but in Donor 1 the initial pH was higher, which may have an adverse effect on the proliferation of some microbial populations (Ilhan, Marcus, Kang, Rittmann, & Krajmalnik-Brown, 2017).

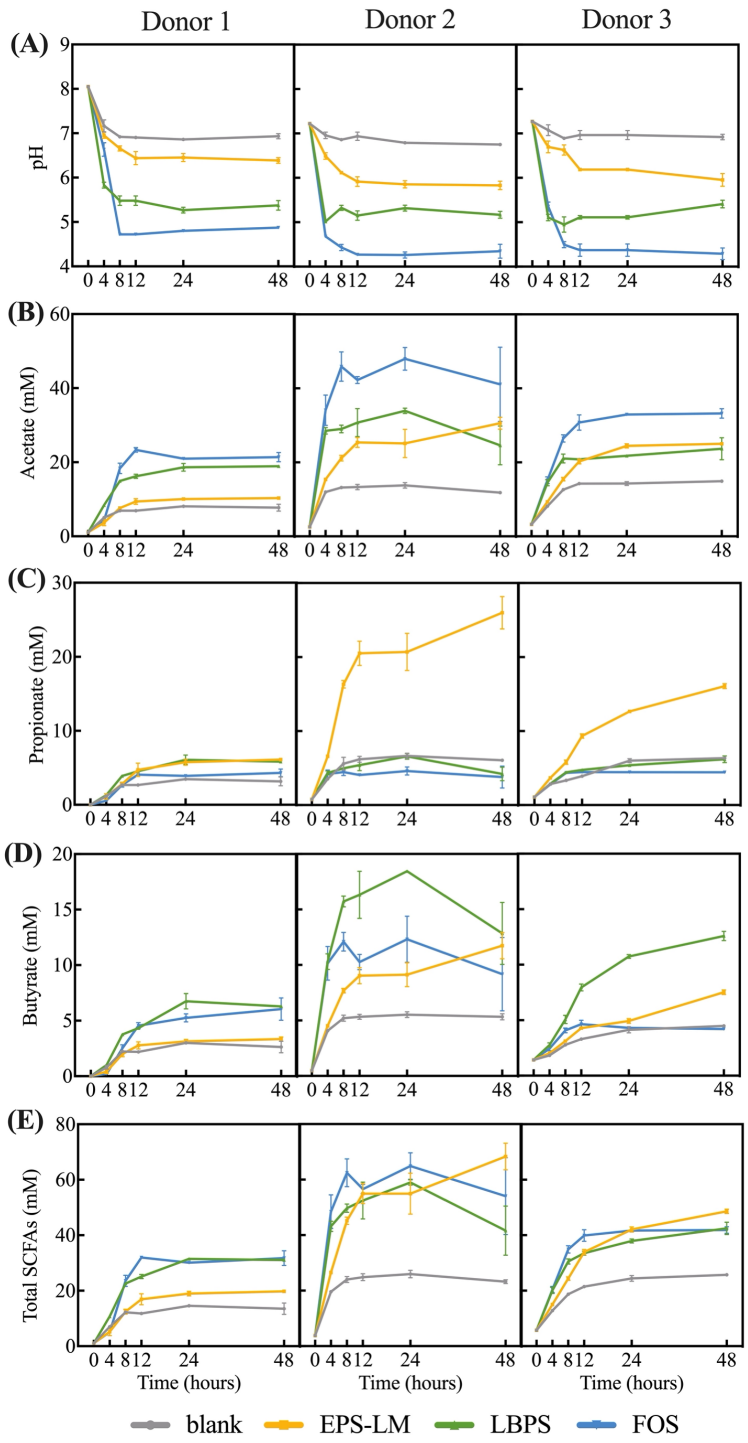

Figure 2-7. Medium pH change and SCFAs production during fecal fermentation with different carbohydrate sources and no carbohydrate nutrient in the blank.

Non-digestible polysaccharides can be fermented and consumed as carbon sources by the gut bacteria to produce SCFAs, including acetic, propionic and butyric acid (Q. Song et al., 2021). **Figure 2-7B-E** and **Table 2-5** shows the concentration changes of acetic, propionic, butyric acid and their total during fecal fermentation in medium supplemented with EPS-LM, LBPS and FOS, respectively. Overall, the total SCFA concentration of EPS-LM, LBPS and FOS group as well as the blank control increased rapidly within the first 12 h of fermentation and increased slightly afterwards. In the blank control group without any carbohydrate, the increased total SCFAs level was probably attributed to the protein degradation by putrefactive bacteria existing in the intestinal environment (Hartemink, Schoustra, & Rombouts, 1999).

Table 2-5. pH value and SCFA productions by human fecal microbiota from *in vitro* fermentations at 48 h.

	Sample	pH	Acetic acid (mM)	Propionic acid (mM)	Butyric acid (mM)	Total (mM)
D1	blank	6.93±0.06^{d}	7.73±0.94^{a}	3.16±0.61^{a}	2.62±0.53^{a}	13.51±2.06^{a}
	EPS-LM	6.39±0.06^{c}	10.31±0.11^{b}	6.11±0.23^{c}	3.34±0.19^{a}	19.74±0.31^{b}
	LBPS	5.37±0.11^{b}	18.92±0.14^{c}	5.83±0.09^{c}	6.28±0.03^{b}	31.04±0.08^{c}
	FOS	4.87±0.03^{a}	21.39±1.25^{d}	4.31±0.52^{b}	6.04±1.01^{b}	31.75±2.65^{c}
D2	blank	6.75±0.02^{d}	11.83±0.31^{a}	6.05±0.21^{a}	5.33±0.28^{a}	23.22±0.67^{a}
	EPS-LM	5.83±0.11^{c}	30.57±1.61^{bc}	25.97±2.18^{b}	11.73±1.18^{b}	68.28±4.82^{c}
	LBPS	5.17±0.08^{b}	24.58±5.22^{ab}	4.21±0.91^{a}	12.84±2.79^{b}	41.62±8.84^{ab}
	FOS	4.35±0.16^{a}	41.09±10.04^{c}	3.78±1.48^{a}	9.17±3.31^{ab}	54.04±13.86^{bc}
D3	blank	6.92±0.06^{d}	14.91±0.17^{a}	6.34±0.09^{b}	4.48±0.09^{a}	25.73±0.24^{a}
	EPS-LM	5.95±0.14^{c}	24.99±0.36^{b}	16.08±0.33^{c}	7.51±0.21^{b}	48.58±0.78^{c}
	LBPS	5.41±0.09^{b}	23.67±2.96^{b}	6.19±0.45^{b}	12.58±0.42^{c}	42.45±2.21^{b}
	FOS	4.29±0.13^{a}	33.21±1.27^{c}	4.44±0.18^{a}	4.21±0.06^{a}	41.84±1.17^{b}

Values are expressed as mean ± SD (n = 3). D1, D2, D3 represent Donor1, 2, 3.

Acetic acid is usually the most abundant component accounting for at least half of the total SCFAs produced by gut microbial fermentation (Louis, Scott, Duncan, & Flint, 2007).

Among the three donors, there were notable differences in the production levels of total SCFA and the three SCFAs. Nevertheless, in all three donors, the highest acetic acid was attained in FOS group, the highest butyric acid in LBPS group and the highest propionic acid in EPS-LM group after 48 h fermentation. The differences in the level of propionic acid and butyric acid with EPS-LM and LBPS may be related to the different structural characteristics. This may suggest that EPS-LM could selectively promote the growth of propionate-producing bacteria whereas LBPS favored the growth of butyrate-producing bacteria. The stimulated production of propionic acid and butyric acid by EPS-LM and LBPS group may be more important for improving human health as acetic acid can be produced at a high level by gut bacterial fermentation of any other dietary fibers.

2.3.7. Effect of EPS-LM and LBPS fermentation on α- and β-diversity of fecal microbial community

The effect of EPS-LM and LBPS on the microbiota composition can be drawn from the results of α- and β-diversity analysis as shown in **Figure 2-8** and **Figure 2-9**. As for the α-diversity, the major factors of interest usually include richness (the number of a given microbial species or group), evenness (the relative abundance) and dominance (the dominant degree of some species) with Chao1 presenting species richness and Shannon and Simpson index evenness (Gao, Sun, Zhang, Hu, & Li, 2022). In general, the α-diversity level of EPS-LM and LBPS group varied considerably among the three donors because of differences in the fecal microbiota. According to **Figure 2-8A**, the Chao1 levels of EPS-LM and LBPS group were very similar, but notably higher than that of FOS group. In addition, Shannon and Simpson index were different among three donor groups, especially in between Donor 2 and 3. Furthermore, EPS-LM treatment with Donor 2 and 3 had

significantly higher dominance, implying that after 48 h fermentation, some beneficial bacteria were dominant, and suppressed the growth some harmful gut bacteria. Principal component analysis (PCA) was performed to reflect the difference among different intestinal flora (R. Dong et al., 2021) as shown in **Figure 2-9**. Overall, the initial composition of fecal microbiota as well as that after 48 h fermentation showed notable differences among three donors, due probably to their different gut environments. Furthermore, for each donor, the microbial composition was also significantly different between the EPS-LM and LBPS group after fermentation. These results indicated that EPS-LM and LBPS with different structural characteristics affected the gut microbial diversity differently.

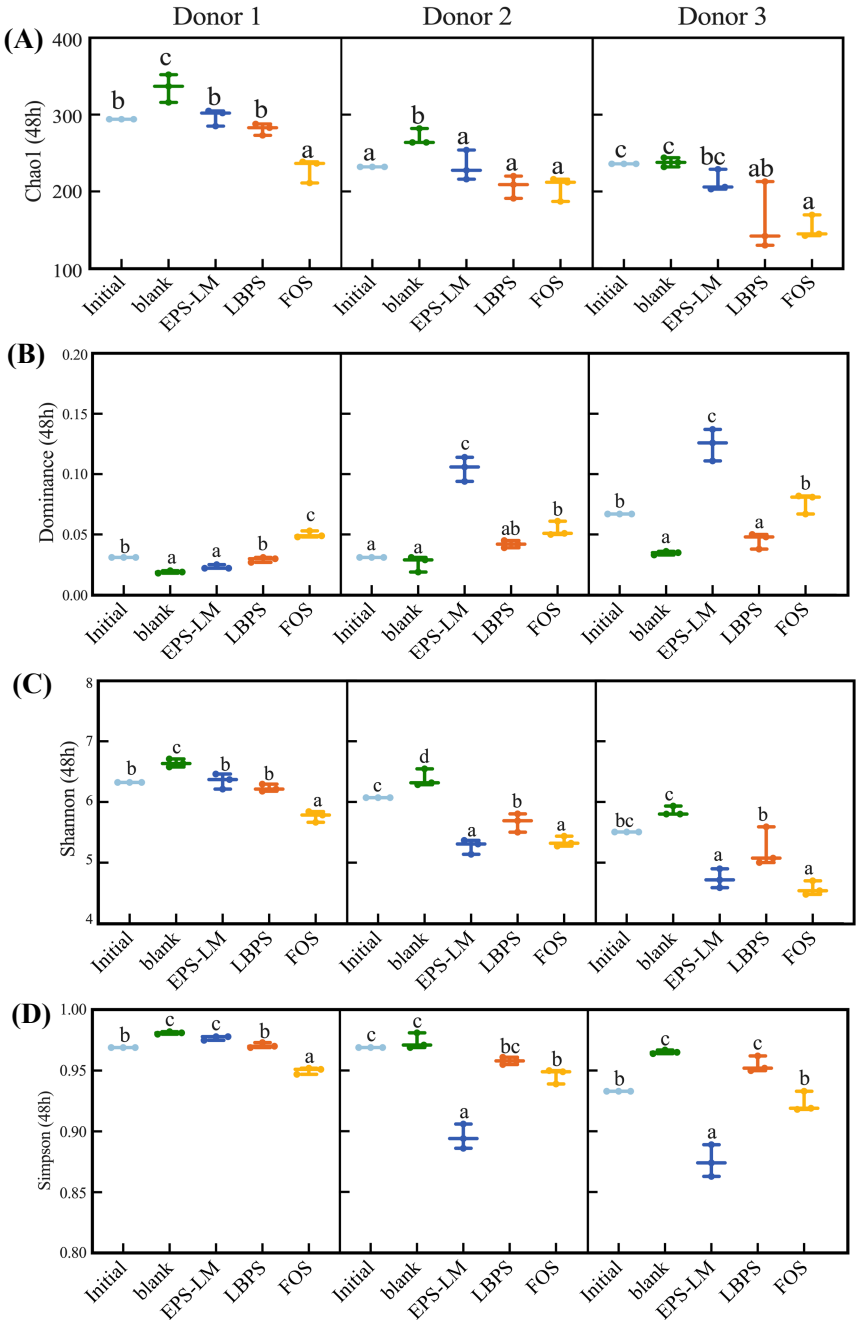

Figure 2-8. α-Diversity analysis of fecal microbial communities throughout *in vitro* fecal fermentation for 24 h of all the donors with different indexes including (A) Chao1, (B) Dominance, (C) Shannon, (D) Simpson. Statistically significant differences comparing the methods were calculated using a Tukey's multiple comparison test, $p < 0.05$.

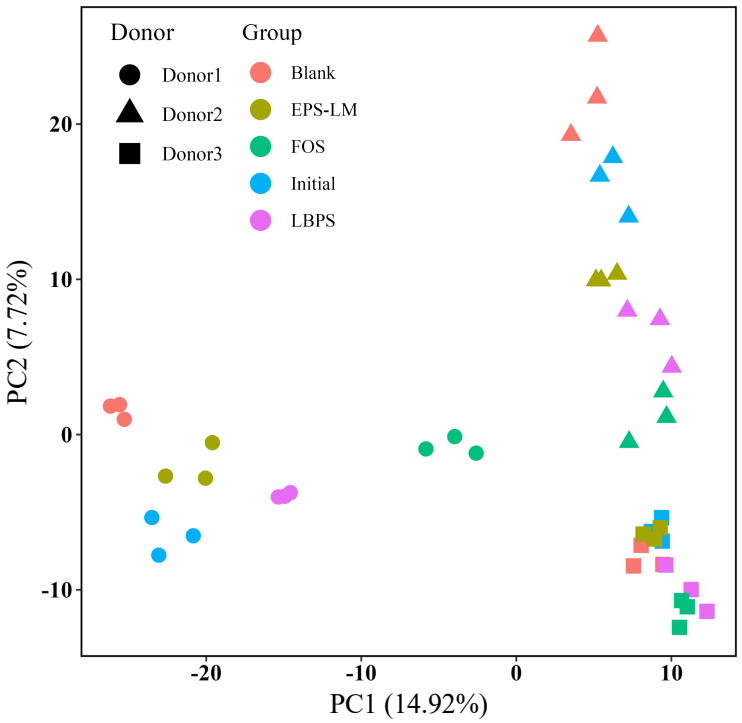

Figure 2-9. β-diversity analysis of fecal microbial communities using principal component analysis (PCA) of fecal microbial communities based on the relative abundances of OTUs at a 97% similarity level.

2.3.8. Effect of EPS-LM and LBPS fermentation on gut microbiota composition

Figure 2-10 shows the spectra of microbiota composition among different donors and carbohydrate groups at phylum and genus level. The initial microbiota showed significance differences among the three donors, such as a higher abundance of *Proteobacteria* in Donor 3 and higher abundance of *Parabacteroides* in Donor 1. At the phylum level (**Figure 2-10A**), the gut microbiota mainly consisted of *Firmicutes*, *Bacteroidetes*, *Actinobacteria*, *Proteobacteria*, *Fusobacteria* and *Verrucomicrobia*, among them *Firmicutes* and *Bacteroidetes*, accounting for 90% (Arumugam et al., 2011; Rinninella et al., 2019). In

general, EPS-LM, LBPS and FOS group showed varied abundance of bacteria for each donor. For example, the levels of *Actinobacteria* with LBPS for Donor 1 and FOS for Donor 3 were up-regulated, which are important in the gut homeostasis maintenance, gastrointestinal and systemic diseases (Binda et al., 2018). Interestingly, all three donor groups, exhibited similar community responses to EPS-LM treatment, especially for the level of *Firmicutes* and *Bacteroidetes* (shown in **Figure 2-10C**). The ratios of *Firmicutes* to *Bacteroidetes* (F/B ratio) of EPS-LM and LBPS group were opposite. F/B ratio is thought to be closely related with obesity as shown by a previous study that genetically obese mice had a higher F/B ratio than lean mice (Ley et al., 2005). At the genus level in **Figure 2-10B**, the relative abundance of bacteria composition was significantly different between EPS-LM and LBPS group. For example, the relative abundance of *Bacteroides*, *Parabacteroides*, *Phascolarctobacterium* treated by EPS-LM group were higher whereas the relative abundance of *Bacteroides*, *Faecalibacterium*, *Blautia*, *Fusicatenibacter* by LBPS group were higher. These species have been suggested to provide many beneficial functions on gut health, e.g. *Parabacteroides* which may be a beneficial species for maintaining the intestinal barrier function (G. Y. Koh, Kane, Wu, & Crott, 2020). Noticeably, although the initial composition of microbiota was quietly different, the gut microbiota of all three donors exhibited similar responses to EPS-LM treatment such as an increase abundance of *Bacteroidetes*, *Parabacteroides* and *Phascolarctobacterium*. EPS-LM seemed to have a strong effect to overcome the gut composition heterogeneity, promote the same beneficial bacteria, and produce the similar components of SCFAs. Compared with FOS and LBPS group, EPS-LM had more consistent effect on gut microbiota. Similar results have also reported that gut microbiota can be alternatively

selected by different structures of Resistant starch type 3 (RS3s) (F. Gu, Li, Hamaker, Gilbert, & Zhang, 2020).

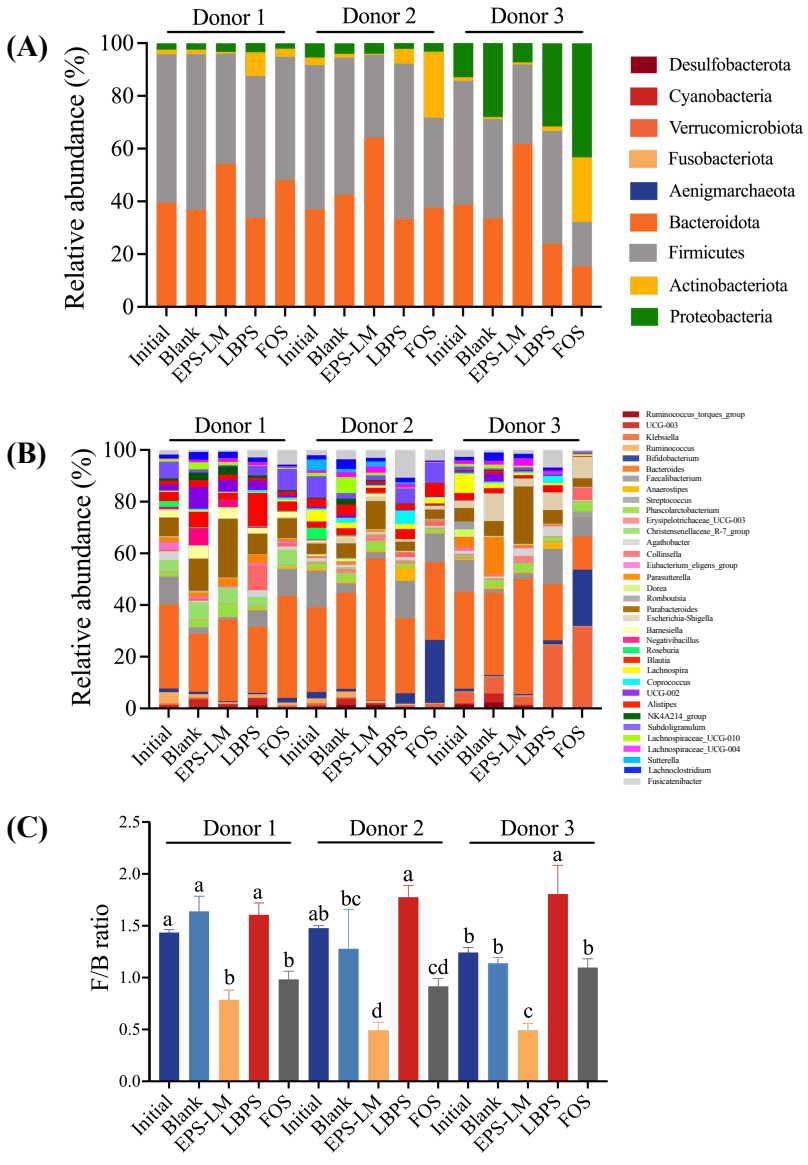

Figure 2-10. Comparisons of different groups on gut microbial composition. Bacterial taxonomic profiling at the (A) phylum level and (B) genus level; (C) The ratio of *Firmicutes* to *Bacteroidetes*.

In the intestinal environment, non-digestible polysaccharides can be utilized and consumed as an essential carbon source by gut bacteria in a way closely dependent on the structural characteristics. It was evident that the glycosidic bonds of polysaccharides could be broken down by the fecal microbiota to lower MW fragments and monosaccharides, and converted into metabolic products (Holscher, 2017). Our results showed that during 48 h fermentation, the total carbohydrate content, molecular weight and monosaccharides content of EPS-LM and LBPS all showed substantial reduction. The fermentative metabolism of polysaccharides by the gut bacteria resulted in increased production of SCFAs and alterations of gut microbiota composition. It has been reported that *Bacteroidetes*, as propionate-producing bacteria, can promote the production of propionic acid through succinate pathway (Reichardt et al., 2014) while *Faecalibacterium* has been recognized as main butyrate-producing bacteria (Kircher et al., 2022). The relative higher levels of SCFAs with LBPS may be attributed to the higher total carbohydrate content of LBPS than EPS-LM. Moreover, the difference in monosaccharide composition between EPS-LM and LBPS may be a major factor on different production levels of SCFAs. For example, it has been suggested that mannan polysaccharides had higher level of propionic acid (Jing Wang, Ke, Strappe, Ning, & Zhou, 2023). The phylum *Bacteroidetes* and genera *Bacteroides*, *Parabacteroides* and *Phascolarctobacterium* in EPS-LM treatment group had a significantly higher abundance than other groups, providing the degradation enzymes for degrading polysaccharide and producing propionic acid and other beneficial metabolites in the human gut (F. Wu et al., 2017; X. Xu, Xu, Ma, Tang, & Zhang, 2013). In addition, EPS-LM reduced F/B ratio more significantly than LBPS. Previous studies have shown that LBPS had significant anti-obesity effects together with the alternation of the

abundance of *Firmicutes* and *Bacteroidetes* in high-fat diet induced mice model (Y. Yang et al., 2021). Therefore, the significant suppression of the F/B ratio by EPS-LM may suggest its potential function for body weight management as well as or better than the LEPS. Moreover, the detailed or specific structural characteristics of polysaccharides such a α- or β-configuration, glycosidic linkage type, and the structure and position of side chain may also affect their metabolism in the gut microbiota and the gut microbial composition (Bie, Duan, Meng, Guo, & Wang, 2021; Yaşar et al., 2024). Similarly the relative richness of *Phascolarctobacterium* has been reported to be positively associated with the mannose and glucose content of polysaccharides derived from *Grifola frondose* fungus (G. Bai et al., 2024). Polysaccharides with α-configurations, such as α-(1→3) glucans has been shown to enrich beneficial gut bacteria, such as *Prevotella* spp., a propionic acid producer (Sajnaga et al., 2023). However, the relationship between the effects on the gut microbiota and the structural characteristics is still too complicated to define.

2.4. Conclusions

As the representative bioactive polysaccharides from two valuable and well-known medicinal fungus or plant, EPS-LM and LBPS have differences in chemical composition and molecular properties. However, they showed some similar changes and effects during simulated gastrointestinal digestion and human fecal fermentation. Both EPS-LM and LBPS were resistant to enzyme and acid hydrolysis in the upper GIT. They were mainly consumed by gut bacterial fermentation in the large intestine. Nevertheless, there were notable differences in the selective consumption of monosaccharides, production of short chain fatty acids and modulation of gut microbial populations between the two polysaccharides during *in vitro* human fecal fermentation, which may lead to different

effects on the host health. Notably, the monosaccharide composition of EPS-LM and LBPS plays a crucial role in their metabolic impact on gut microbiota. It is interesting that the monosaccharide composition, instead of the molecular weight, of the polysaccharides appeared to be a significant factor for their different metabolic outcomes in the gut microbiota. For example, the mannose-rich EPS-LM resulted in a higher level of propionic acid and the glucose-rich LPBS a higher level of butyric acid, while FOS produced more acetic acid. The two polysaccharides also affected the microbiota composition differently, particularly the relative abundance of gut bacterial populations such as EPS-LM significantly decreasing the ratio of *Firmicutes* to *Bacteroidetes* in human feces. The initial differences in the microbiota composition among the different human fecal donors only had subtle and minor influence on the results. Our findings also provided a theoretical basis for the prebiotic effects of EPS-LM and its potential application in functional food products. Further research is still needed to investigate the metabolic pathways for fermentative metabolism of the polysaccharides and the relationship to their molecular properties.

Chapter 3 Human fecal fermentation of high/low-molecular weight EPS from Cs-HK1 and anti-inflammatory protection on gut barrier function

3.1 Introduction

The gut barrier integrity is crucial for maintaining gut health and providing strong protection against harmful antigens and microorganisms (Celebi Sozener et al., 2022). However, existing pharmacological interventions often present significant side effects and lack specificity, it is necessary to develop safe and effective alternative therapies. Gut microbiota plays a critical role in maintaining the integrity and function of the gut barrier. Consisting of over 1000 species, the composition of the gut microbiota is closely associated with intestinal barrier function and the development of various diseases, while certain phyla, such as Firmicutes, Bacteroidetes, Actinobacteria, Proteobacteria, and Verrucomicrobia, are of particular significance (Celebi Sozener et al., 2022). For instance, *Bifidobacteria* species are known to influence multiple protein kinase signaling pathways, which subsequently induce the phosphorylation of tight junction (TJ) proteins. Such phosphorylation events can facilitate the formation of TJs, as well as their redistribution and stabilization within the cellular complex (Hsieh et al., 2015; Xiang, Peng, Du, & Wei, 2016). Similarly, *Faecalibacterium prausnitzii*, a prominent member of the Firmicutes phylum, exerts anti-inflammatory effects by producing SCFAs, such as butyrate that supports intestinal epithelial health (Lenoir et al., 2020). The metabolic byproducts of gut microbiota such as SCFAs, bile acids, and tryptophan metabolites play a vital role in modulating the intestinal barrier function (Ghosh, Whitley, Haribabu, & Jala, 2021). In particular, SCFAs including acetic, propionic, and butyric acid, serve as the primary energy sources for colonocytes and also exhibit anti-pathogenic properties by lowering luminal pH.

Recently considerable research effort has been devoted to the prebiotic functions of natural polysaccharides from various sources on the gut microbiota and their beneficial contributions to human health (Goushki et al., 2025; Ho Do, Seo, & Park, 2021; Y. Yu et al., 2018). As the human genome does not encode digestive enzymes for breaking down polysaccharides, most natural polysaccharides are indigestible in the stomach or small intestine (Kaoutari, Armougom, Gordon, Raoult, & Henrissat, 2013). Instead, these polysaccharides are fermented in the colon by gut microbiota that is equipped with a diverse array of carbohydrate-active enzymes (CAZymes), such as glycoside hydrolases and polysaccharide lyases (Wardman, Bains, Rahfeld, & Withers, 2022). During fermentation, the polysaccharides can be can be degraded and utilized as a carbon source by the gut bacteria, yielding beneficial metabolite products such as SCFAs. On the other hand, the fermentative metabolism of polysaccharides may modulate the composition and relative abundance of microbial populations in the gut microbiota, contributing to improved host health and reduced metabolic diseases.

The structure characteristics of natural polysaccharides, such as molecular weight, monosaccharide composition, and glycosidic linkage patterns are key factors for their effects on the gut microbiota. Among the natural polysaccharides from various sources, those from edible and medicinal fungi have attracted wide attention due to their notable bioactivities and abundant contents. The Chinese caterpillar fungus, *C. sinensis*, is a well-known edible and medicinal fungus. As natural Chinese caterpillar fungus is rare and expensive, mycelial fermentation is an efficient and economical process for production of fungal biomass and polysaccharides. Cs-HK1 is a C. sinensis fungus and has been applied to mycelial fermentation for production of bioactive EPS (P. Leung, Q. Zhang, & J. Wu, 2006). The EPS has a wide molecular weight MW range and is composed primarily of mannose, glucose, and galactose, which have been shown to affect their prebiotic effects and anti-inflammatory activities (L.-Q.

Li et al., 2021; Mao et al., 2020; A.-X. Song et al., 2019). It is of significance to further assess the properties and activities of the fermentation products of EPS in human gut microbiota.

The present study was to further examine the prebiotic properties of two different EPS fractions and the gut barrier protective effects of their fermentation products through simulated human gastrointestinal digestion and gut microbial fermentation. It was hypothesized that the EPS fractions are resistant to the digestive enzymes and gastric acid in the upper gastrointestinal tract but can be well fermented, and utilized as a carbon source by the gut microbiota. The EPS was isolated from the Cs-HK1 fermentation medium and separated into a high- and a low-MW EPS fraction, EPS-HM and EPS-LM with significantly different chemical compositions. Measurements were performed on the degradation and consumption of EPS and resultant SCFAs production and influence on the composition and abundance of microbiota. The fermentation products were assessed for anti-inflammatory protection on gut barrier function using a lipopolysaccharide (LPS)-induced Caco-2/RAW264.7 coculture cell model.

3.2 Materials and methods

3.2.1 Chemicals and reagents

Dextran molecular weight standards (1–670 kDa) were obtained from International Laboratory USA (San Bruno, CA, USA) and pepsin (3,000 U/g), trypsin (250 U/g), and bile salts and Fructooligosaccharide (FOS) from Solarbio (Beijing, China). Gastric lipase (100,000 U/g) and pancreatin (250 U/mg) were acquired from Yuanye (Shanghai, China); monosaccharide standards (Mannose, rhamnose, glucuronic acid, galacturonic acid, glucose, galactose, xylose, arabinose and fucose), trifluoroacetic acid (TFA), acetonitrile (ACN, HPLC grade), methanol (MeOH), lipopolysaccharide (LPS), and phenazine methosulfate (PMS) from Sigma-Aldrich (St. Louis, MO, USA). Dilbecco's modified Eagle's medium (DMEM) and fetal bovine serum (FBS) were from Gibco (Grand Island, NY, USA), and 3-(4,5-

dimethylthiazol-2-yl)-5-(3-carbo3xymethoxyphenyl)-2-(4-sulfophenyl)-2H-tetrazolium (MTS) from Promega (Madison, WI, USA). Other reagents were purchased commercially as analytical grade products.

3.2.2 Cs-HK1 mycelial fermentation and isolation of high- and low-MW EPS fractions

As reported previously, the Cs-HK1 fungus strain was preserved in mycelial culture on solid PDA agar (F. T. Gu, Li, et al., 2025). For EPS production, the Cs-HK1 mycelial stock culture was transferred into a liquid medium, which was composed of 40 g/L glucose, 5 g/L peptone, 1 g/L KH_2PO_4, 0.5 g/L $MgSO_4 \cdot 7H_2O$, and 10 g/L yeast extract. The Cs-HK1 mycelial fermentation was carried out in shake flasks at 250 rpm and 20 °C for 7 days. Then the fermentation liquid was centrifuged at 9,000 rpm for 30 min and the supernatant was collected for EPS isolation by ethanol precipitation. For isolation of higher- and lower-MW EPS separately, the ethanol precipitated was performed in two steps, using 40 % (v/v) ethanol in the first step and 80 % (v/v) ethanol in the second step. In the first step, ethanol was gradually added with stirring to the supernatant medium to the desired concentration of 40 % (v/v), and then kept static at 4 °C for 40 min. The solid was then separated from the liquid mixture by centrifugation, deproteinized and collected as EPS-HM. In the second step, ethanol was added to the liquid to a final ethanol concentration of 80 % (v/v) and left at 4 °C overnight. Then the liquid was centrifuged at 9,000 rpm for 30 min to collect the precipitate as EPS-LM. Both EPS fractions were deproteinized by the Sevag method. EPS fractions were mixed with the Sevag reagent (chloroform: n-butanol=4:1) and vortexed vigorously for 20 min. The solutions were then centrifuged at 4,000 rpm for 10 min to collect the EPS-containing supernatant. This procedure was repeated until the protein interphase was absent and the deproteinized EPS fractions were freeze-dried for the following analysis and assessment.

3.2.3 *In vitro* gastrointestinal digestion of EPS fractions

The *in vitro* or simulated human gastrointestinal digestion of EPS fractions was performed as described in section 2.2.3 with some modifications. Samples were taken for further investigation after 0.5, 1, 2 and 4 h of incubation and heated for enzyme inactivation.

3.2.4 *In vitro* human fecal fermentation

The *in vitro* human fecal fermentation of EPS fractions was performed as described in section 2.2.5 with some modifications. The culture tubes were incubated for fecal fermentation for 0, 6, 12, 24 and 48 h and then taken out promptly from the incubator for analysis and activity assessment. The medium pH of each tube was measured with a PHS-3C pH meter (Sanxin Shanghai, China) and then divided into several aliquots. One aliquot was immediately frozen at -80 °C for DNA extraction and the residues were centrifugated (12,000 rpm, 10 min, 4 °C) and the supernatants were collected for further analysis. FOS, a well-known prebiotic fructo-oligosaccharide, was included for comparison with the EPS and the carbohydrate-free medium as the blank control in the fecal fermentation. Carbohydrate-free medium without fermentation was taken as the initial group.

3.2.5 Analysis of the original EPS and the digested/fermented carbohydrates

Total carbohydrate content in the original EPS and fecal fermentation medium was determined by Anthrone test in reference to glucose and total protein content by Lowry method in reference to bovine albumin, as reported previously (F. T. Gu, Li, et al., 2025). The MW profiles of original EPS-LM, EPS-HM and the products after gastrointestinal digestion and fecal fermentation were analyzed as described in section 2.2.7.

The reducing sugars (C_R) in the digestion and fermentation samples were analyzed by DNS method (Miller, 1959), by measurement of absorbance at 550 nm using glucose as the reference.

The constituent monosaccharides in the original EPS and fecal fermentation medium were analyzed as described in 2.2.8.

3.2.6 Analysis of short-chain fatty acids (SCFAs) in fecal fermentation medium

SCFAs were analyzed as described in 2.2.9.

3.2.7 Genomic analysis of fecal microflora

The microbial populations of fecal microflora were analyzed by 16S rRNA gene sequencing. The fermented samples were defrosted on ice and the DNA was extracted from the samples using the Tiangen stool DNA extraction kit (Tiangen, Beijing, China). The extraction protocol was performed according to the manufacturer's instructions. DNA concentrations were measured using a Nanodrop 2000 (ThermoFisher, Massachusetts, USA).

To amplify the V3-V4 region of the 16S rRNA gene, PCR was performed using the extracted DNA. The primers used were 341F (CCTACGGGNGGCWGCAG) and 785R (GACTACHVGGGTATCTAATCC) (Klindworth et al., 2013). The amplified DNA was then sequenced using Illumina MiSeq (Illumina, Inc., San Diego, CA, USA).

The raw sequencing reads were merged, demultiplexed and quality-filtered through QIIME 2.0, and the obtained reads were clustered into Operational Taxonomic Units (OTUs) with 97% distance-based similarity threshold via the Greengenes (version 13_8) database (McDonald et al., 2012). OTU clusters served as the basis for all of the subsequent analysis. Microbial community diversity was assessed through two approaches: α-diversity metrics calculated using Mothur and β-diversity metrics calculated using the Bray-Curtis dissimilarity (Lozupone & Knight, 2005).

3.2.8 Cell culture model for assessment of fecal fermentation products on gut barrier function

3.2.8.1 Cell cultures

Human intestinal epithelium Caco-2 cell line and murine macrophage RAW264.7 cell line were obtained from the American Type Culture Collection (ATCC, Manassas, VA, USA). Both were cultured in Dulbecco's modified Eagle medium (DMEM) supplemented with 10% (v/v) FBS at 37 °C in 5% CO_2 atmosphere. The culture medium was changed every 2 days and the cells used in the experiments were 20-30 generations. Fecal fermentation samples were centrifuged (12,000 rpm, 10min) and the supernatant was collected and filtered through 0.22 μm membrane for the tests.

Cells were seeded in a 96-well plate at 1×10^4 cells/mL and incubated for 24 h to reach the exponential growth phase. The fecal fermentation liquid was added to the wells at selected concentrations (final volume 200 μL in each well) and incubated for another 24 h. Cell viability was measured by the CellTiter 96 Aqueous Assay (Promega, Madison, WI, USA) according to the supplier's instructions. After the incubation, the absorbance was measured at 490 nm using a microplate reader (Thermo Scientific, USA).

3.2.8.2 Establishment of Caco-2/Raw264.7 co-culture model

The Caco-2/RAW264.7 co-culture model was established on 24-well Transwell® plates with a membrane pore size of 0.4 μm (SPLInsert^{TM} Hanging, SPL, Korea). Caco-2 cells were inoculated at 3×10^4 cells/well in the apical chamber of the 24-well plate and incubated for 21 days during which the culture medium was changed every 2 days. RAW264.7 cells were inoculated at 2×10^5 cells/well into 24-well plate and incubated for 24 h. When the trans-epithelial resistance (TEER) value of the Caco-2 cell layer was above 300 $\Omega\cdot cm^2$, read by an EVOM2 Epithelial Voltohmeter (World Precision Instruments Inc, Sarasota, FL, USA), the

Caco-2 cell inserts were transferred into 24-well plate seeded with RAW 264.7 cells. Briefly, the apical chamber contained different concentrations (125 μg/mL and 250 μg/mL) of fecal fermentation samples (no carbon source group, EPS-LM and EPS-HM group). The basolateral side was added with LPS (1 μg/mL) IFN-γ (50 ng/mL) and incubated for 24 h to stimulate RAW 264.7 cells. After 24 h incubation, the TEER value was measured again to assess the permeability of Caco-2 monolayer. Then the cells and medium were collected for the following measurements.

3.2.8.3 NO and IL-1β analysis

The Caco-2/RAW264.7 co-culture liquid was centrifuged (1,000 rpm, 10 min, 4°C) and the supernatant was collected. The NO content was determined by the Griess assay and IL-1β content by Elisa kit according to the manufacturer's instructions.

3.2.8.4 Immunofluorescence analysis of tight junction (TJ) proteins

Two TJ proteins, ZO-1 and Claudin-1, were quantified by immunohistochemistry staining according to the literature (Buckley et al., 2018). The cells were washed twice with pre-cooled PBS and then fixed with 1:1 methanol and acetone at -20 °C for 10 min, and the permeabilized with 0.2% Triton X-100 in PBS for 15 min. This was followed by treatment with blocking PBS solution containing 5% goat serum, 5% FBS and 2% bovine serum albumin (BSA) for 1 h. The cells were then incubated with primary antibodies (rabbit ZO-1, and mouse Claudin-1 antibodies) at 4 °C overnight, followed by treatment with secondary antibodies and 4′,6-diamidino-2-phenylindole (DAPI) at room temperature for 1 h. The treated cells were examined under a confocal microscope (Leica TCS SPE, Leica, Germany).

3.2.8.5 Quantitative real-time polymerase chain reaction (q-PCR) analysis

Total RNA was extracted from cells by TransZol Up Plus RNA Kit (TransGen Biotech, China) according to the manufacturer's instructions. The cDNA was synthesized using the TransScript® one-step gDNA removal and cDNA synthesis SuperMix (TransGen Biotech, China) according to the manufacturer's protocol. At RT-PCR step, the cDNA was used for quantitative real-time PCR using Taq Pro Universal SYBR qPCR Master Mix (Vazyme, China). The primer sequence of each gene was as follows: GAPDH: GCGCCCAATACGACCAAATC (F) and GACAGTCAGCCGCATCTTCT (R); Claudin-1: CCAGGTACGAATTTGGTCAGG (F) and TGGTGTTGGGTAAGAGGTTGT (R); Occludin: CTTCCAATGGCAAAGTGAATG (F) and TACCACCGCTGCTGTAACGAG (R); ZO-1: GGTGAAGTGAAGACAATG (F) and GGTAATATGGTGAAGTTAGAG (R).

3.2.9 Statistical analysis

Each experiment was run in triplicate and the data were shown as the mean ± standard deviation (SD) using various software packages including SPSS (version 26.0; IBM Inc., Chicago, IL, USA), GraphPad Prism 9 for Mac OS X (GraphPad Software, Inc., La Jolla, CA, US), and RStudio software. To assess statistical significance, a one-way analysis of variance (ANOVA) was performed, followed by Tukey's pairwise comparison at a significance level of $p < 0.05$.

3.3 Results and discussion

3.3.1 Molecular properties of EPS fractions

Table 3-1 shows the composition and molecular weight MW of EPS-LM and EPS-HM. EPS-LM had 70% total carbohydrate, 11% protein and an average MW of 4.55×10^6 Da. EPS-HM had nearly 90% total carbohydrate, only 3% protein content and an MW of 9.48×10^7 Da. EPS-LM has a lower MW than EPS-HM, which suggests that with the ethanol concentration

increasing, extracted EPS has a lower MW. Besides, both EPS fractions were hetero-polysaccharides mainly composed of Man, Glc and Gal and the most abundant monosaccharide was Man in EPS-LM and Glc in EPS-HM, which were generally consistent with the previous results (Mao et al., 2020).

Table 3-1. Chemical composition and molecular weight of EPS-LM and EPS-HM.

	Total carbohydrate (wt%)	Total protein (wt%)	MW (Da)	Monosaccharide molar ratio			
				Man	Rha	Glc	Gal
EPS-LM	70.21±1.23	11.24±0.32	4.55×10^6	72.7	1	12.7	38.6
EPS-HM	89.53±1.35	3.41±0.76	9.48×10^7	1	-	5.3	0.4

Figure 3-1 shows FT-IR spectra of EPS-LM and EPS-HM. Overall, both EPS-LM and EPS-HM had typical bands of carbohydrates, which were from 500-3900 cm^{-1}. The absorption peak near 3400 cm^{-1} was caused by the -OH stretching vibration in the molecular structure indicating the interactions of the PS chains (G. Chen et al., 2021). The band at 2900 cm^{-1} and 1408 cm^{-1} was due to C-H stretching and bending vibration including CH, CH_2 and CH_3 (L. Zhang et al., 2018). The absorption peak at around 1637 cm^{-1} and 1067 cm^{-1} was associated with C=O stretching (S. Yuan et al., 2023). The absorption bands at around 1067 cm^{-1} suggested a pyranose form of the glucosyl residue and a slight peak around 880 cm^{-1} indicated the presence of β-glycosidic bond (G. Chen et al., 2021). On the other hand, EPS-HM has more peaks around 1384 cm^{-1} and 1202 cm^{-1} corresponding to C-OH side group and C-C band stretching vibrations (X. Ma et al., 2016). This suggested a complex structure with various functional groups of EPS-HM.

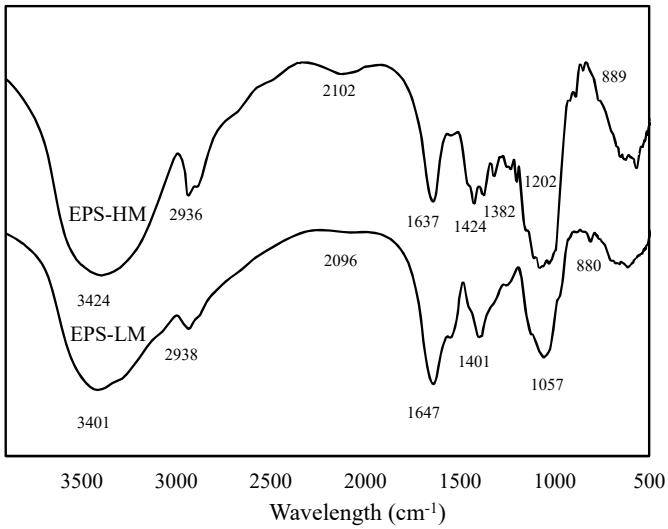

Figure 3-1. FT-IR spectra of EPS-LM and EPS-HM.

3.3.2 Changes of EPS fractions in simulated gastrointestinal digestion

The simulated upper gastrointestinal tract (GIT) includes the saliva, stomach and small intestine, and it aids in the digestion and absorption of food components through enzymes like α-amylase, trypsin, and lipase found in digestive juices (Sensoy, 2021). Growing evidence indicates that polysaccharides cannot be broken down by digestive enzymes (M. Zhang et al., 2025), though some polysaccharides have been shown to be partially degraded in the acidic environment of the stomach. To evaluate the digestive properties of EPS fractions, the reducing sugar content and molecular weight were measured and shown in **Table 3-2**. The reducing sugar content and MW of EPS fractions showed no significant change before and after saliva digestion, indicating negligible amylase degradation of the EPS fractions. Similarly, there was no significant change in the reducing sugar content or molecular weight of EPS fractions during simulated gastric or intestinal digestion. These results indicated that EPS-LM and EPS-HM were highly resistant to the digestive systems without degradation.

Table 3-2. Reducing sugars (C_R) contents and changes of molecular weight during *in vitro* simulated gastrointestinal digestion of EPS-LM and EPS-HM.

	EPS-LM		EPS-HM	
	C_R (mg/mL)	MW (Da)	C_R (mg/mL)	MW (Da)
Saliva				
0 min	0.13±0.03[a]	4.23×10^6(±4.26%)[a]	0.21±0.05[a]	8.84×10^7(±6.55%)[a]
20 min	0.11±0.05[a]	4.46×10^6(±3.47%) [a]	0.18±0.03[a]	9.10×10^7(±5.60%)[a]
Gastric				
0.5 h	0.11±0.10[a]	4.68×10^6(±6.21%)[a]	0.16±0.05[a]	9.55×10^7(±4.68%)[a]
1 h	0.18±0.03[a]	4.50×10^6(±5.58%)[a]	0.26±0.11[a]	9.67×10^7(±6.58%)[a]
2 h	0.11±0.05[a]	4.17×10^6(±4.97%)[a]	0.26±0.05[a]	9.34×10^7(±5.35%)[a]
Small intestinal				
0.5 h	0.09±0.07[a]	4.65×10^6(±6.35%)[a]	0.26±0.05[a]	9.14×10^7(±5.47%)[a]
1 h	0.06±0.05[a]	4.57×10^6(±3.54%)[a]	0.24±0.08[a]	9.84×10^7(±5.49%)[a]
2 h	0.21±0.09[a]	4.98×10^6(±5.98%)[a]	0.28±0.15[a]	9.79×10^7(±5.94%)[a]
4 h	0.18±0.08[a]	4.67×10^6(±4.67%)[a]	0.27±0.10[a]	9.67×10^7(±5.94%)[a]

Values are expressed as mean ± SD, n = 3.

3.3.3 Degradation and consumption of EPS during fecal fermentation

Previous studies have shown that the MW of EPS could affect the degradation rate and products of fecal fermentation (Q.-Y. Li et al., 2022). These degraded fragments are further utilized by the microbiota to produce metabolic products such as SCFAs. As illustrated in **Figure 3-2**, the molecular weight of EPS-LM and EPS-HM fell progressively during *in vitro* fermentation. Within the first 6 h, the molecular weight of EPS-LM and EPS-HM decreased dramatically and additional peaks with lower MW appeared, indicating the degradation of EPS by the fecal fermentation. Notably, the high-MW EPS EPS-HM showed a more rapid degradation than EPS-LM, corresponding to a rapid consumption of the total carbohydrate as shown in **Figure 3-2C**. This indicated a higher susceptibility of high-MW EPS to the fermentation by the intestinal microbiota during the early stages, agreeing with a previous study that blackberry PS with higher molecular weight were more degraded in the initial 4 h (Q.-Y.

Li et al., 2022). These findings highlight the distinct fermentation characteristics of EPS-LM and EPS-HM, suggesting that the initial MW is a significant factor in the fermentation and utilization by gut microorganisms.

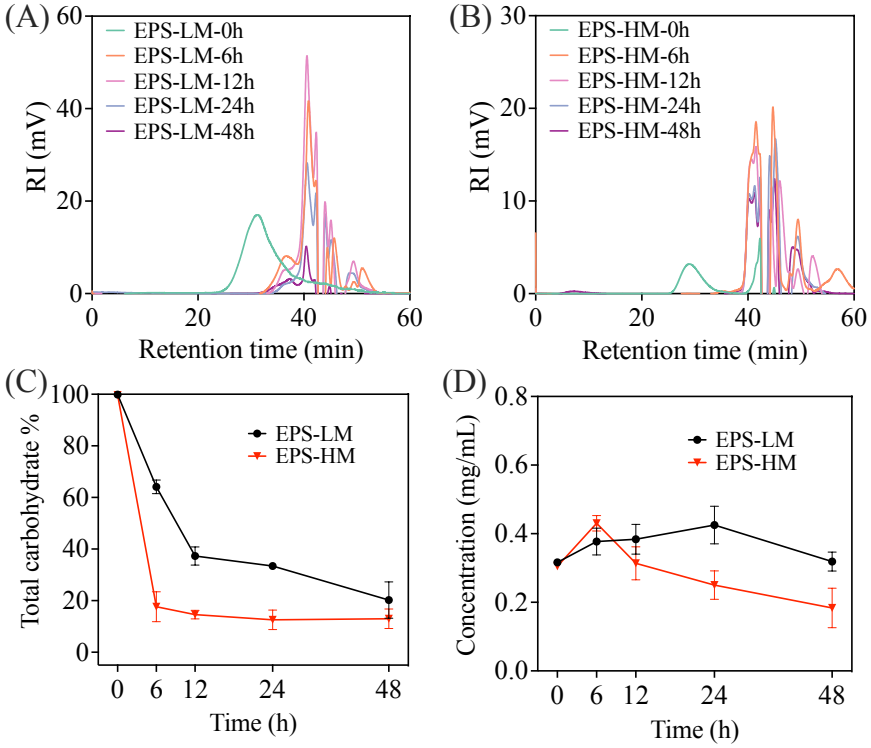

Figure 3-2. Changes in GPC profiles of the EPS MW : (A) EPS-LM and (B) EPS-HM during fecal fermentation; Changes in (C) the total carbohydrate consumption and (D) concentration of reducing sugars during fecal fermentation (n = 3).

With an increase in fermentation time, the consumption of EPS fractions gradually increased. As shown in **Figure 3-2C**, EPS-HM had an 82% total carbohydrate consumption within 6 h, while for EPS-LM, the fermentation rate from 0 to 12 h was faster than that from 12 to 48 h, and gut microbiota utilized EPS-LM gradually and continuously. The different time courses of consumption may be attributed to their differences in the monosaccharide composition. For EPS-HM, glucose accounts for 76.5% of the monosaccharide composition, which agreed with the study that glucose is the most preferred monosaccharide by intestinal flora (Y. Zhao et al., 2024), leading to a rapid depletion of the EPS-HM in less than 6 hours.

Besides, protein is also likely to be fermented and affect the carbohydrate consumption by gut microbiota (C. K. Yao, Muir, & Gibson, 2016).

In addition, as shown in **Figure 3-2D**, the reducing sugars released from EPS-HM remarkably increased to the high content (0.43 mg/mL) after 6 h fermentation and then decreased (to 0.18 mg/mL) with the increasing fermentation time. These changes implied that the glycosidic bonds of EPS-HM were hydrolyzed during fermentation, exposing reducing ends and increasing sugar content (J.-L. Hu, Nie, Min, & Xie, 2013). After 6 h, the consumption rate of reducing sugars by gut microbiota exceeded their release, as they were consumed and utilized as carbon sources by gut microbiota. Similar changes have been reported in other studies, such as polysaccharides from straw mushroom (*Volvariella volvacea*) during fecal fermentation (W. Hu et al., 2023). Besides, for EPS-LM, the reducing sugar content showed an upward during the 24 h fermentation process, from 0.31 to 0.42 mg/mL and then decreased to 0.32 mg/mL. These results revealed that both EPS-HM and EPS-LM could be utilized by gut microbes, exhibiting distinct fermentative properties. EPS-HM was utilized remarkably and rapidly, while EPS-LM was utilized more slowly.

3.3.4 Changes in constituent monosaccharides of EPS

Molar ratios of monosaccharide composition in natural polysaccharides can be altered during fecal fermentation by human colonic microbiota. **Table 3-3** showed the monosaccharide contents changing during fecal fermentation of EPS-LM and EPS-HM (original HPLC profiles of monosaccharides in Supplemental data, **Figure 3-3**). With the increase in the fermentation time, the level of all the monosaccharides showed a decrease. For EPS-LM, the initial composition was dominated by Man (58.2 %) and Gal (30.9 %), with lower levels of Glc (10.2 %) and Rham (0.8 %). Over the period, Man and Gal decreased significantly, with Man dropping from 56.6 % to 29.1 % and Gal from 32.7 % to 7.1 %, indicating substantial utilization by gut microbiota. In contrast, Glc showed the most dramatic increase, rising from 9.9 % to

61.7 %, suggesting slower consumption rates. Rham remained relatively stable, increasing only slightly from 0.8 % to 2.3 %, indicating the least microbial utilization. For EPS-HM, the initial composition was dominated by Glc (79.4 %), with lower levels of Man (15.1 %) and Gal (5.6 %). During fermentation, Glc decreased significantly from 79.4 % to 30.2 %, showing it was the most utilized monosaccharide. Man increased slightly from 15.1 % to 25.8 % and Gal increased substantially from 5.6 % to 44.1 %. This suggests that for EPS-HM, Glc was the primary energy source for gut microbiota. The metabolism of different monosaccharides requires specific enzymes, and these bacteria may encode enzymes that are specifically adapted for the degradation of these monosaccharides (Rodionova et al., 2013). This also suggests that their different fermentation characteristics and the composition of the microbiota.

Table 3-3. Monosaccharide composition (mol%) of original EPS and changes during fecal fermentation from HPLC analysis.

	EPS-LM				EPS-HM		
Time (h)	Man	Rham	Glc	Gal	Man	Glc	Gal
0	58.2±6.1^{c}	0.8±0.1^{a}	10.2±1.2^{a}	30.9±2.9^{c}	15.1±0.1^{a}	79.4±1.7^{c}	5.6±1.2^{a}
6	57.9±26.8^{bc}	1.1±0.2^{a}	15.2±4.1^{a}	25.8±6.9^{c}	19.7±0.2^{a}	63.9±1.1^{bc}	16.3±0.3^{a}
12	53.1±4.7^{bc}	0.9±0.1^{a}	23.7±2.5^{ab}	22.3±1.1^{bc}	18.3±0.4^{a}	44.1±0.2^{ab}	37.7±0.2^{b}
24	46.3±2.8^{b}	2.2±0.1^{a}	35.1±1.4^{b}	16.5±1.6^{b}	15.4±0.1^{a}	38.5±0.2^{ab}	46.1±0.1^{b}
48	29.1±4.2^{a}	2.3±0.1^{a}	61.7±2.1^{c}	7.1±1.8^{a}	25.8±0.3^{a}	30.2±0.1^{a}	44.1±0.2^{b}

Values are expressed as mean ± SD, n = 3.

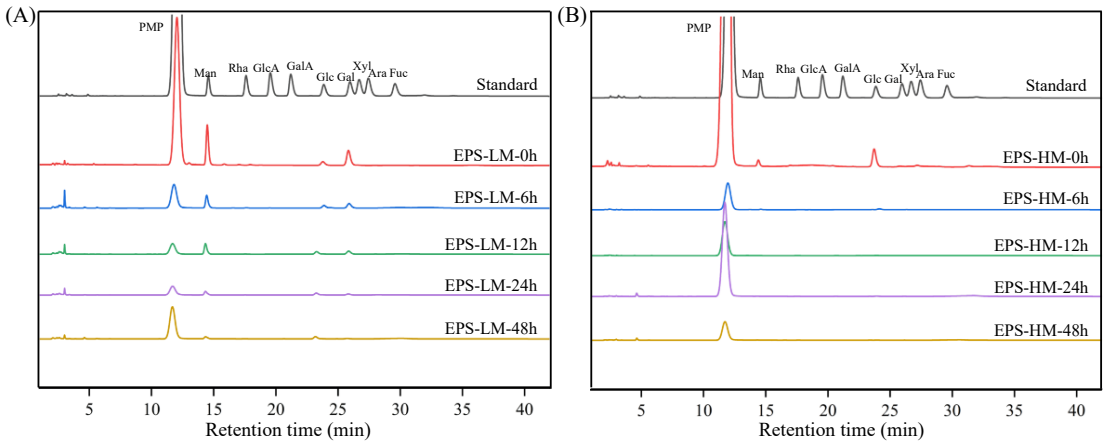

Figure 3-3. HPLC profiles of monosaccharides in EPS-LM and EPS-HM during fecal fermentation.

3.3.5 Medium pH change and SCFA production during fecal fermentation

Figure 3-4 shows the trends of medium pH change and three SCFAs during the fecal fermentation. As shown in **Figure 3-4A**, the pH decreased rapidly in FOS fermentation and gradually in EPS-LM and EPS-HM and only slightly in carbohydrate-free blank group. During 48 h fermentation, the pH decreased from the initial pH 7.58 to 3.76 in the FOS group, to 4.90 in EPS-HM, to 5.26 in EPS-LM group and to 6.74 in Blank group. The alteration in pH value can be a monitor of assessing the acidic environment in the intestine, with the decrease reflecting the utilization of polysaccharides by gut bacteria.

SCFAs including acetic, propionic, and butyric acids are the main end products by anaerobic fermentation of polysaccharides in gut microbiota. SCFAs play a crucial role in maintaining normal physiological functions of the intestinal tract, such as enhancing gut barrier integrity and regulating the immune system and inflammatory response (A. Nogal, A. M. Valdes, & C. Menni, 2021). As shown in **Figure 3-4B-D**, during the fecal fermentation, the concentration of acetic, propionic, and butyric acids in FOS and EPS groups significantly increased compared with Blank group. Acetic acid was produced at the highest level, accounting for a major portion of the total SCFAs. Acetate is primarily produced via the acetyl-CoA and Wood-Ljungdahl pathways (A. Koh et al., 2016; Louis et al., 2007). Besides, EPS-HM (39.07 mM) produced more acetic acid than EPS-LM (32.14 mM), which was consistent with the pH change. Besides, after 48 h fermentation, compared with the Blank group, the propionic acid production of EPS-LM and EPS-HM groups were 130% and 66.9% higher, respectively. EPS-LM group can produce much more propionic acid than EPS-HM group while the trend reversed for butyric acid production. Propionate can reduce food intake and regulate the immune response to cardiovascular diseases (Bartolomaeus et al., 2019; M. Wang et al.,

2019). Butyrate may offer beneficial effects on the damage to the intestine, inflammatory bowel disease and metabolic diseases (Stoeva et al., 2021). The different production levels of SCFAs with the different carbohydrates can be attributed to variations in molecular weight, monosaccharide composition and other molecular properties. Overall, the production of SCFAs from fecal fermentation of EPS fractions suggests their beneficial effects on human health.

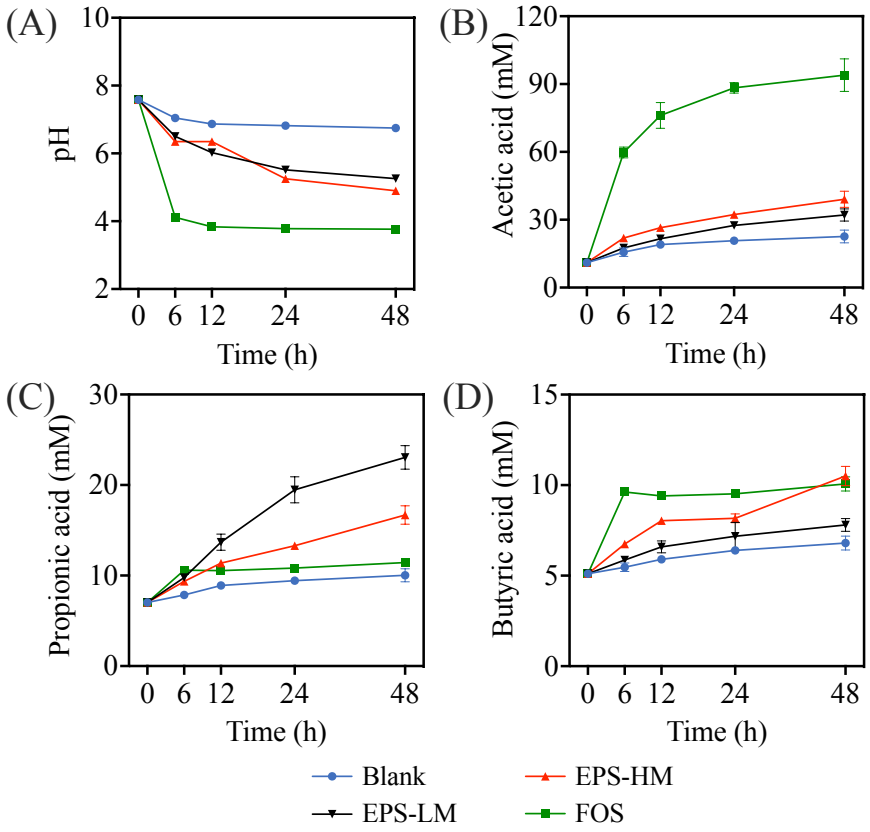

Figure 3-4. Time courses of medium pH change and production of SCFAs of different carbohydrate sources and the carbohydrate-free blank during fecal fermentation: (A) pH, (B) acetic acid, (C) propionic acid, (D) butyric acid. Blank: no additional carbohydrate source; FOS (fructo-oligosaccharide): a probiotic reference; EPS-LM and EPS-HM: the experimental group (n = 3).

3.3.6 Gut microbiota profiles

In order to investigate the effects of EPS fractions on gut microbiota, high-throughput sequencing was performed. The α-diversity of the microbial community was shown in **Figure**

3-5A-C, including Chao1 index to represent for richness of bacterial community, and Shannon and Simpson index to represent for diversity of bacterial community. The results showed the richness and diversity of EPS fractions and FOS groups were lower than Blank group, which were similar to the previous results (G. Ma, Xu, Du, Muinde Kimatu, et al., 2022; D.-T. Wu et al., 2021). Besides, there was no significant difference between the two EPS fractions. These trends were also similar to the effects of Blackberry polysaccharides (Q.-Y. Li et al., 2022). In addition, principal component analysis (PCA) displays the microbial community diversity of different groups (**Figure 3-5D**). Component 1 (PC1) could explain 62.8% of the difference among groups and Component 2 (PC2) could explain 22.2% of the difference among groups. The total variance was 85%, accounting for the overall difference in the microbial composition. The distance among different groups showed that each group changed and reshaped gut microbiota, with EPS fractions having a great influence on microbial community compared with Blank. As shown in **Figure 3-5E**, the significant distinction among different groups displayed the difference in microbiota composition, which was consistent with the results of PCA. These findings showed EPS fractions are beneficial for regulating the microbial community.

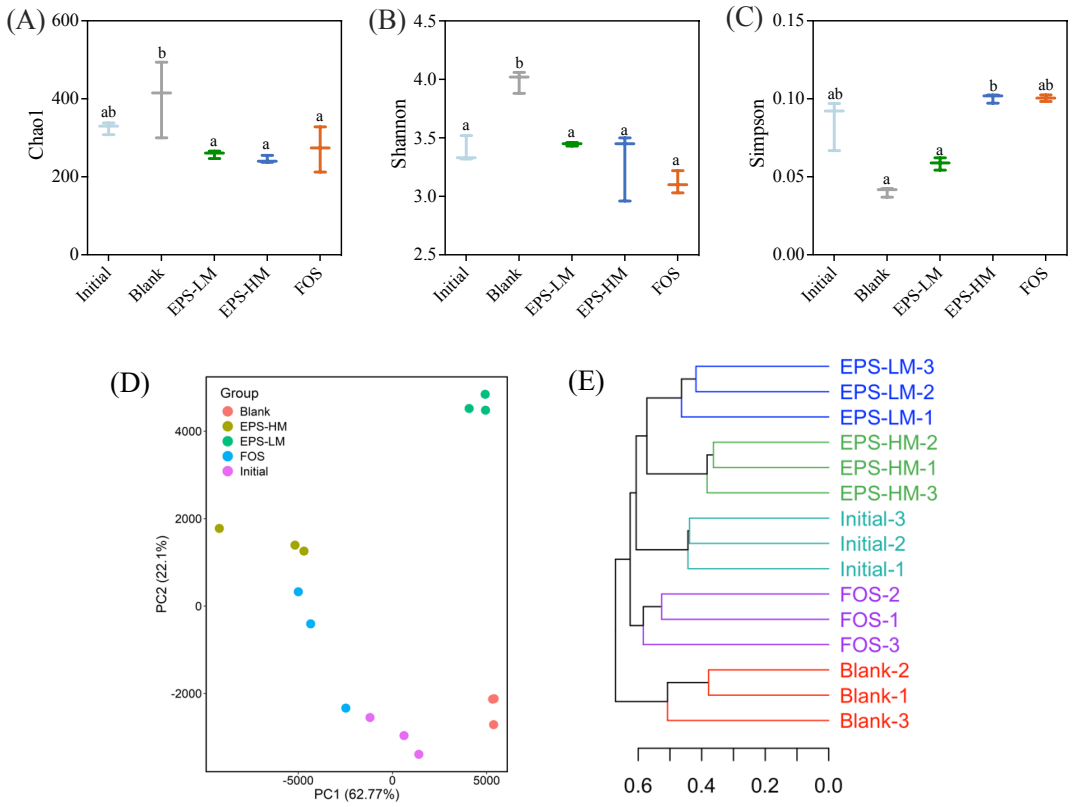

Figure 3-5. α-Diversity analysis of fecal microbial communities throughout *in vitro* fecal fermentation for 0 (Initial group) and 48 h of different carbohydrate sources and carbohydrate blank with different indexes including (A) Chao1, (B) Shannon, (C) Simpson, statistically significant differences between the methods were determined using Tukey's multiple comparison test, with $p<0.05$; β-diversity analysis of fecal microbial communities using (D) principal component analysis (PCA) of fecal microbial communities based on the relative abundances of OTUs at a 97% similarity level and (E) multivariate analysis of variance from matrix scores based on Bray-Curtis method at the genus level. Blank: no additional carbohydrate source; FOS (fructo-oligosaccharide): a probiotic reference; EPS-LM and EPS-HM: the experimental group (n = 3).

Figure 3-6A shows the composition of intestinal microbiota at the phylum level. At the phylum level, the gut microbiota mainly consisted of Bacteroides, Firmicutes, Proteobacteria and Actinobacteria (Faith et al., 2013), with Firmicutes and Bacteroidetes accounting for over

90% (Arumugam et al., 2011). Compared with Blank group, EPS-HM group increased the level of Bacteroides and Firmicutes and decreased the level of Proteobacteria. EPS-LM group increased the level of Bacteroides and Proteobacteria and decreased the level of Firmicutes. Especially, EPS-LM had the lowest ratio of Firmicutes to Bacteroidetes (F/B), where an increased F/B ratio is closely associated with obesity (Crovesy, Masterson, & Rosado, 2020). The results were in line with the previous study that lower molecular weight of polysaccharides from *Ficus carica* Linn. also had a lower F/B ratio (B. Xu et al., 2024). At the genus level (**Figure 3-6B**), among the groups, the abundance of *Prevotella 9* and *Lachnoclostridium* was the highest in EPS-HM group while the abundance of *Bacteroides*, *Parabacteroides*, *Faecalibacterium* was at the highest level in EPS-LM group. An increasing number of evidence has proved that these bacteria are beneficial gut microbiota. For example, *Lachnoclostridium* was proven to potentially improve colonic inflammation (M. Zhang et al., 2024). *Bacteroides* and *Parabacteroides* can alleviate gut epithelial barrier and intestinal inflammation (H. Deng et al., 2018; Lai et al., 2022). **Figure 3-6C** showed the heatmap based on the top 20 different taxa to analyse the microbial composition among different treatment groups. *Blautia* was abundant in EPS fractions and FOS group. As found in a previous study, FOS high-dose treatment in mice increased the relative abundance of Blautia (García et al., 2023). EPS fractions also upregulated the abundance of *Fusicatenibacter* and *Eubacterium rectale group* when comparing with Blank group. *Fusicatenibacter* was suggested to have anti-inflammatory activity through inhibiting the production of proinflammatory cytokines such as IL-6, TNF-α, and IL-1β (Voorhies et al., 2019). Additionally, *Eubacterium rectale group* can promote the production of butyrate and valerate and suppress the intestinal lymphomagenesis (H. Lu et al., 2022). Besides, based on **Figure 3-6D-E**, the linear discriminant analysis (LDA) and effect size (LEfSe) were carried out to compare the gut species in different groups. Different colors represent microbiota with significant differences in each group. There were significant

differences (LDA score >4) in different groups, in that 9, 15, 18, 11 and 13 OTUs among Initial, Blank, EPS-LM, EPS-HM and FOS group, respectively.

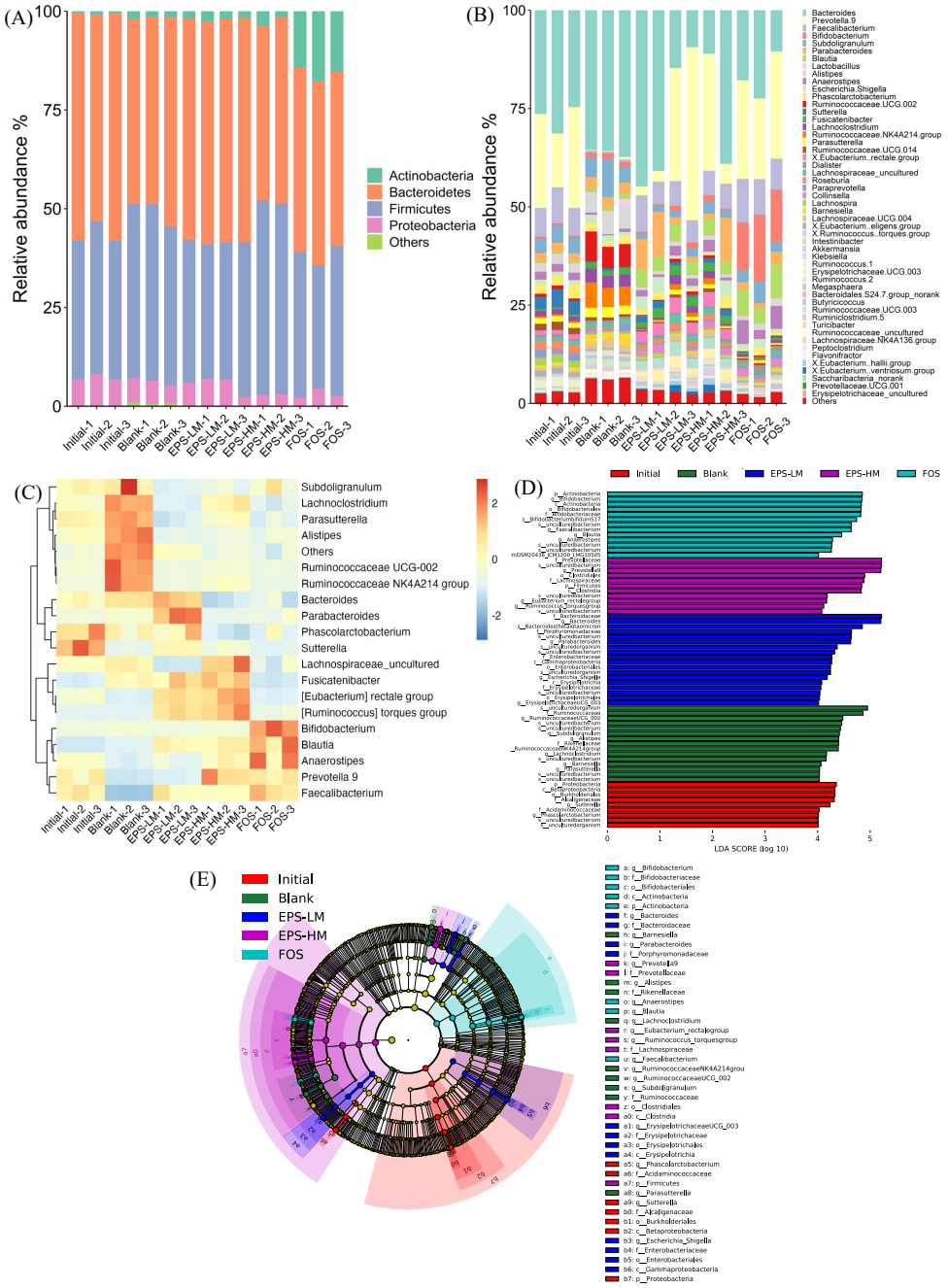

Figure 3-6. Comparisons of different groups on gut microbial composition for 0 (Initial group) and 48 h fermentation. Bacterial taxonomic profiling at the (A) phylum level and (B) genus level; Bacterial analysis based on (C) heatmap at genus level; Species difference of gut microbiota based on (D) Linear discriminant analysis (LDA) score and (E) LEfSe diagram.

Blank: no additional carbohydrate source; FOS (fructo-oligosaccharide): a probiotic reference; EPS-LM and EPS-HM: the experimental group (n = 3).

Therefore, the properties of EPS-LM and EPS-HM selectively altered their fermentative behavior during fermentation. Although EPS-HM possessed a higher molecular weight, higher purity of polysaccharide content and simpler monosaccharide composition (mainly consisting of Glc) made it faster degradation. Glc was a prior carbon source for gut microbiota and much easier to be utilized (Y. Zhao et al., 2024). In contrast, EPS-LM had lower molecular weight and degradation of Man and Gal relay on more specific enzymes, such as GH 92 and GH27 (Alonso-Gil, Parkan, Kaminský, Pohl, & Miyazaki, 2022; Reddy et al., 2016) which could decrease the fermentation efficiency. Additionally, the difference in monosaccharide composition also regulated the composition of gut microbiota. *Lachnoclostridum* preferentially utilized Glc to produce butyric acid, resulting in higher levels of butyric acid in EPS-HM group. Meanwhile, *Faecaliacterium* and *Bacteroides* highly expressed mannosidase and galactosidase, which allowed them to preferentially catabolize Man and Gal to produce propionic acid, contributing to the elevated levels of propionic acid in the EPS-LM group (Keung et al., 2025).

3.3.7 Fecal fermentation products affecting LPS-induced inflammation in Caco-2/RAW264.7 co-culture models

The gut barrier connects gut microbes and the intestinal immune system, and damaged gut barrier function is commonly associated with a variety of gastrointestinal disorders, including inflammatory bowel disease (Luissint, Parkos, & Nusrat, 2016; Turner, 2009). As illustrated in **Figure 3-7A-B**, the LPS-stimulated Caco-2/RAW264.7 co-cultured model exhibited a significant upregulation of key signalling molecules and proinflammatory cytokines, including nitric oxide (NO) and interleukin-1β (IL-1β), indicative of a robust inflammatory response. However, the EPS-LM and EPS-HM fermented groups markedly inhibited these inflammatory

markers, with both polysaccharides demonstrating a dose-dependent reduction in NO and IL-1β levels compared to the LPS-treated group. This anti-inflammatory effect suggests that the fermented metabolites of EPS-LM and EPS-HM possess potent immunomodulatory properties.

Furthermore, **Figure 3-7C** highlights the protective effects of EPS-LM and EPS-HM metabolites on intestinal barrier integrity measured by TEER. LPS treatment significantly reduced the TEER level compared to the NC group, reflecting compromised barrier function and increased paracellular permeability due to inflammatory damage. In contrast, the metabolites of EPS-LM and EPS-HM at various concentrations significantly restored the TEER level, indicating their ability to mitigate LPS-induced barrier disruption. This restoration of TEER suggests the potential of EPS for enhancement of epithelial tight junction integrity and protection against inflammatory damage.

The protective effects of EPS-LM and EPS-HM were further corroborated by the mRNA expression levels of tight junction (TJ) proteins, as shown in **Figure 3-7D-F**. LPS stimulation significantly downregulated the expression of Claudin-1, Occludin, and ZO-1 compared to the NC group, reflecting the damaged impact of inflammation on intestinal barrier function. However, treatment with EPS-LM and EPS-HM metabolites upregulated the expression of these TJ proteins, suggesting their role in reinforcing the intestinal epithelial barrier. This upregulation of TJ proteins is critical for maintaining barrier integrity and preventing the translocation of luminal pathogens, which are hallmarks of inflammatory bowel diseases (Kaminsky, Al-Sadi, & Ma, 2021).

Immunofluorescence analysis (**Figure 3-7G**) provided additional insights into the localization and distribution of TJ proteins. In the control Caco-2 cell monolayers, ZO-1 and Claudin-1 exhibited a continuous and well-defined immunolocalization pattern at the junctional regions of the cell membrane, indicative of intact barrier function. In contrast, LPS treatment resulted in faint, discontinuous immunolocalization of TJ proteins, with ZO-1 mis-

localized to the cytosolic space, reflecting severe disruption of the epithelial barrier. Remarkably, treatment with EPS-LM and EPS-HM metabolites restored the expression and proper localization of TJ proteins, further supporting their protective role in maintaining barrier integrity under inflammatory conditions. These results showed the importance of utilization of EPS fractions by gut microbiota. For example, EPS-HM upgraded the abundance of *Lachnoclostridium*, a butyrate producer. Butyrate synergistically inhibited the HDAC8/NF-κB pathway and enhanced TJ protein (ZO-1, Occludin, Claudin-1) expression (Kang et al., 2021; Peng et al., 2024). Taken together, these findings demonstrate that the fermented metabolites of EPS-LM and EPS-HM exert significant anti-inflammatory and barrier-protective effects in the LPS-induced Caco-2/RAW264.7 co-culture model.

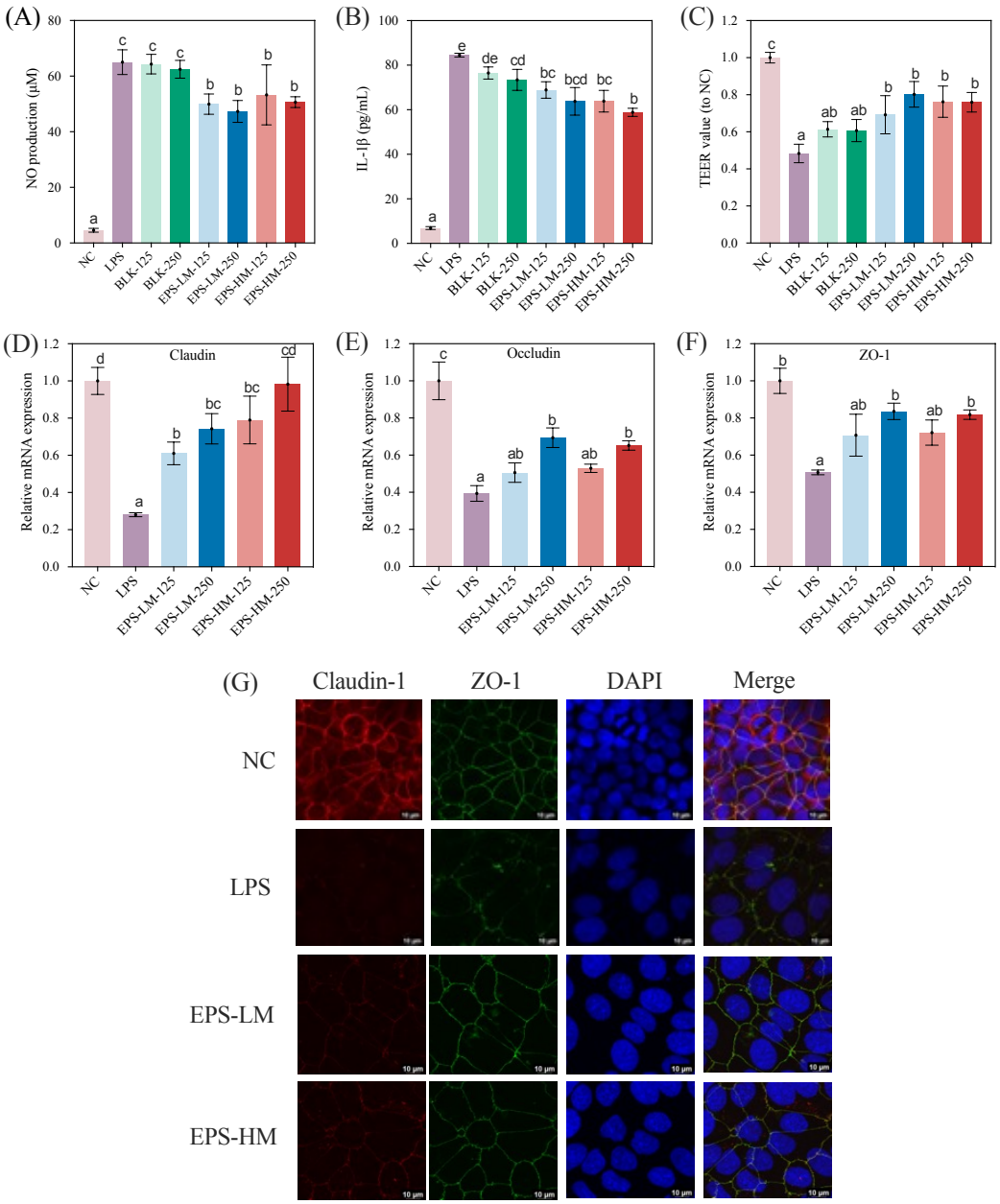

Figure 3-7. EPS-LM and EPS-HM fermented products reduced the levels of proinflammatory cytokines in LPS-treated Caco-2/RAW264.7 co-culture. (A) NO production using the Griess method, (B) IL-1β level using the Elisa kit; (C) TEER value; the mRNA expression level of (D) Claudin-1, (E) Occludin, (F) ZO-1 and cellular localization of (G) Claudin-1and ZO-1 in Caco-2 cells. NC: negative control group with cell culture medium only; Blank: the blank control, no additional carbohydrate source fermented group; EPS-LM and EPS-HM: the experimental fermented group (n = 3).

3.4 Conclusions

In this study, EPS-LM and EPS-HM showed highly resistant in upper GI tract and well-utilized by gut microbes. During fecal fermentation, EPS-LM and EPS-HM showed different trends in the MW reduction, carbohydrate consumption, and reducing sugar production due to their differences in MW and monosaccharide composition. The progressive fermentation of EPS-LM (low MW, mannose/galactose-based) relied more on the synergistic metabolism of Proteobacteria and increased propionic acid content. In contrast, rapid fermentation of EPS-HM (high MW, glucose-dominated) enriched the Bacteroides and Firmicutes as a core group of bacteria whose metabolites were dominated by acetic and butyric acids. Nevertheless, the fermentation products of both EPS fractions exhibited significant and dose-dependent anti-inflammatory and barrier-protective effects. This study not only provides a theoretical basis for the precise application of natural polysaccharides but also opens up a new direction for the intestinal barrier recovery based on microbiota metabolism. Moreover, the anti-inflammatory and gut barrier protective effects as well as the probiotic properties of EPS fractions suggest their potential as functional food ingredients for promoting gut health and enhancing metabolic functions.

Chapter 4 Isolation, purification, structural characterization, hypoglycemic and antioxidant activities of a low-MW EPS from Cs-HK1

4.1 Introduction

Elevated blood glucose level or hyperglycemia is recognized as a crucial factor contributing to metabolic and cardiovascular diseases (CVDs) (S. Jin & Kang, 2024; Poznyak, Litvinova, Poggio, Sukhorukov, & Orekhov, 2022). Persistent or chronic hyperglycemia can induce oxidative stress, which in turn leads to cellular dysfunction and damage to various tissues, such as vascular endothelium, which is a key player in maintaining vascular health (Y. An et al., 2023). Oxidative stress occurs when there is an imbalance between the production of reactive oxygen species (ROS) and cell not able to repair the resulting damage. The overproduction of ROS, including H_2O_2, $HO\cdot$, and O^{2-} can lead to endothelial damage, which is a signal of several metabolic disorders and CVDs, including atherosclerosis, hypertension and myocardial infarction (Dubois-Deruy, Peugnet, Turkieh, & Pinet, 2020; Pizzino et al., 2017). A major source of elevated blood glucose is the rapid digestion of carbohydrates, facilitated by enzymes such as α-amylase and α-glucosidase, which break down complex carbohydrates into absorbable glucose (L. Sun & Miao, 2020). Controlling these enzymes is an effective measure for managing postprandial blood glucose levels to lower the risk of associated complications. The current drugs for these diseases have many side effects on the patients, including chronic diarrhea and weight loss (Susilawati, Levita, Susilawati, & Sumiwi, 2023). Therefore, considerable effort has been devoted to seek natural remedies that can effectively reduce blood sugar and oxidative stress without causing harmful effects to human health and quality of life.

Natural polysaccharides from edible and medicinal sources have been shown a wide range of biological activities and potential therapeutic effects on metabolic diseases and CVDs (Q. Jin, Lin, & Lu, 2025). For example, pumpkin polysaccharides have been shown to enhance

antioxidant enzymes and reduce fasting blood glucose level on T2DM rats (A. Lu et al., 2019). Polysaccharides from American crabapple fruits have shown potential hypoglycemic activity by significantly inhibiting α-amylase and α-glucosidase *in vitro* (Q. Sun et al., 2025). Polysaccharide extracted from *Pleurotus citrinopileatus* fungal mycelia could effectively inhibit α-glucosidase and improve insulin resistance in HepG2 cells (Hao, Sun, Zhang, Wu, & Zhu, 2020). *C. sinensis* (=*Ophiocordyceps sinensis*), generally known as the Chinese caterpillar fungus, is a valued medicinal fungus in traditional Chinese medicine including Tibetan medicine. Polysaccharides represent a major class of nutritional and bioactive biomacromolecules with multiple biological activities such as immunomodulation, anti-tumor, anti-diabetic, and, antioxidant effects (Elnahas, Elkhateeb, & Daba, 2024). However, *C. sinensis* is a rare in nature and expensive, mycelial fermentation has become a major process for commercial production of the fungal materials.

Cs-HK1 is a fungus isolated from the fruiting body of a natural *C. sinensis* caterpillar fungus by Wu's group (P. H. Leung et al., 2006). Cs-HK1 mycelial culture has been applied to liquid fermentation for production of the fungal biomass and polysaccharides. The EPS from liquid fermentation of Cs-HK1 mycelia have shown multiple bioactivities, such as anti-inflammatory, immunomodulatory and antioxidant properties (L.-Q. Li et al., 2020; J.-K. Yan, Wang, & Wu, 2014). It is well known that the structural characteristics of polysaccharides are the determining factors on their biological activities. Therefore, it is of significance to analyze the EPS structural properties and to further investigate the structure-activity relationship. In our previous studies, the lower-MW EPS fraction, EPS-LM isolated from the Cs-HK1 mycelial fermentation medium has shown more significant anti-inflammatory and antioxidant activities (Q.-L. Huang, Siu, Wang, Cheung, & Wu, 2013; L.-Q. Li et al., 2020).

In this study, a major polysaccharide fraction, EPS-LM-n, was isolated from EPS-LM and purified to homogeneity by liquid chromatography. Its detailed structural characteristics were

derived through a series of analytical experiments analysis including molecular weight, monosaccharide composition, FTIR, methylation analysis and NMR. The hypoglycemic activity of EPS-LM-n was evaluated by measurement of α-amylase and α-glucosidase inhibitory and antioxidant activity by radical scavenging and reducing power assays. Its potential for cardiovascular protection against oxidative damage was tested in EA.hy926 cell culture.

4.2 Materials and methods

4.2.1 Chemicals

Iron (II) sulfate heptahydrate, iron (III) chloride hexahydrate, Deuterium oxide (D_2O), ascorbic acid, Penicillin, streptomycin, lipopolysaccharide, sulphanilamide, N-1-naphthyl ethylenediamine dihydrochloride were obtained from Sigma-Aldrich (St. Louis, MO, USA). ABTS (2,2'-azino- bis(3-ethylbenzothiazoline-6-sulfonic acid) was sourced from Roche (Mannheim, Germany), while Trolox ((S)-(2)- 6-hydroxy-2,5,7,8-tetramethyl-chroman-2-carboxylic acid) was obtained from Calbiochem (San Diego, CA, United States). Phosphate-buffered saline (PBS) was acquired from Macklin. All other chemicals were of analytical reagent (AR) grade or higher and were obtained from reputable suppliers.

4.2.2 Cs-HK1 mycelial fermentation and EPS extraction

EPS-LM was extracted from Cs-HK1 mycelial fermentation, described as section 2.2.2.

4.2.3 Separation and purification of EPS-LM-n

EPS-LM was firstly deproteinated by Sevag method (F. T. Gu, Zhao, et al., 2025), dialyzed with 3,500-Da MW cut-off membrane for 3 days and then lyophilized. Further purification used DEAE-52 cellulose column (ϕ3.5 cm×33 cm). The mobile phase was different concentrations of NaCl solutions (0, 0.1M, 0.2M, 0.5M, 1M) with a flow rate of 1.3 mL/min, respectively. From each tube, 9.1 mL eluent was collected with an automatic fractional

collector and phenol-sulfuric acid method (J.-K. Yan, Li, Wang, & Wu, 2010) was used to obtain the elution profile, with glucose as a standard at 490 nm. A major fraction was collected, combined, concentrated, and lyophilized, designated EPS-LM-1. EPS-LM-1 was loaded onto a HiLoad 16/600 Superdex 200 pg column (ϕ1.6 cm×60 cm), which was eluted with distilled water at a flow rate of 2 mL/min. The major fraction was collected, concentrated, dialyzed and lyophilized, yielding the final purified fraction EPS-LM-n, which was a neutral polysaccharide.

4.2.3 Chemical and structure analysis of EPS-LM-n

4.2.3.1 Molecular weight analysis

Molecular weight of EPS-LM-n was analyzed as described in section 2.2.7.

4.2.3.2 Chemical composition analysis

Total carbohydrate of EPS-LM-n were determined as described in section 2.2.6 and protein content by Lowry method using bovine albumin as a reference (F. T. Gu, Li, et al., 2025).

Monosaccharide composition of EPS-LM-n was determined as described in section 2.2.8.

4.2.3.3 Fourier transform infrared spectroscopy (FT-IR) analysis

FTIR spectroscopy was performed to characterize the structural attributes of EPS-LM-n. EPS-LM-n was analysed as described in section 2.2.3.

4.2.3.4 Methylation and GC-MS analysis

Methylation analysis of EPS-LM-n was conducted with a modified method (X. Li, Chen, Liu, Xu, & Zhang, 2021). The polysaccharide was first dissolved in anhydrous DMSO, followed by the addition of NaOH powder and stirring for 3 h to facilitate methylation. Iodomethane was subsequently introduced and successful methylation was indicated by the absence of O-H absorption (3200–3700 cm^{-1}) in the IR spectrum. The methylated sample was then hydrolyzed, reduced and acetylated to yield partial methylated alditol acetates (PMAAs).

These PMAAs were analyzed using a GC-MS (Agilent Technology 6890A-5975C, USA) with a BPX70 column (30 m × 0.25 mm, 0.25 μm, SGE, Australia). The GC-MS conditions were as follows: carrier gas was high purity helium with a split ratio of 10:1, injection volume was 1 μL, initial temperature was held at 140 °C for 2.0 min, followed by an increase to 230 °C at a rate of 3 °C/min for 3 min. Mass spectra were scanned from m/z 30 to 600. PMAAs were identified by comparing retention times and fragmentation patterns to those in established databases (Sassaki, Gorin, Souza, Czelusniak, & Iacomini, 2005).

4.2.3.5 Nuclear magnetic resonance (NMR) spectroscopy analysis

NMR spectra of the polysaccharide was recorded using a 600 MHz NMR spectrometer (Bruker AVANCE-III 600MHZ, Switzerland) at 25 °C. A total of 50 mg of the dried polysaccharide was dissolved in D_2O, ensuring complete dissolution before lyophilization. This process was repeated twice and the final sample was reconstituted in 0.6 mL of D_2O. Following this treatment, the ^{1}H, ^{13}C NMR and 2D NMR spectrum (including COSY, HSQC and HMBC) were measured.

4.2.4 Assays for α-Amylase and α-Glucosidase inhibitory activity of EPS-LM-n

The inhibition of digestive enzymes such as α-amylase and α-glucosidase can prevent carbohydrates from being broken down into easily digestible and absorbable substances (J. Wu, Shi, Wang, & Wang, 2016). The inhibition of these enzymes is a promising way to prevent CVDs conditions. Therefore, assessing α-amylase and α-glucosidase inhibitory activities can investigate the hypoglycemic activities of polysaccharides.

4.2.4.1 α-Amylase inhibitory activity

α-Amylase inhibitory activity of EPS-LM-n and acarbose (as positive control) was determined according to previous method (Jiaxin Chen, Zhou, Liu, & Bi, 2022) with some modifications. EPS-LM-n sample or acarbose (40 μL) with different concentrations (0.2-1

mg/mL) was mixed with 40 μL α-amylase (1 U/mL) and incubated at 37 °C for 10 min, followed with the addition of 80 μL starch solution (0.5%, w/v) and incubated at 37 °C for another 10 min. After that, 160 μL of 3, 5-dinitrosalicylic acid reagent was added and the mixture was incubated in boiling water for 10 min to stop the reaction. The absorbance of each vial was measured at 540 nm and the enzyme inhibition activity (%) was calculated by $[1-(A_1-A_2)/A_0] \times 100$, where A_0 is the absorbance of α-amylase and starch solution (control), A_1 is the absorbance of α-amylase, starch and EPS-LM-n solution, A_2 is the absorbance of EPS-LM-n and starch solution.

4.2.4.2 α-Glucosidase inhibitory activity

α-Glucosidase inhibitory activity of EPS-LM-n and acarbose (used as positive control) was determined from previous method (Jiaxin Chen et al., 2022) with some modifications. Briefly, 50 μL of EPS-LM-n or acarbose at various concentrations (0.2, 0.4, 0.6, 0.8, 1 mg/mL) were mixed with 100 μL of α-glucosidase (0.5 U/mL) and incubated at 37 °C for 10 min. Subsequently, 100 μL of p-nitrophenyl-α-D-glucopyranoside (5 mM) was added to each vial and incubated 37 °C for a further 20 min. The reaction was terminated by adding 1 mL of Na_2CO_3 (1 M). The absorbance of each vial was measured at 405 nm and the inhibition rate of α-glucosidase was calculated by $[1-(A_1-A_2)/A_0] \times 100$, where A_0 is the absorbance of pPNG and α-glucosidase, A_1 is the absorbance of pPNG, α-glucosidase and EPS-LM-n or acarbose, A_2 is the absorbance of pPNG and EPS-LM-n or acarbose.

4.2.5 Antioxidant activity assays

4.2.5.1 Hydroxyl radical scavenging activity

Hydroxyl radical scavenging activity was determined by the method (Yangbian Guo et al., 2024) with some modifications. EPS-LM-n sample solution was prepared at different concentrations (0.2-1 mg/mL) and 0.2 mL of the solution was mixed with 0.2 mL of 5 mM

$FeSO_4$ solution. Then, 0.2 mL of 1% (v/v) H_2O_2 was added to the mixture and incubate at 37 °C for 60 min. Distilled water was used as a blank control and ascorbic acid (Vc) as a positive control. Afterward, the absorbance of the mixture was measured at 510 nm. The hydroxyl radical scavenging effect was calculated by $[(A_0 - A)/A_0] \times 100$, where A_0 is the absorbance of the control solution (without EPS-LM-n or Vc) and A is the absorbance of the sample (EPS-LM-n or Vc).

4.2.5.2 DPPH radical scavenging activity

The $DPPH^+$ scavenging activity of the samples were assessed using a previous established method (Schlesier, Harwat, Böhm, & Bitsch, 2002). In brief, 3 mL sample at varying concentrations (0, 0.2, 0.4, 0.6, 0.8, 1 mg/mL) and mixed with 1 mL of $DPPH^+$-C_2H_5OH solution (0.1 mM). The mixture was shaken thoroughly and then incubated at room temperature for 30 min in the dark. The absorbance was measured at 517 nm using a UV-vis spectrophotometer (UV-2450, Shimadzu, Japan). Ethanol served as a negative control, while Vc was used as a positive control at the same concentration. All experiments were conducted in triplicate and $DPPH^+$ scavenging activity of sample was calculated by $[1- (A_1 – A_2) /A_0] \times 100$, where A_0 is the absorbance of control ($DPPH^+$ solution without sample), A_1 is the absorbance of EPS-LM-n or Vc with $DPPH^+$ solution, A_2 is the absorbance of EPS-LM-n or Vc.

4.2.5.3 Trolox equivalent antioxidant capacity (TEAC)

The TEAC assay assesses the ability of a sample to scavenge $ABTS^+$ radicals, using Trolox as a reference antioxidant (Schlesier et al., 2002). $ABTS^+$ radicals were generated through the oxidation of ABTS by potassium persulfate ($K_2S_2O_8$). Specifically, a 7.4 mM ABTS solution in distilled water was combined with 2.45 mM $K_2S_2O_8$ and allowed to react at room temperature in the dark for 16 h. Following this, 500 μL of the resultant $ABTS^+$ solution was

mixed with samples at varying concentrations to achieve an initial absorbance of approximately 0.70 at 734 nm. The mixture was then left at room temperature in dark for 2 h before measuring absorbance at 734 nm. TEAC of samples was reported as μmol Trolox/g sample.

4.2.5.4 Ferric-reducing antioxidant power (FRAP) assay

The FRAP assay measures the reducing power of a sample by transferring a single electron to $Fe(TPTZ)_2(III)$, resulting in $Fe(TPTZ)_2(II)$ (Schlesier et al., 2002). The FRAP reagent was freshly prepared by mixing 3 M acetate buffer (pH 3.6), 0.1 M 2,4,6-Tris(2-pyridyl)-s-triazine (TPTZ) solution in 0.4 M HCl and 0.2 M ferric chloride hexahydrate ($FeCl_3 \cdot 6H_2O$) at 10:1:1 volume ratio and incubated at 37 °C. Different concentrations (0, 0.2, 0.4, 0.6, 0.8, 1 mg/mL) of sample solution (3.62 mL) was mixed with 0.38 mL FRAP reagent and incubated at room temperature for 15 min. The absorbance of the mixture was then measured at 593 nm using ferrous sulfate ($FeSO_4$) as a reference. FRAP activity of sample was expressed as μmol Fe^{2+}/g sample.

4.2.6 Cell culture assays for assessing protective effects of EPS-LM-n on H_2O_2-induced EA. hy926 cell line

4.2.6.1 Cell line and culture conditions

The EA. hy926 human endothelial cell line was purchased from Invitrogen Life Technologies (Carlsbad, CA, USA) and cultured in DMEM/F-12 medium (Gibco Life Technologies, Rockville, MD, USA) supplemented with 10% fetal bovine serum (Gibco Life Technologies, Rockville, MD, USA) and 1% penicillin/streptomycin (Gibco Life Technologies, Rockville, MD, USA). Media were replaced every days after 50% cell density. The cell culture was maintained at 37℃ with 5% CO_2 in the atmosphere. As the cell culture reached ~80% confluence, the cells were treated with different concentrations of H_2O_2 with 2×10^4/mL.

4.2.6.2 Measurement of cell viability

Cells were incubated in 96-well plate after 24 h incubation and were tested using the CellTiter 96 cytotoxicity assay (Promega, Madison, Wis). The plate was incubated 2-2.5 h and optical density (OD) was then read directly at 492 nm.

4.2.6.3 Intracellular ROS level determination

Cells was seeded on 96 well for 24 hours and were incubated with the carboxy-2,7-dichlorofluorescein diacetate (DCFH-DA) probe (with 10 ppm final concentration) for 1 hour, add 300 μM of hydrogen peroxide (H_2O_2 to stimulate the cells. The reactive oxygen detection assay detects reactive oxygen using the fluorescent probe DCFH-DA. DCFH-DA does not emit light and can easily pass across the cell membrane. It can be digested by the internal enzyme system to become DCFH after entering the cell. DCFH is unable to cross the cell membrane, allowing the probe to be inserted into the cell readily. In the cell, reactive oxygen may oxidize non-fluorescent DCFH to become fluorescent DCF. The concentration of oxidative stress in cell can be determined by measuring the fluorescence of DCF. After incubating at 37 ℃ for 2 hours, fluorescence was measured from 485 nm (excitation) to 527 nm (emission) wavelengths on a microplate reader (Molecular Devices Spectra MAX Gemini X). All experiments and measurements were performed in triplicate.

4.2.6.4. Cell apoptosis by flow cytometry

EA.hy926 cells were cultured in 6 well plates with 2×10^5/ml and treated by different concentrations of H_2O_2 and EPS-LM-n. After incubation, cells were prepared according to the instructions of the Annexin V-FITC/PI Apoptosis Detection Kit (Beyotime, Beijing, China). Specifically, 1×10^5 cells were collected and rinsed twice with cold PBS. They were then resuspended in 100 μL of binding buffer, to which 5 μL of FITC Annexin V and 5 μL of propidium iodide (PI) were added. This mixture was incubated for 15 min at 25 °C in the dark.

Following the incubation, 400 μL of binding buffer was added and the cells were analyzed using a FACScan flow cytometer (BD Biosciences, San Jose, CA, USA). The cells were quantitatively detected using the BD Accuri C6.

4.2.7 Data analysis

All the experiments were performed in triplicate or more repeats. The data were analyzed by SPSS (version 26.0, IBM Inc., Chicago, IL, USA). Descriptive statistics were calculated for all numerical variables, with results expressed as mean ± standard deviation. A one-way analysis of variance (ANOVA) was performed to evaluate statistical significance, followed by Tukey's pairwise comparisons with a significance level set at $p < 0.05$.

4.3 Results and discussion

4.3.1 Isolation and purification of EPS-LM-n

EPS-LM, a crude low-MW fraction of exopolysaccharide, was isolated from Cs-HK1 mycelial fermentation. After DEAE-52 chromatography fractionation, two separate peaks were isolated, named EPS-LM-1and EPS-LM-2 (**Figure 4-1A**). EPS-LM-1 was a neutral polysaccharide eluted with water. Then, EPS-LM-1 with a higher peak was further purified through a Sephadex G-200 pg, yielding a predominant peak (**Figure 4-1B**), named EPS-LM-n. The sugar content of EPS-LM-n was 79.50 ± 0.01%. There was negligible peaks at 260 nm and 280 nm (**Figure 4-1C**), indicating the absence of protein and nucleic acids in EPS-LM-n (Porterfield & Zlotnick, 2010). HPGPC analysis of EPS-LM-n revealed a sharp, narrow and symmetrical peak (**Figure 4-1D**), confirming its homogeneity. EPS-LM-n was determined to have a weight-average MW (Mw) of be 417 kDa, a number-average MW (Mn) of 359 kDa and a polydispersity index (Mw/Mn) of 1.154. The GPC results suggested that MW of EPS-LM-n was consistent with the findings from a previous study (L. Q. Li, A. X. Song, W. T. Wong, & J. Y. Wu, 2021a). As shown in the previous study (L. Q. Li et al., 2021a), the lower-MW

fraction of Cs-HK1 EPS collected from the 2nd step of ethanol precipitation had stronger anti-inflammatory activities. Consistently, another reported study (Y. Shi et al., 2016) has also found that lower-MW polysaccharides from another source had higher bioactivities and water solubility.

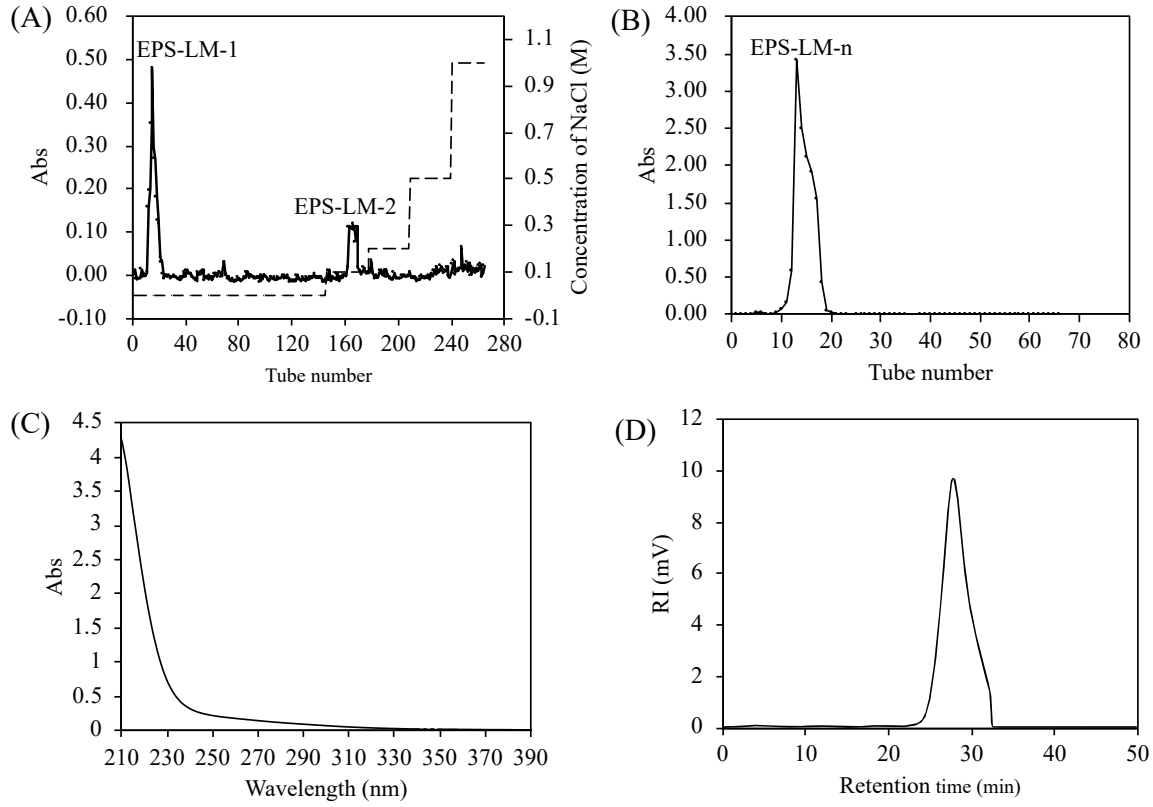

Figure 4-1. Extraction and isolation of EPS-LM. (A) Elution curve of EPS-LM on DEAE-52 column; (B) Elution curve of EPS-LM-n on Sephadex G-100 column; (C) UV spectrum of EPS-LM-n; (D) GPC profile of EPS-LM-n.

Table 4-1. The chemical composition and molecular weight distribution of EPS-LM-n.

Item	Value
Sugar content % (w/w)	79.50±0.01
Protein content % (w/w)	1.66±0.08
Monosaccharide molar ratio	Man:Glc:Gal=1: 0.49:0.21
Mw (kDa)	417
Mn (kDa)	359
Polydispersity (Mw/Mn)	1.154

4.3.2 FT-IR spectroscopy and monosaccharide composition of EPS-LM-n

As shown in **Figure 4-2A**, FT-IR spectrum was determined ranging from 4000 to 500 cm^{-1} to characterize the functional groups of EPS-LM-n. The intense broad peak near 3340 cm^{-1} was caused by the -OH stretching vibration in the molecular structure indicating the interactions of the PS chains. The band at 2930 cm^{-1} was due to C-H stretching vibration. The absorption peak near 1643 cm^{-1} was attributed to the scissoring vibration of bound water (Y.-X. Wang et al., 2022). The absorption peak near 1384 cm^{-1} was assigned to $-CH_3$ group bending vibration or O-H deformation vibration (J. H. Li et al., 2023; Y.-X. Wang et al., 2022). The characteristic peaks at 1054 cm^{-1} was due to C-O-C structures, the existence of glycosides (Y. He, Peng, Zhang, Liu, & Sun, 2021). Additionally, the peaks at 1072 and 1054 cm^{-1} suggested the presence of pyran-glycosides (M. Wu et al., 2020). These FT-IR results confirmed the characteristic functional bands of purified EPS.

The HPLC spectrum of EPS-LM-n presented three major monosaccharide peaks in **Figure 4-2B,** which were identified as Man, Glc and Gal by the reference chromatogram. The molar ratio of Man:Glc:Gal was 1:0.49:0.21 in **Table 4-1**, indicated that mannose was the most abundant monosaccharide constituent of EPS-LM-n. In combination with the FT-IR analysis, the results suggested the existence of mannopyranose (Man*p*) C-O-C linkages and glucopyranose (Glc*p*) C-O-C bonds in EPS-LM-n.

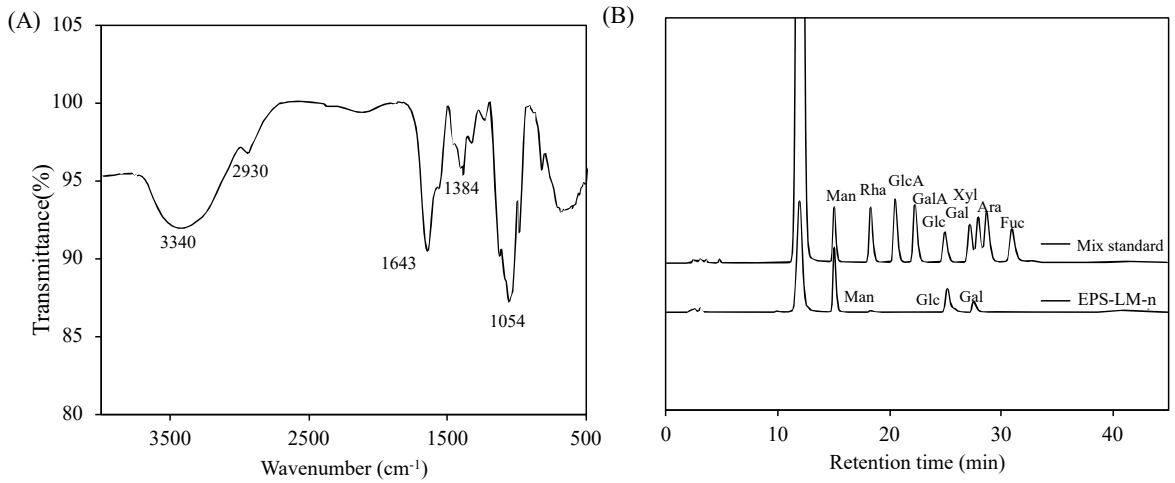

Figure 4-2. (A) FT-IR spectrum of EPS-LM-n; (B) Monosaccharide composition of EPS-LM-n.

4.3.3 Methylation analysis

Methylation analysis is a useful method for detecting the types and ratio of glycosidic linkages in polysaccharides (Qingbin Guo, Ai, & Cui, 2019). As shown in **Table 4-2**, EPS-LM-n had a diverse linkage pattern of seven glycosidic types. Man residues (62.35%) had terminal Man*p* (40.47%), 1,2-Man*p* (13.12%) and 1,2,6-Man*p* (8.76%) linkages, Glc residues (25.86%) had terminal Glc*p* (7.23%) and 1,4-Glc*p* (18.63%) linkages, and Gal residues (11.8%) had terminal Gal*p* (8.24%) and 1,3-Gal*p* (3.56%) linkages. The proportion of glycosidic bond residues with Man:Glc:Gal (1:0.49:0.21) were consistent with results of monosaccharide composition analysis. Total proportion of terminal Man*p*, Glc*p*, Gal*p* was 55.94%, suggesting that EPS-LM-n was a highly branched heteropolysaccharide. Among these linkages, the terminal Man*p* has the highest proportion of 40.47% indicating the main backbone structure of EPS-LM-n.

Table 4-2. Methylation analysis of EPS-LM-n (RT: retention time).

RT (min)	Linkage patterns	Derivative name	Content (mol%)
8.901	t-Man(*p*)	1,5-di-O-acetyl-2,3,4,6-tetra-O-methyl mannitol	40.47
9.001	t-Glc(*p*)	1,5-di-O-acetyl-2,3,4,6-tetra-O-methyl glucitol	7.23
9.992	t-Gal(*p*)	1,5-di-O-acetyl-2,3,4,6-tetra-O-methyl galactitol	8.24
12.382	1,3-Gal(*p*)	1,3,5-tri-O-acetyl-2,4,6-tri-O-methyl galactitol	3.56
12.45	1,2-Man(*p*)	1,2,5-tri-O-acetyl-3,4,6-tri-O-methyl mannitol	13.12
14.102	1,4-Glc(*p*)	1,4,5-di-O-acetyl-2,3,6-tetra-O-methyl glucitol	18.63
18.31	1,2,6-Man(*p*)	1,2,5,6-tetra-O-acetyl-3,4-di-O-methyl mannitol	8.76

4.3.4 NMR analysis

To further analyze the structural properties of EPS-LM-n, ^{1}H NMR, ^{13}C NMR and 2D NMR spectroscopy was used. In the ^{1}H NMR spectrum (**Figure 4-3A**), eight anomeric signals in the region 5.25−4.8 ppm were designated as A–H. Signal at δ 5.21, 5.14 and 4.96 were attributed to Man. Signal at δ 4.95, 4.89 and 4.83 were attributed to Glc. Signal at δ 4.97 and 4.99 was attributed to Gal (Yin Chen, Wang, Zhang, Zhang, & Linhardt, 2021; J. H. Li et al., 2023; J. Wu et al., 2021). The ^{13}C NMR spectrum (**Figure 4-3B**) contained several major signals around δ 102, 101, 100 and 98 in the anomeric carbon region (δ 90–110), suggesting α-configuration (H.-Y.-Y. Yao et al., 2021). Subsequent analysis was to identify the sequence and linkage types of glycosidic bonds of several residues by 2D NMR including COSY, HSQC and HMBC (**Figure 4-3C-E**). By combination of 1D and 2D NMR spectra, the proton and carbon chemical shifts of some of the major residues (labeled A-H) are summarized and assigned in **Table 4-3**.

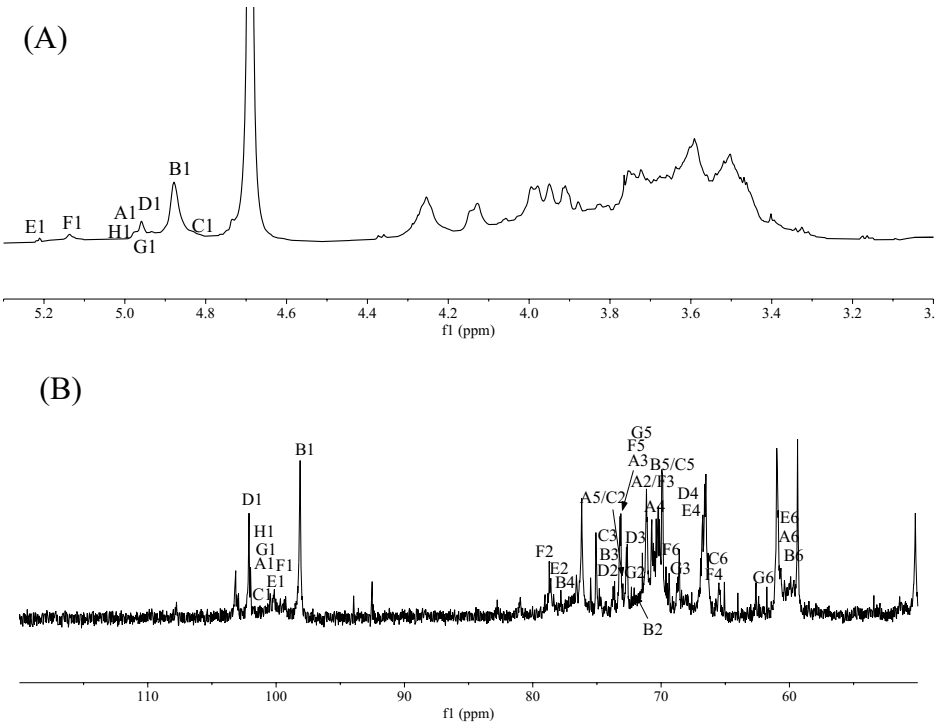

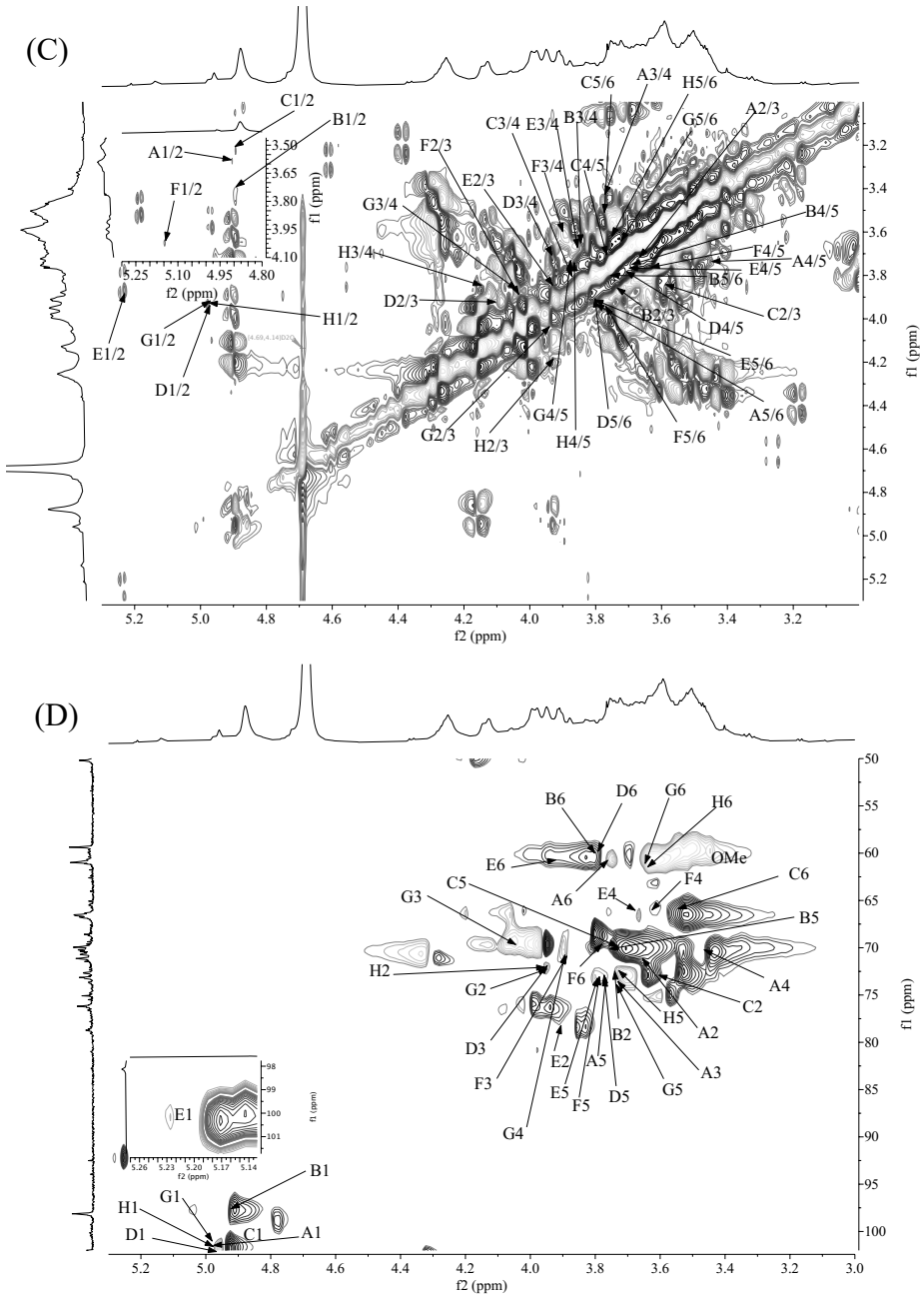
(C)
C1/2
B1/2
A1/2
F1/2
E1/2
G1/2
D1/2
H1/2
C5/6
A3/4
H5/6
C3/4
E3/4
B3/4
G5/6
A2/3
F2/3
F3/4
C4/5
E2/3
D3/4
G3/4
B4/5
H3/4
F4/5
A4/5
E4/5
B5/6
D2/3
B2/3
C2/3
D4/5
E5/6
A5/6
G4/5
D5/6
F5/6
G2/3
H2/3
H4/5
f2 (ppm)
f1 (ppm)
(D)
B6
D6
G6
H6
E6
OMe
F4
C6
C5
A6
E4
G3
B5
H2
F6
G2
A4
C2
H5
A2
D3
B2
E2
A5
A3
F3
E5
F5
D5
G5
G4
E1
B1
G1
H1
D1
C1
A1
f2 (ppm)
f1 (ppm)

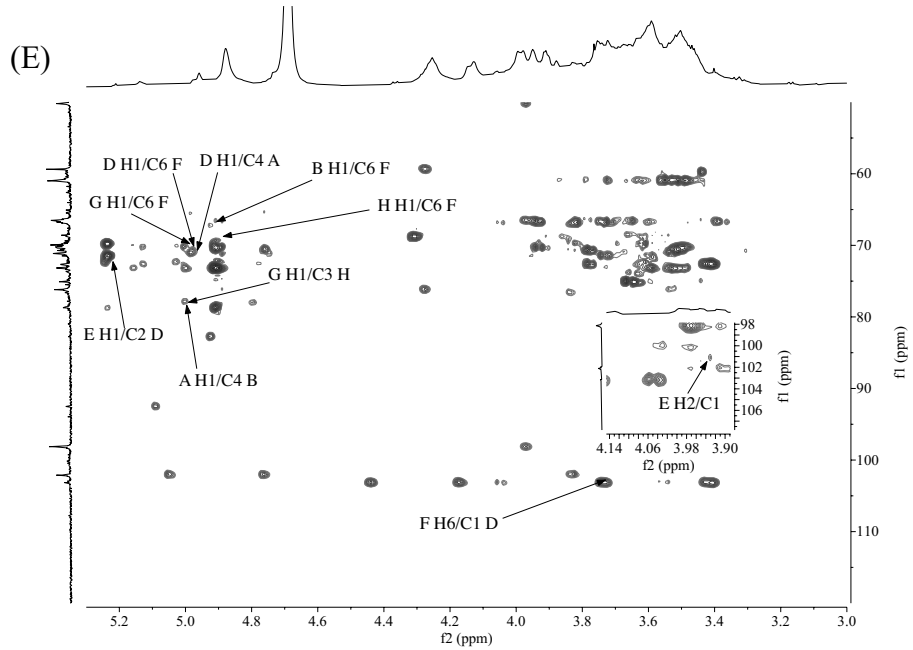

Figure 4-3. 1D-NMR spectra of EPS-LM-n. (A) ^{1}H NMR and (B) ^{13}C NMR spectrum of EPS-LM-n. 2D-NMR spectra of EPS-LM-n. (C) COSY; (D) HSQC; (E) HMBC. Experiments were performed in D_2O at 25 °C (chemical shifts are expressed in δ ppm).

Table 4-3. ^{1}H and ^{13}C NMR chemical shifts chemical shift assignments of EPS-LM-n.

Residues	Chemical shift (ppm)					
	H1 (C1)	H2 (C2)	H3 (C3)	H4 (C4)	H5 (C5)	H6 (C6)
A: α-Glc*p*-(1→	4.95 (101.84)	3.65 (71.28)	3.74 (73.07)	3.45 (70.73)	3.75 (72.88)	3.75/3.92 (60.55)
B: (1→4)-α-Glc*p*	4.89 (98.03)	3.73 (72.71)	3.83 (73.46)	3.67 (77.81)	3.74 (70.01)	3.80/3.98 (60.16)
C: (1→4)-6-Me-α-Glc*p*	4.83 (101.61)	3.59 (72.88)	3.86 (73.53)	3.75 (77.94)	3.74 (70.01)	3.53 (66.02)
D: α-Man*p*-(1→	4.96 (102.23)	4.10 (73.59)	3.93 (71.64)	3.70 (66.78)	3.78 (73.76)	3.77/3.92 (60.35)
E: (1→2)-α-Man*p*	5.21 (100.11)	3.91 (78.56)	3.84 (71.28)	3.67 (66.72)	3.79 (73.40)	3.78/3.92 (60.55)
F: (1→2,6)-α-Man*p*	5.14 (100.05)	4.03 (78.59)	3.88 (71.28)	3.62 (66.03)	3.78 (73.08)	3.77/3.92 (70.11)
G: α-Gal*p*-(1→	4.96 (101.69)	3.94 (72.16)	4.02 (69.59)	3.87 (71.28)	3.72 (73.01)	3.64/3.54 (61.26)
H: (1→3)-α-Gal*p*	4.99 (101.86)	3.93 (72.26)	4.14 (78.62)	3.86 (71.15)	3.73 (72.58)	3.63 (61.17)

By correlating the peaks of HSQC spectrum based on ^{1}H NMR and ^{13}C NMR, the anomeric signals of EPS-LM-n were identified to be δ 4.95/101.84, δ 4.89/98.03, δ 4.96/102.23, δ 4.83/101.61, δ 5.21/100.11, δ 5.14/100.05, δ 4.96/101.69, δ 4.99/101.86. For residue A, proton signal at δ 4.95 with carbon signal at δ 101.84 confirmed it α-Glc*p*-(1→. Furthermore, compared with glucose standard, the signals of C1 and C4 shifted to the downfield, confirming that residue B was (1→4)-α-Glc*p* (Y. Wang et al., 2019). For residue C, the downfield resonance of C4 at δ 77.94 and C6 at δ 66.02 indicated 4-O and 6-O substitutions. Proton signal at δ 3.41 had a corresponding carbon signal at δ 60.89 in HSQC spectrum, suggesting the presence of *O*-methyl groups (OMe). The inter-residual cross signals of OMe H/C6 C and C H6/C OMe at δ 3.41/66.02 and δ 3.53/60.89 in HMBC spectrum (**Figure 4-3D**) suggests that OMe group is linked to the C6 position of residue C. These evidences demonstrated that residue C was (1→4)-α-6-O-Me-α-Glc*p* (Z. Liang et al., 2022). The proton signal at 4.96 ppm and carbon signal at 102.23 ppm was the signal of α-Man*p*-(1→, which was residue D. For residue E, the signals of C1 and C2 shifted to the downfield, confirming the presence of (1→2)-α-Man*p*. Residue F was confirmed to be (1→2,6)-α-Man*p* based on the chemical shift of C2 (δ 78.59), C6 (δ 70.11) to the low field (Y. Chen et al., 2021). The proton signal at δ 4.96 and carbon signal at δ 101.69 demonstrated that residue G was α-Gal*p*-(1→ (Clarke et al., 2018). The carbon signal of C3 at δ 78.62 shifted to the downfield, suggesting (1→3)-α-Gal*p* of residue H (Stojkovic et al., 2017).

The structure and connection mode of EPS-LM-n was shown in **Figure 4-3D**. The cross-peaks A H1/C4 B revealed the linkage of α-Glc*p*-(1→4)-α-Glc*p*-(1→ and B H1/C6 F revealed the linkage of →4)-α-Glc*p*-(1→2,6)-α-Man*p*-(1→. The cross-peaks H H1/C6 F indicated the linkage of →3)-α-Gal*p*-(1→2,6)-α-Man*p*. G H1/C6 F and G H1/C3 H indicated terminal α-Gal*p*-(1→2,6)-α-Man*p*-(1→ and α-Gal*p*-(1→3)-α-Gal*p*-(1→. E H2/C1 and E H1/C2 D indicated that the backbone of the polysaccharide mainly consisted of (1→2)-α-Man*p* (Y. Chen

et al., 2021). The signals of δ 3.77/102.23 (F H6/C1 D) and δ 4.96/70.11 (D H1/C6 F) implied the linkage of α-Man*p*-(1→2,6)-α-Man*p*-(1→. The signal of δ 4.95/70.11 (G H1/C6 F) indicated the presence of the linkage of α-Gal*p*-(1→2,6)-α-Man*p*-(1→.

Based on the monosaccharide composition analysis, methylation results and NMR spectrum, the structure for EPS-LM-n had a backbone of →2)-α-Man*p*-(1→ branched at the O-6. The side-chains were composed of →4)-α-Glc*p*-(1→, which were located outside of the Man core and mostly linked to O-6 of the →2)-α-Man*p*-(1→. Some of the →4)-α-Glc*p*-(1→ residues had 6-O methyl modification. The site of Gal was at a more outer position. This has an →3)-α-Gal*p*-(1→ linked to O-6 of the →2)-α-Man*p*-(1→. In addition, α-Man*p*-(1→ residues and α-Gal*p*-(1→ residues were present in the side-chains.

4.3.5 Hypoglycemic activities

In the in the of human digestive system, α-amylase which mainly exists in the pancreas specifically hydrolyzing the α-1,4-glycosidic bonds of starch into disaccharides and oligosaccharides. Disaccharides and oligosaccharides are further hydrolyzed into glucose by α-glucosidase in the brush border of the small intestine for intestinal absorption. Therefore, inhibition of these enzyme activities can effectively slow down the rate of dietary glucose release. As shown in **Figure 4-4A**, the inhibitory effects of EPS-LM-n against α-amylase followed a concentration-dependent trend, ranging from 0.2 to 1 mg/mL, though with significantly lower potency than commercial anti-diabetes drug, acarbose. The IC_{50} of EPS-LM-n was about 0.64 mg/mL, which was significantly lower and more potent than some reported fungal polysaccharides, such as those from *Lentinula edodes* (more than 1.22 mg/mL) (Yin et al., 2023) and *Tricholoma matsutake* (3.75 mg/mL) (H.-R. Yang, Chen, & Zeng, 2021). As shown in **Figure 4-4B** the α-glucosidase inhibitory activity of EPS-LM-n and acarbose increased with higher concentrations and was concentration-dependent. The IC_{50} value of EPS-LM-n was 0.74 mg/mL, which was also higher than that of acarbose (0.49 mg/mL). At 0.2

mg/mL, EPS-LM-n showed only 12.19% inhibition and gradually increased to 52.6% inhibition at 1 mg/mL. Besides, EPS-LM-n showed a much higher inhibitory activity compared with EPS-III extracted from *Cordyceps militaris*, which was around 40.5% (H. Sun, Yu, Li, & Zhu, 2021). Although the positive control acarbose (diabetes drug) had a stronger activity than EPS-LM-n, it may produce side effects on patients such as flatulence and diarrhea accompanying (Y. Dong et al., 2022). In contrast, EPS-LM-n may have lower or no side effects and also have other health benefits and a favourable and potential α-amylase and α-glucosidase inhibitor.

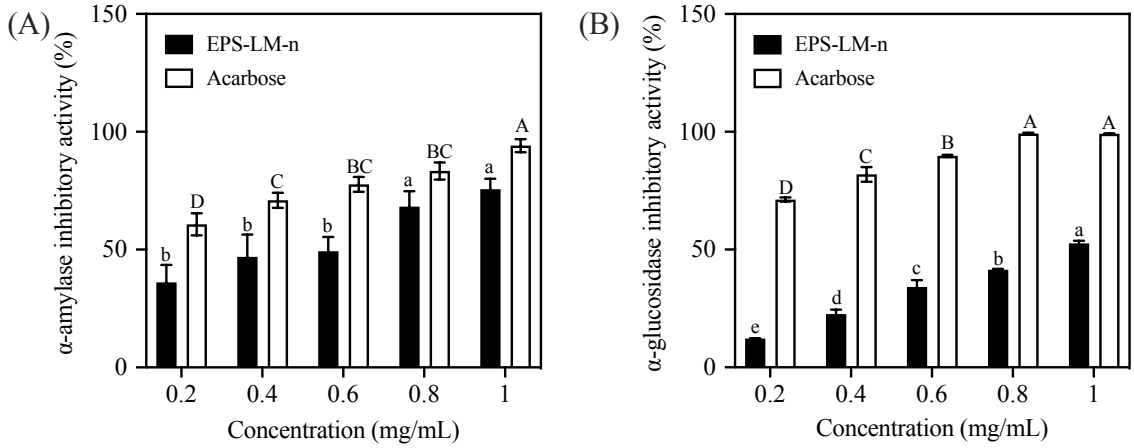

Figure 4-4. α-amylase (A) and α-glucosidase (B) inhibitory activities of EPS-LM-n *in vitro*, acarbose as a positive control.

The monosaccharide composition and structural characterization of EPS-LM-n played an important role in hypoglycemic activities. EPS-LM-n was a mannan-based polysaccharide and exhibited a backbone dominated by (1→2)-α-linked mannose residues, which is critical for its enzyme-inhibitory function. Mannans are recognized for their ability to modulate glucose metabolism by reducing postprandial blood glucose and enhancing insulin sensitivity (Z. Huang et al., 2020). This aligned with studies demonstrating that α-mannose linkages, particularly (1→2)-α-Man*p* and (1→2,6)-α-Man*p*, directly affect digestive enzymes (Jing, Zong, Li, Surhio, & Ye, 2016). Beyond Man, the presence of Glc and Gal in EPS-LM-n

significantly contributed to the hypoglycemic bioactivity. Hsu et. al (Hsu et al., 2013) established a quantitative structure-relationship showing that Glc and Gal linearly correlated with α-glucosidase inhibition. In addition, the complex structure of EPS-LM-n, characterized by its branched side chains, such as →4)-α-Glc*p*-(1→, →3)-α-Gal*p*-(1→, may physically hinder the binding of create α-amylase and α-glucosidase to the substrates. These branched side chains could create spatial barriers that inhibit the access of enzymes to the active sites, thereby disrupting their function. Furthermore, EPS-LM-n is likely to function as a competitive inhibitor to starch and reduce the hydrolysis of substrates. Deng et. al (Y. Deng et al., 2020) uncovered that polysaccharides may attach to the starch and hinder the hydrolysis of starch by α-amylase and affect the spatial configuration of α-amylase. Moreover, the existence of polysaccharides leaded to changes in the polarity and molecular conformation of α-glucosidase, resulting in the loss of the enzyme activities (J.-Q. Zhang et al., 2019). Overall, gradual increase in inhibitory activity suggests potential for hypoglycemic activity of EPS-LM-n.

4.3.6 Antioxidant activities

Excessive free radicals can compromise the body's defense mechanisms and lead to chronic diseases, making free radical scavenging an essential measure of antioxidant capacity (Yakun Zhang et al., 2023). **Figure 4-5A** showed the hydroxyl radical scavenging activities of EPS-LM-n and Vc at various concentrations. The scavenging activity of EPS-LM-n was significantly increased from 42.8% to 80.62% with increasing concentration. Vc tended to scavenge hydroxyl radicals from 59.32% to 87.91%. Within the tested concentration range, the scavenging activity of EPS-LM-n was much stronger than that of an extracellular polysaccharide from *Cordyceps militaris* (Yangbian Guo et al., 2024). It demonstrated that EPS-LM-n had potential antioxidant activity for scavenging hydroxyl radicals.

The DPPH radical scavenging assay evaluates antioxidants based on their hydrogen-donating capabilities and is widely recognized as a reliable method for measuring the free-

radical scavenging activities of such compounds (Z. Chen et al., 2020). **Figure 4-5B** showed the DPPH radicals scavenging activities of EPS-LM-n and Vc with various concentrations. Obviously, EPS-LM-n exhibited a concentration-dependent scavenging DPPH activity, increasing from 41.97% to 62.9% in the concentration range of 0.2-1.0 mg/mL. Similar scavenging ability has been reported of a purified EPS from *Paecilomyces cicadae* (Miq.) Samson (L. He, Wu, Cheng, Li, & Lu, 2010). Vc showed a potent activity to scavenge DPPH radicals completely even at the lowest concentration.

The ABTS radical scavenging assay is commonly accepted as an effective method for assessing the total antioxidant capacity of natural products (Khaskheli et al., 2015). **Figure 4-5C** showed the ABTS radicals scavenging activities of EPS-LM-n and Vc with various concentrations. At an initial concentration of 0.2 mg/mL, the scavenging rate was only 23.46%. However, with the increasing concentrations, EPS-LM-n exhibited a certain dose-effect relationship and compared with the previous literature, EPS-LM-n showed stronger ABTS radical scavenging activity than the polysaccharides from a cultured *Ophiocordyceps sinensis* fungus (Huynh, Tran, & Dinh, 2024).

The FRAP capacity of EPS-LM-n was determined and shown in **Figure 4-5D**. The antioxidant potential of various samples were assessed by their capability to convert the TPTZ–Fe (III) complex into the TPTZ–Fe (II) complex. While Vc demonstrated significantly greater FRAP ability compared to EPS-LM-n, the latter showed a concentration-dependent FRAP ability within the range of 0.2 to 1.0 mg/mL, in that the FRAP values from 36.04 μM to 597.48 μM. Moreover, the FRAP value of EPS-LM-n at 1 mg/mL was higher than of the two polysaccharides, CMP-3 and CMP-4, extracted from *Cordyceps militaris* (R. Chen et al., 2014). These results implied that EPS-LM-n possessed noticeable antioxidant activities.

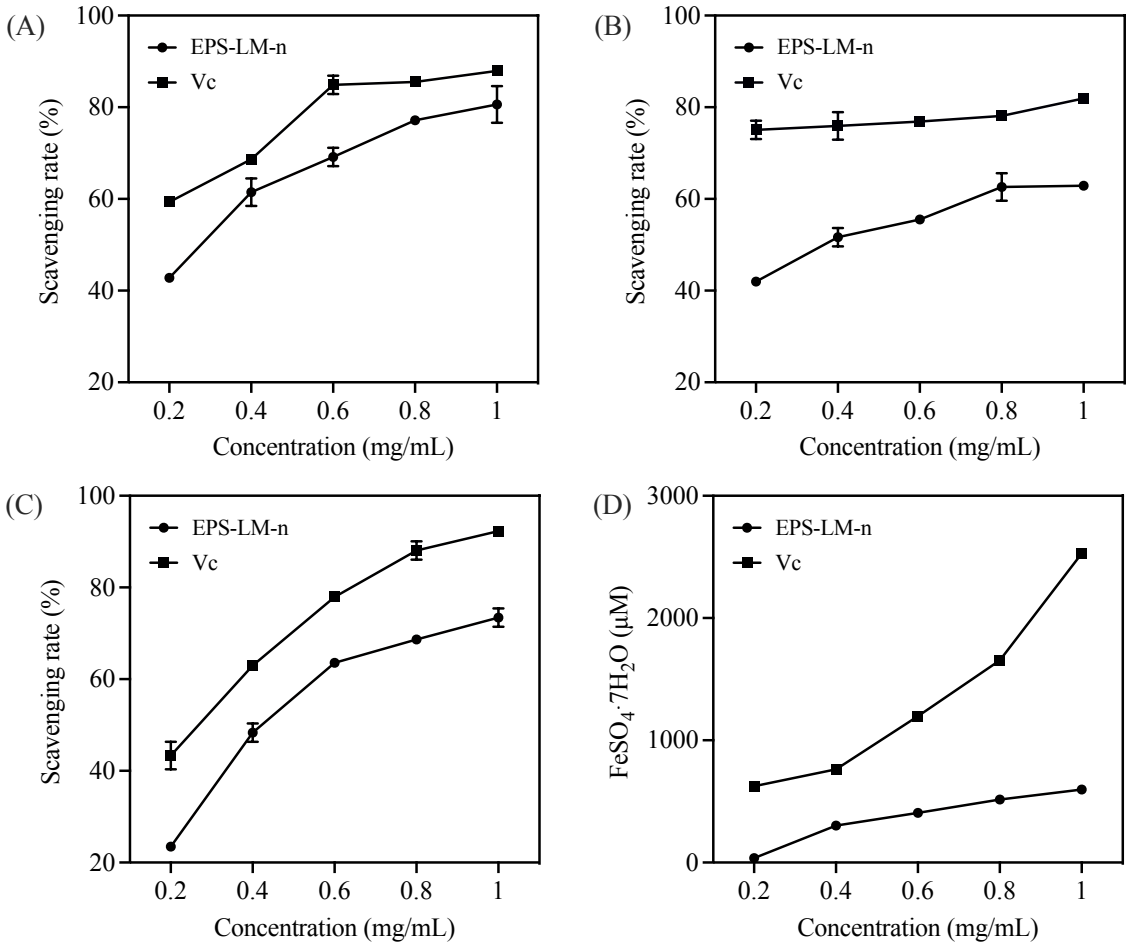

Figure 4-5. Antioxidant activities of EPS-LM-n. (A) Hydroxyl radical scavenging activity; (B) DPPH radicals scavenging activity; (C) ABTS radicals scavenging activity; (D) FRAP ability.

4.3.7 Protective effects of EPS-LM-n on EA. hy926 cells against oxidative damage

4.3.7.1 Effects of EPS-LM-n on cell viability and intracellular ROS generation

As shown in **Figure 4-6A**, H_2O_2 with varying concentrations (50-700 μM) reduced the cell viability in EA.hy 926 cells compared with untreated cells (with medium only). It illustrated that the viability of EA.hy926 cells diminished in a concentration-dependent manner upon H_2O_2 treatment. Similar to previous studies that a cell-challenged model can be successfully constructed by reducing cell viability to approximately 50 % through H_2O_2 induction (R. Liang, Zhang, & Lin, 2017), the cell culture treated with 300 μM H_2O_2 exhibited a viability of 44.46 ± 0.03%, and was for subsequent experiments. As shown in **Figure 4-6B**, all concentrations of

EPS-LM-n showed no-toxic to EA. hy926 cell in the concentrations range of 50-300 μg/mL and it did not interfere with the cell growth and viability. Compared with untreated cells, EPS-LM-n could significantly restore the cell viability impaired by H_2O_2 (300 μM), with cell viability from 49.91% to 95.41%, exhibited in **Figure 4-6C**.

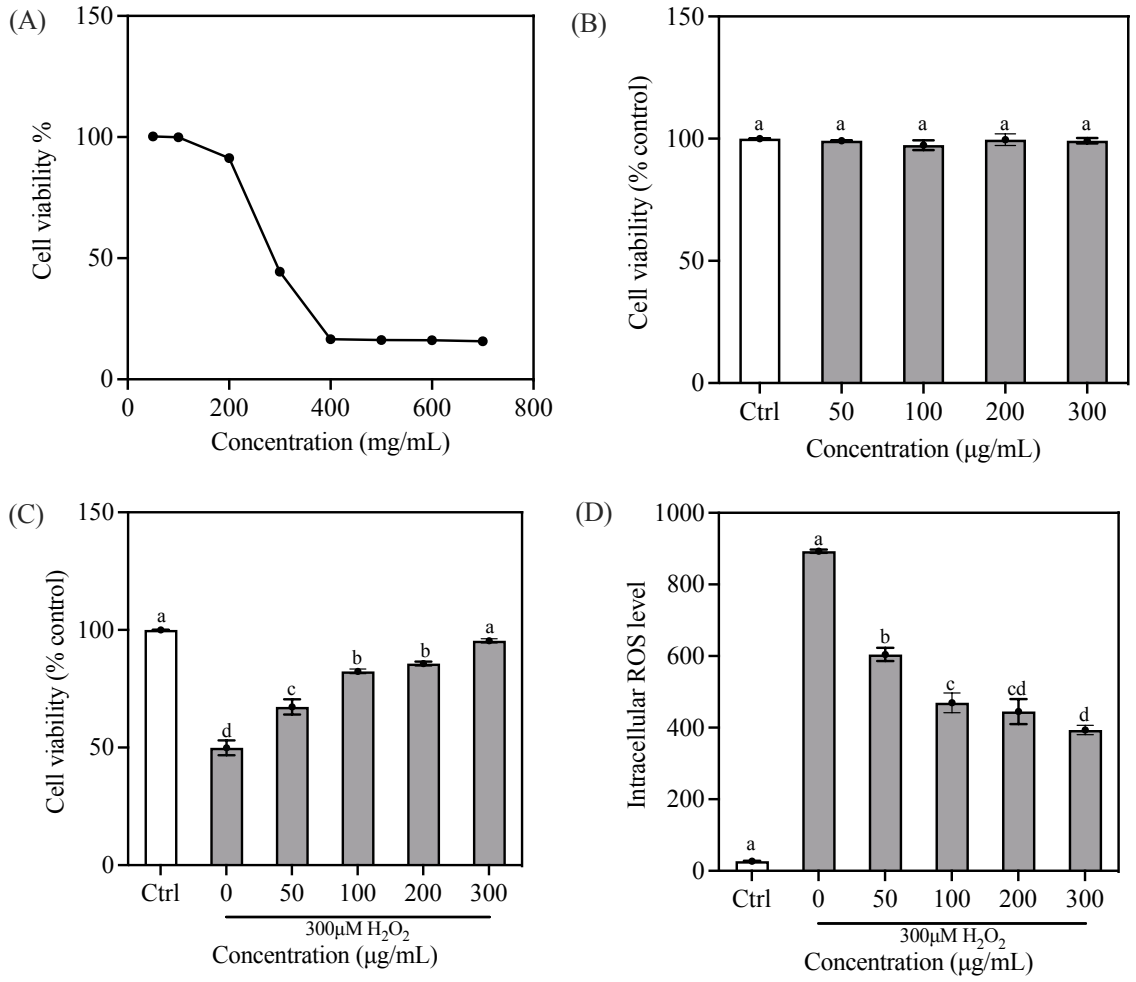

Figure 4-6. (A) Cell viability of EA. hy926 cells treated with different concentrations of H_2O_2; Effects of EPS-LM-n on EA. hy926 cells at different concentrations: (B) Cell viability in normal culture; (C) Cell viability in culture exposed to 300 μM H_2O_2; (D) Intracellular ROS levels in culture exposed to 300 μM H_2O_2. (Cell viability values were expressed as percentage of the untreated group which was normalized to 100%).

DCFH-DA is a widely utilized probe for monitoring cellular redox activities and was also applied in the present study. **Figure 4-6D** shows the intracellular ROS levels in EA.hy926 cells

exposed to 300 μM H_2O_2 and after treatment with EPS-LM-n. Compared to the normal culture, a significant increase in ROS levels was observed in cells exposed with 300 μM H_2O_2 only, which was notably reduced by EPS-LM-n at 50-300 mg/mL. Furthermore, EPS-LM-n demonstrated a dose-dependent decrease in ROS levels in H_2O_2-induced EA.hy926 cells. Specifically, ROS levels in the group treated with 300 μg/mL EPS-LM-n were reduced by 56.05% relative to the group treated with 300 μM H_2O_2 alone. These findings suggest that EPS-LM-n effectively scavenges intracellular ROS.

4.3.7.2 Effects of EPS-LM-n on ROS-induced apoptosis of EA. hy926 cells

As shown in **Figure 4-7A**, the percentage of apoptotic cells induced by H_2O_2 was significantly decreased in EA.hy926 cells upon treatment with EPS-LM-n at 100 and 300 μg/mL. The normal culture group without any treatment showed normal cells 96.1%, early apoptotic cells 1.63%, late apoptotic cells 0.71% and necrotic cells 1.52%. The H_2O_2 treated group showed normal cells 33.9%, early apoptotic cells 56%, late apoptotic cells 3.51% and necrotic cells 6.58%. The percentage of normal cells in H_2O_2-treated group was increased to 69.3% with 100 μg/mL EPS-LM-n and to 73.1% with 300 μg/mL EPS-LM-n. The increasing percentage of apoptotic cells induced by H_2O_2 in EA.hy926 cells (**Figure 4-7B**) was effectively reduced with the treatment of EPS-LM-n. These results suggested that EPS-LM-n could effectively reduce oxidative damage and intracellular ROS level and protect the EA.hy926 cells against H_2O_2-induced apoptosis.

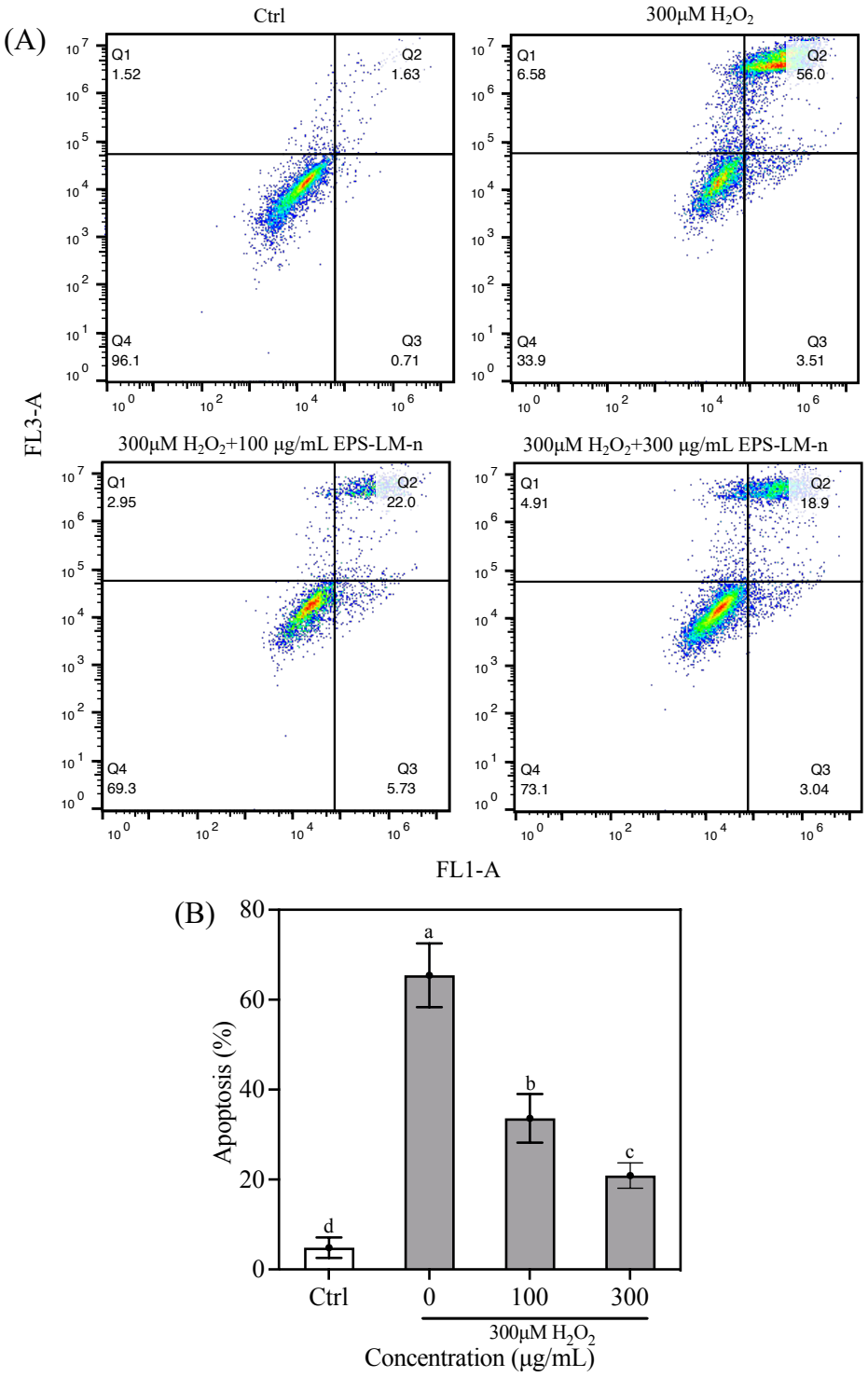

Figure 4-7. EPS-LM-n significantly decreased cell apoptosis in H_2O_2-treated EA.hy926 cells. (A) Cells were treated with different concentrations of H_2O_2 and EPS-LM-n. (B) Results were quantitively analyzed. Cells were seeded with 5×10^5/mL and incubated for 24 h.

These results indicated that EPS-LM-n exhibited dual bioactivities, specifically hypoglycemic and antioxidant activities. Both hyperglycemia and oxidative stress are known to drive vascular endothelial dysfunction, contributing to CVDs (S. Jin & Kang, 2024; Poznyak et al., 2022). EPS-LM-n significantly inhibited the activities of α-glucosidase and α-amylase *in vitro*, suggesting that EPS-LM-n could effectively slow down the degradation of carbohydrates into glucose and reduce the level of postprandial blood glucose (Y. Yao et al., 2024). Whereas hyperglycemia, or elevated glucose levels, are closely associated with excessive ROS production in cells, which poses a major risk of endothelial damage (D. R. Yang, Wang, Zhang, & Wang, 2024). By inhibiting these enzymes, EPS-LM-n may not only help manage hyperglycemia but also contribute to reducing oxidative stress and endothelial dysfunction. On the other hand, H_2O_2-induced cell model directly demonstrated that EPS-LM-n effectively reduced intracellular ROS accumulation and suppressed apoptosis, thereby enhancing the viability of oxidatively stressed EA. hy926 cells. These evidence strongly supported the ability of EPS-LM-n to repair the oxidative damage at the cellular level. Therefore, targeting endothelial injury and potentially mitigating the progression of CVDs, EPS-LM-n could serves as a dual-action agent that scavenges ROS, protect endothelial cells from apoptosis and indirectly mitigate hyperglycemia-induced oxidative stress (**Figure 4-8**).

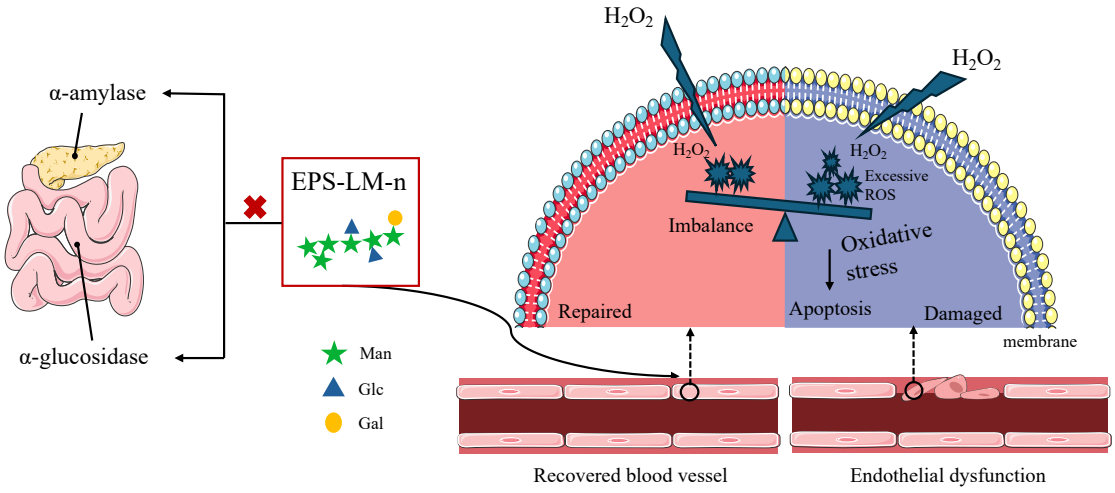

Figure 4-8. Schematic illustration of EPS-LM-n protective effects against H_2O_2-treated EA.hy926 cells.

Overall, the relationship between structural characteristics of polysaccharides from different fungal species and their biological functions are closely related. For example, a neutral EPS composed of Man, Glc and Gal, designated EPS-III, from an edible fungus *Cordyceps militaris* showed significant α-glucosidase inhibitory activity (H. Sun et al., 2021). This suggested that the presence of mannose may enhance the ability of EPS-LM-n to regulate glucose levels. Similarly, mannose-rich polysaccharide from *Auricularia auricula-judae* (Bull.) Quél. was shown to significantly reduce oxidative stress and improve glucose metabolism disorder (Q. Shi et al., 2024). The high content of mannose in these polysaccharides is likely to contribute to their bioactivity, as mannose has been proved to participate in various metabolic activities and cellular signalling pathways (Dhanalakshmi et al., 2023). Furthermore, an EPS from *Streptomyces* strain composed of Man and Glc (molar ratio 4.1:1) showed antioxidant activities by effectively scavenging DPPH and hydroxyl radicals. Additionally, a heteropolysaccharide isolated from the fruit body of *Cordyceps militaris*, composed of (1→2)-α-D-Man*p* residue showed significant antioxidant and immunoregulation activities (Ying Zhang et al., 2020). Similar to EPS-LM-n, all these fungal polysaccharides in the literature contained mannose as a major monosaccharide and some also contained →2)-α-Man*p*-(1→ in the chain structure. In addition, MW was another crucial factor as previous studies have shown that lower MW tend to have higher antioxidant activities (L. Zheng et al., 2021). The findings from studies are supportive to the significance of the mannan-rich composition along with a (1→2)-α-Man*p* backbone of EPS-LM-n in the bioactivities against hyperglycemia and oxidative stress and protective effect on the vascular endothelial cells.

4.4 Conclusions

Through this study, a neutral and mannose-rich heteropolysaccharide, designated EPS-LM-n, was isolated and purified from the lower-MW fraction of Cs-HK1 EPS a homogenous MW of 417 kDa. Its structure was fully characterized and elucidated as a backbone of a →2)-α-Man*p*-(1→ linkage, complemented by branched structures of →4)-α-Glc*p*-(1→, →3)-α-Gal*p*-(1→. EPS-LM-n effectively inhibited two major digestive enzymes, α-glucosidase and α-amylase, suggesting its potential hypoglycemic activity. EPS-LM-n also exhibited significant antioxidant activities, as evidenced by its ability to scavenge hydroxyl radicals and protect EA.hy926 vascular endothelial cells from oxidative damage. This protective effect was characterized by increased cell viability, reduced reactive oxygen species levels and decreased apoptosis rates. Overall, the results and findings signified the potential of EPS-LM-n as a nutraceutical ingredient for managing hyperglycemic and oxidative stress-related disorders. While the *in vitro* results are promising, further investigations, especially *in vivo* studies, are essential to fully assess the mechanisms of action and therapeutic efficacy of EPS-LM-n. More systematic assessment and comprehensive understanding of the structure-activity relationship pave the way for development and application of EPS-LM-n for dietary intervention and therapeutic treatment of metabolic and cardiovascular diseases.

Chapter 5 General conclusions and future studies

5.1 General conclusions

This research has completed an experimental study on different fractions of exopolysaccharide (EPS) from Cs-HK 1 fungal mycelial fermentation. The chief findings from this study are summarized below.

1) *In vitro* fecal fermentation studies showed that EPS-LM, EPS-HM and LBPS with different molecular compositions and properties were resistant to enzyme and acid hydrolysis during *in vitro* simulated gastrointestinal digestion and mainly consumed by gut bacterial fermentation in the large intestine. The monosaccharide composition, instead of the molecular weight, of the polysaccharides appeared to be a significant factor for their different metabolic outcomes in the gut microbiota.
2) EPS-LM and LBPS altered the microbiota composition differently particularly the relative abundance of gut bacterial populations such as the ratio of *Firmicutes* to *Bacteroidetes*. The initial differences in the microbiota composition among the different human fecal donors only had subtle and minor influence on the results.
3) Mannose and galactose-rich EPS-LM significantly increased the production of propionic acid, glucose-rich EPS-HM was found to enhance the production of butyric acid. Both EPS fractions metabolites could decrease NO and IL-1β levels, increase TEER value, upgrade the mRNA expression levels of Claudin-1, Occludin and ZO-1, and protein expression levels of ZO-1 and Claudin-1 in LPS-induced Caco-2/RAW264.7 co-culture model.
4) Through DEAE and superdex purification, a neutral polysaccharide, EPS-LM-n was obtained, with a homogenous MW 417kDa. EPS-LM-n consisted of Man, Glc and Gal with molar ratio 1:0.49:0.21. The backbone of EPS-LM-n consisted of a →2)-α-Man*p*(1→ with branches →4)-α-Glc*p*(1→, →3)-β-Gal*p*(1→. EPS-LM-n had an

inhibitory effect on α-glucosidase and α-amylase, exhibiting potent hypoglycemic effects.

5) Antioxidant activities of EPS-LM-n was also evaluated *in vitro*. Results of hydroxyl, ABTS, DPPH radical scavenging and FRAP ability assays showed that EPS-LM-n had potential antioxidant activities. EPS-LM-n significantly increased cell viability, decreased ROS level and cell apoptosis on EA.hy926 cells with H_2O_2 induced oxidative damage.

5.2 Future studies

The results from this research provide useful reference and foundation for further study, development and application of fungi EPS with strong prebiotic potential for modulating the gut microbiota and hypoglycemic and antioxidant activities. Specifically, the following studies are recommended for future work.

1) DSS/LPS induced inflammatory bowel disease (IBD) animal models will be employed to validate the specific roles of Cs-HK1 EPS in intestinal metabolism, focusing on the regulatory mechanisms that control their effects on gut function and interactions with host. EPS-LM (mannose-rich) and EPS-HM (glucose-rich) will treat the animal models with low, medium and high dose (50 mg/kg/d, 100 mg/kg/d and 200 mg/kg/d).
2) The anti-inflammatory mechanisms will be elucidated using LPS-induced inflammation models, focusing on the inflammatory signaling pathways to determine how EPS metabolites exhibit their protective effects.
3) The high-fat diet-fed mouse model will be utilized to verify the hypoglycemic activities of EPS-LM-n. We will further perform controlled enzymatic degradation of EPS-LM-n to obtain specific oligosaccharides, and compare their *in vitro* and *in vivo* activities with the native polymer to establish a precise structure-activity relationship.

4) A comparative structural and biological analysis of diverse fungal EPS will be conducted to identify the structural similarities that correlate with their biological activities. A comparative genomics and glycomics analysis will be conducted on EPS from different medicinal fungi. We will also correlate glycosidic linkage patterns and branching degrees with their prebiotic selectivity and bioactivity profiles, thereby enhancing our understanding of fungal polysaccharides functional potential.

References

Ahmadi, E., Rezadoost, H., Alilou, M., Stuppner, H., & Farimani, M. M. (2022). Purification, structural characterization and antioxidant activity of a new arabinogalactan from Dorema ammoniacum gum. *International Journal of Biological Macromolecules, 194*, 1019-1028.

Alonso-Gil, S., Parkan, K., Kaminský, J., Pohl, R., & Miyazaki, T. (2022). Unlocking the Hydrolytic Mechanism of GH92 α-1,2-Mannosidases: Computation Inspires the use of C-Glycosides as Michaelis Complex Mimics. *Chemistry – A European Journal, 28*(14), e202200148.

An, X., Bao, Q., Di, S., Zhao, Y., Zhao, S., Zhang, H., Lian, F., & Tong, X. (2019). The interaction between the gut Microbiota and herbal medicines. *Biomed Pharmacother, 118*, 109252.

An, Y., Xu, B.-T., Wan, S.-R., Ma, X.-M., Long, Y., Xu, Y., & Jiang, Z.-Z. (2023). The role of oxidative stress in diabetes mellitus-induced vascular endothelial dysfunction. *Cardiovascular Diabetology, 22*(1), 237.

Arumugam, M., Raes, J., Pelletier, E., Le Paslier, D., Yamada, T., Mende, D. R., Fernandes, G. R., Tap, J., Bruls, T., & Batto, J.-M. (2011). Enterotypes of the human gut microbiome. *Nature, 473*(7346), 174-180.

Bai, G., Xie, Y., Gao, X., Xiao, C., Yong, T., Huang, L., Cai, M., Liu, Y., Hu, H., & Chen, S. (2024). Selective impact of three homogenous polysaccharides with different structural characteristics from Grifola frondosa on human gut microbial composition and the structure-activity relationship. *International Journal of Biological Macromolecules, 269*, Article 132143.

Bai, J., Li, T., Zhang, W., Fan, M., Qian, H., Li, Y., & Wang, L. (2021). Systematic assessment of oat β-glucan catabolism during in vitro digestion and fermentation. *Food Chemistry, 348*, Article 129116.

Bai, Y., Liu, L., Zhang, R., Huang, F., Deng, Y., & Zhang, M. (2017). Ultrahigh pressure-assisted enzymatic extraction maximizes the yield of longan pulp polysaccharides and their acetylcholinesterase inhibitory activity in vitro. *International Journal of Biological Macromolecules, 96*, 214-222.

Bartolomaeus, H., Balogh, A., Yakoub, M., Homann, S., Markó, L., Höges, S., Tsvetkov, D., Krannich, A., Wundersitz, S., & Avery, E. G. (2019). Short-chain fatty acid propionate protects from hypertensive cardiovascular damage. *Circulation, 139*(11), 1407-1421.

Bie, N., Duan, S., Meng, M., Guo, M., & Wang, C. (2021). Regulatory effect of non-starch polysaccharides from purple sweet potato on intestinal microbiota of mice with antibiotic-associated diarrhea. *Food & Function, 12*(12), 5563-5575.

Binda, C., Lopetuso, L. R., Rizzatti, G., Gibiino, G., Cennamo, V., & Gasbarrini, A. (2018). Actinobacteria: a relevant minority for the maintenance of gut homeostasis. *Digestive and Liver Disease, 50*(5), 421-428.

Black, I., Heiss, C., & Azadi, P. (2019). Comprehensive Monosaccharide Composition Analysis of Insoluble Polysaccharides by Permethylation To Produce Methyl Alditol Derivatives for Gas Chromatography/Mass Spectrometry. *Analytical chemistry, 91*(21), 13787-13793.

Brodkorb, A., Egger, L., Alminger, M., Alvito, P., Assunção, R., Ballance, S., Bohn, T., Bourlieu-Lacanal, C., Boutrou, R., & Carrière, F. (2019). INFOGEST static in vitro simulation of gastrointestinal food digestion. *Nature protocols, 14*(4), 991-1014.

Buckley, A. G., Looi, K., Iosifidis, T., Ling, K.-M., Sutanto, E. N., Martinovich, K. M., Kicic-Starcevich, E., Garratt, L. W., Shaw, N. C., & Lannigan, F. J. (2018). Visualisation of multiple tight junctional complexes in human airway epithelial cells. *Biological procedures online, 20*, 1-9.

Celebi Sozener, Z., Ozdel Ozturk, B., Cerci, P., Turk, M., Gorgulu Akin, B., Akdis, M., Altiner, S., Ozbey, U., Ogulur, I., & Mitamura, Y. (2022). Epithelial barrier hypothesis: effect of the external exposome on the microbiome and epithelial barriers in allergic disease. *Allergy, 77*(5), 1418-1449.

Chang, S. T., & Wasser, S. P. (2018). Current and future research trends in agricultural and biomedical applications of medicinal mushrooms and mushroom products. *International Journal of Medicinal Mushrooms, 20*(12).

Chen, C., Wu, W., Xu, X., Zhang, L., Liu, Y., & Wang, K. (2014). Chain conformation and anti-tumor activity of derivatives of polysaccharide from Rhizoma Panacis Japonici. *Carbohydrate Polymers, 105*, 308-316.

Chen, G., Bai, Y., Zeng, Z., Peng, Y., Zhou, W., Shen, W., Zeng, X., & Liu, Z. (2021). Structural characterization and immunostimulatory activity of heteropolysaccharides from Fuzhuan brick tea. *Journal of Agricultural and Food Chemistry, 69*(4), 1368-1378.

Chen, J., & Seviour, R. (2007). Medicinal importance of fungal beta-(1-->3), (1-->6)-glucans. *Mycol Res, 111*(Pt 6), 635-652.

Chen, J., Zhang, W., Lu, T., Li, J., Zheng, Y., & Kong, L. (2006). Morphological and genetic characterization of a cultivated Cordyceps sinensis fungus and its polysaccharide

component possessing antioxidant property in H22 tumor-bearing mice. *Life Sciences, 78*(23), 2742-2748.

Chen, J., Zhou, M., Liu, M., & Bi, J. (2022). Physicochemical, rheological properties and in vitro hypoglycemic activities of polysaccharide fractions from peach gum. *Carbohydrate Polymers, 296*, 119954.

Chen, R., Jin, C., Li, H., Liu, Z., Lu, J., Li, S., & Yang, S. (2014). Ultrahigh pressure extraction of polysaccharides from Cordyceps militaris and evaluation of antioxidant activity. *Separation and Purification Technology, 134*, 90-99.

Chen, Y., Wang, T., Zhang, X., Zhang, F., & Linhardt, R. J. (2021). Structural and immunological studies on the polysaccharide from spores of a medicinal entomogenous fungus Paecilomyces cicadae. *Carbohydrate Polymers, 254*, 117462.

Chen, Y., Xie, M.-Y., & Gong, X.-F. (2007). Microwave-assisted extraction used for the isolation of total triterpenoid saponins from Ganoderma atrum. *Journal of Food Engineering, 81*(1), 162-170.

Chen, Z., Zhao, Y., Zhang, M., Yang, X., Yue, P., Tang, D., & Wei, X. (2020). Structural characterization and antioxidant activity of a new polysaccharide from Bletilla striata fibrous roots. *Carbohydrate Polymers, 227*, 115362.

Clarke, B. R., Ovchinnikova, O. G., Kelly, S. D., Williamson, M. L., Butler, J. E., Liu, B., Wang, L., Gou, X., Follador, R., Lowary, T. L., & Whitfield, C. (2018). Molecular basis for the structural diversity in serogroup O2-antigen polysaccharides in Klebsiella pneumoniae. *Journal of Biological Chemistry, 293*(13), 4666-4679.

Crovesy, L., Masterson, D., & Rosado, E. L. (2020). Profile of the gut microbiota of adults with obesity: a systematic review. *European journal of clinical nutrition, 74*(9), 1251-1262.

da Rosa, B. V., Bresolin, T. H., Ugalde, G. A., & Kuhn, R. C. (2024). Purification of bioactive polysaccharides from Lentinula edodes using fixed-bed column with activated carbon. *Separation Science and Technology, 59*(5), 762-772.

da Silva Fonseca, M., Marchioro, M. L. K., Guimarães, D. K., Góes-Neto, A., Drechsler-Santos, E. R., Santos, V. A., Barbosa-Dekker, A. M., Dekker, R. F., & Cunha, M. A. (2020). Neodeightonia phoenicum CMIB-151: isolation, molecular identification, and production and characterization of an exopolysaccharide. *Journal of Polymers and the Environment, 28*, 1954-1966.

Dabke, K., Hendrick, G., & Devkota, S. (2019). The gut microbiome and metabolic syndrome. *The Journal of clinical investigation, 129*(10), 4050-4057.

Deng, H., Yang, S., Zhang, Y., Qian, K., Zhang, Z., Liu, Y., Wang, Y., Bai, Y., Fan, H., & Zhao, X. (2018). Bacteroides fragilis prevents Clostridium difficile infection in a mouse model by restoring gut barrier and microbiome regulation. *Frontiers in microbiology, 9*, 2976.

Deng, Y., Huang, L., Zhang, C., Xie, P., Cheng, J., Wang, X., & Liu, L. (2020). Novel polysaccharide from Chaenomeles speciosa seeds: Structural characterization, α-amylase and α-glucosidase inhibitory activity evaluation. *International Journal of Biological Macromolecules, 153*, 755-766.

Dhanalakshmi, M., Sruthi, D., Jinuraj, K. R., Das, K., Dave, S., Andal, N. M., & Das, J. (2023). Mannose: a potential saccharide candidate in disease management. *Medicinal Chemistry Research, 32*(3), 391-408.

Dong, R., Liu, S., Xie, J., Chen, Y., Zheng, Y., Zhang, X., Zhao, E., Wang, Z., Xu, H., & Yu, Q. (2021). The recovery, catabolism and potential bioactivity of polyphenols from carrot subjected to in vitro simulated digestion and colonic fermentation. *Food Research International, 143*, Article 110263.

Dong, Y., Sui, L., Yang, F., Ren, X., Xing, Y., & Xiu, Z. (2022). Reducing the intestinal side effects of acarbose by baicalein through the regulation of gut microbiota: An in vitro study. *Food Chemistry, 394*, 133561.

Dou, Z., Chen, C., & Fu, X. (2019). The effect of ultrasound irradiation on the physicochemical properties and α-glucosidase inhibitory effect of blackberry fruit polysaccharide. *Food Hydrocolloids, 96*, 568-576.

Duan, C., Qiao, S., Wang, N., Zhao, Y., Qi, C., & Yao, X. (2001). Studies on the active polysaccharides from Lycium barbarum L. *Yao xue xue bao= Acta pharmaceutica Sinica, 36*(3), 196-199.

Dubois-Deruy, E., Peugnet, V., Turkieh, A., & Pinet, F. (2020). Oxidative Stress in Cardiovascular Diseases. *Antioxidants, 9*(9), 864.

Elisashvili, V., Kachlishvili, E., & Wasser, S. (2009). Carbon and nitrogen source effects on basidiomycetes exopolysaccharide production. *Applied Biochemistry and Microbiology, 45*(5), 531-535.

Elnahas, M. O., Elkhateeb, W. A., & Daba, G. M. (2024). Nutritive profile, pharmaceutical potentials, and structural analysis of multifunctional bioactive fungal polysaccharides—A review. *International Journal of Biological Macromolecules, 266*, 130893.

Elsehemy, I. A., El Deen, A. M. N., Awad, H. M., Kalaba, M. H., Moghannem, S. A., Tolba, I. H., & Farid, M. A. (2020). Structural, physical characteristics and biological activities assessment of scleroglucan from a local strain Athelia rolfsii TEMG. *International Journal of Biological Macromolecules, 163*, 1196-1207.

Faith, J. J., Guruge, J. L., Charbonneau, M., Subramanian, S., Seedorf, H., Goodman, A. L., Clemente, J. C., Knight, R., Heath, A. C., & Leibel, R. L. (2013). The long-term stability of the human gut microbiota. *Science, 341*(6141), 1237439.

Fan, Y., & Pedersen, O. (2021). Gut microbiota in human metabolic health and disease. *Nature Reviews Microbiology, 19*(1), 55-71.

Feng, Y., Song, Y., Zhou, J., Duan, Y., Kong, T., Ma, H., & Zhang, H. (2022). Recent progress of Lycium barbarum polysaccharides on intestinal microbiota, microbial metabolites and health: A review. *Critical Reviews in Food Science and Nutrition*, 1-24.

Ferraboschi, P., Ciceri, S., & Grisenti, P. (2021). Applications of lysozyme, an innate immune defense factor, as an alternative antibiotic. *Antibiotics, 10*(12), 1534.

Gao, X., Sun, C., Zhang, Y., Hu, S., & Li, D. (2022). Dietary supplementation of L-carnitine ameliorates metabolic syndrome independent of trimethylamine N-oxide produced by gut microbes in high-fat diet-induced obese mice. *Food & Function, 13*(23), 12039-12050.

García, G., Martínez, D., Soto, J., Rodríguez, L., Nuez, M., Domínguez, N., Buchaca, E. F., Hernández, C., Sobrino, A., & Pérez, E. R. (2023). Short-Chain Fructooligosaccharides Improve Gut Microbiota Composition in Patients with Type 2 Diabetes. A randomized, Open-Label, Controlled Pilot Clinical Trial. *Journal of Biotechnology and Biomedicine, 6*(2), 244-258.

Ghosh, S., Whitley, C. S., Haribabu, B., & Jala, V. R. (2021). Regulation of Intestinal Barrier Function by Microbial Metabolites. *Cell Mol Gastroenterol Hepatol, 11*(5), 1463-1482.

Gil-Ramírez, A., Smiderle, F. R., Morales, D., Iacomini, M., & Soler-Rivas, C. (2019). Strengths and weaknesses of the aniline-blue method used to test mushroom (1→ 3)-β-d-glucans obtained by microwave-assisted extractions. *Carbohydrate Polymers, 217*, 135-143.

Gong, M., Zhu, Q., Wang, T., Wang, X., Ma, J., & Zhang, W. (1990). Molecular structure and immunoactivity of the polysaccharide from Cordyceps sinensis (Berk.) Sacc. *Sheng Wu Hua Hsueh Tsa Chih, 6*(6), 486-492.

Goushki, M. A., Kharat, Z., Fehrenbach, G. W., Murphy, E. J., Devine, D., Gately, N., & Fuemayor, E. (2025). Exploring the role of polysaccharides from macroalgae in shaping

gut microbiome and promoting anti-obesity outcomes. *Food Hydrocolloids, 160*, 110758.

Gu, F., Li, C., Hamaker, B. R., Gilbert, R. G., & Zhang, X. (2020). Fecal microbiota responses to rice RS3 are specific to amylose molecular structure. *Carbohydrate Polymers, 243*, Article 116475.

Gu, F. T., Li, J. H., Zhao, Z. C., Zhu, Y. Y., Huang, L. X., & Wu, J. Y. (2025). Metabolic outcomes of Cordyceps fungus and Goji plant polysaccharides during in vitro human fecal fermentation. *Carbohydrate Polymers, 350*, 123019.

Gu, F. T., Zhao, Z. C., Zhu, Y. Y., Huang, L. X., Li, J. H., Liu, X., & Wu, J. Y. (2025). Human fecal fermentation of high/low-molecular weight exopolysaccharides from a medicinal fungus Cs-HK1 and anti-inflammatory protection on gut barrier function. *International Journal of Biological Macromolecules, 319*, 145481.

Gulcin, İ. (2020). Antioxidants and antioxidant methods: An updated overview. *Archives of toxicology, 94*(3), 651-715.

Guo, Q., Ai, L., & Cui, S. (2019). *Methodology for structural analysis of polysaccharides*: Springer.

Guo, Q., Liang, S., Xiao, Z., & Ge, C. (2023). Research progress on extraction technology and biological activity of polysaccharides from Edible Fungi: A review. *Food Reviews International, 39*(8), 4909-4940.

Guo, Y., Cao, L., Zhao, Q., Zhang, L., Chen, J., Liu, B., & Zhao, B. (2016). Preliminary characterizations, antioxidant and hepatoprotective activity of polysaccharide from Cistanche deserticola. *International Journal of Biological Macromolecules, 93*, 678-685.

Guo, Y., Wei, Y., Liu, C., Li, H., Du, X., Meng, J., Liu, J., & Li, Q. (2024). Elucidation of antioxidant activities of intracellular and extracellular polysaccharides from Cordyceps militaris in vitro and their protective effects on ulcerative colitis in vivo. *International Journal of Biological Macromolecules, 267*, 131385.

Halliwell, B. (2006). Phagocyte-derived reactive species: salvation or suicide? *Trends in biochemical sciences, 31*(9), 509-515.

Hao, Y., Sun, H., Zhang, X., Wu, L., & Zhu, Z. (2020). A novel polysaccharide from Pleurotus citrinopileatus mycelia: Structural characterization, hypoglycemic activity and mechanism. *Food bioscience, 37*, 100735.

Hartemink, R., Schoustra, S. E., & Rombouts, F. M. (1999). Degradation of Guar Gum by Intestinal Bacteria. *Bioscience and Microflora, 18*(1), 17-25.

He, L., Wu, X., Cheng, J., Li, H., & Lu, X. (2010). Purification, composition analysis, and antioxidant activity of exopolysaccharides from mycelial culture of Paecilomyces cicadae (Miq.) Samson (Ascomycetes). *International Journal of Medicinal Mushrooms, 12*(1).

He, P., Zhang, A., Zhang, F., Linhardt, R. J., & Sun, P. (2016). Structure and bioactivity of a polysaccharide containing uronic acid from Polyporus umbellatus sclerotia. *Carbohydrate Polymers, 152*, 222-230.

He, Y., Peng, H., Zhang, H., Liu, Y., & Sun, H. (2021). Structural characteristics and immunopotentiation activity of two polysaccharides from the petal of Crocus sativus. *International Journal of Biological Macromolecules, 180*, 129-142.

Ho Do, M., Seo, Y. S., & Park, H.-Y. (2021). Polysaccharides: bowel health and gut microbiota. *Critical Reviews in Food Science and Nutrition, 61*(7), 1212-1224.

Holscher, H. D. (2017). Dietary fiber and prebiotics and the gastrointestinal microbiota. *Gut Microbes, 8*(2), 172-184.

Hsieh, C.-Y., Osaka, T., Moriyama, E., Date, Y., Kikuchi, J., & Tsuneda, S. (2015). Strengthening of the intestinal epithelial tight junction by Bifidobacterium bifidum. *Physiological Reports, 3*(3), e12327.

Hsu, W.-k., Hsu, T.-h., Lin, F.-y., Cheng, Y.-k., & Yang, J. P.-w. (2013). Separation, purification, and α-glucosidase inhibition of polysaccharides from Coriolus versicolor LH1 mycelia. *Carbohydrate Polymers, 92*(1), 297-306.

Hu, J.-L., Nie, S.-P., Min, F.-F., & Xie, M.-Y. (2013). Artificial simulated saliva, gastric and intestinal digestion of polysaccharide from the seeds of Plantago asiatica L. *Carbohydrate Polymers, 92*(2), 1143-1150.

Hu, T., Jiang, C., Huang, Q., & Sun, F. (2016). A comb-like branched β-D-glucan produced by a Cordyceps sinensis fungus and its protective effect against cyclophosphamide-induced immunosuppression in mice. *Carbohydrate Polymers, 142*, 259-267.

Hu, W., Di, Q., Liang, T., Zhou, N., Chen, H., Zeng, Z., Luo, Y., & Shaker, M. (2023). Effects of in vitro simulated digestion and fecal fermentation of polysaccharides from straw mushroom (Volvariella volvacea) on its physicochemical properties and human gut microbiota. *International Journal of Biological Macromolecules, 239*, 124188.

Hu, X., Wang, T., & Jin, F. (2016). Alzheimer's disease and gut microbiota. *Science China Life Sciences, 59*, 1006-1023.

Hu, Z., Zhou, H., Li, Y., Wu, M., Yu, M., & Sun, X. (2019). Optimized purification process of polysaccharides from Carex meyeriana Kunth by macroporous resin, its

characterization and immunomodulatory activity. *International Journal of Biological Macromolecules, 132*, 76-86.

Huang, Q.-L., Siu, K.-C., Wang, W.-Q., Cheung, Y.-C., & Wu, J.-Y. (2013). Fractionation, characterization and antioxidant activity of exopolysaccharides from fermentation broth of a Cordyceps sinensis fungus. *Process Biochemistry, 48*(2), 380-386.

Huang, W., Sun, J., Liu, T., Zhao, T., Dong, X., Xu, X., Lu, Y., Lin, X., & Gong, G. (2023). Fingerprint and Chemometric Analysis of Arabinogalactan Derived From Lycium barbarum Fruit. *Natural Product Communications, 18*(5), Article 1934578X231168467.

Huang, Z., Lin, F., Zhu, X., Zhang, C., Jiang, M., & Lu, Z. (2020). An exopolysaccharide from Lactobacillus plantarum H31 in pickled cabbage inhibits pancreas α-amylase and regulating metabolic markers in HepG2 cells by AMPK/PI3K/Akt pathway. *International Journal of Biological Macromolecules, 143*, 775-784.

Huo, J., Liao, Q., Wu, J., Zhao, D., Sun, W., An, M., Li, Y., Huang, M., & Sun, B. (2022). Structure elucidation and intestinal barrier protection of an α-D-glucan in Huangshui. *International Journal of Biological Macromolecules, 223*, 595-605.

Huynh, T., Tran, M.-T., & Dinh, M.-H. (2024). *Antioxidant and cytotoxic effects of isolated polysaccharides from cultured Ophiocordyceps sinensis.* Paper presented at the IOP Conference Series: Earth and Environmental Science.

Ilhan, Z. E., Marcus, A. K., Kang, D.-W., Rittmann, B. E., & Krajmalnik-Brown, R. (2017). pH-mediated microbial and metabolic interactions in fecal enrichment cultures. *Msphere, 2*(3), e00047-00017.

Ji, N.-F., Yao, L.-S., Li, Y., He, W., Yi, K.-S., & Huang, M. (2011). Polysaccharide of cordyceps sinensis enhances cisplatin cytotoxicity in non–small cell lung cancer H157 cell line. *Integrative cancer therapies, 10*(4), 359-367.

Ji, X., Peng, Q., Yuan, Y., Shen, J., Xie, X., & Wang, M. (2017). Isolation, structures and bioactivities of the polysaccharides from jujube fruit (Ziziphus jujuba Mill.): A review. *Food Chemistry, 227*, 349-357.

Jin, Q., Lin, B., & Lu, L. (2025). Potential therapeutic value of dietary polysaccharides in cardiovascular disease: Extraction, mechanisms, applications, and challenges. *International Journal of Biological Macromolecules, 296*, 139573.

Jin, S., & Kang, P. M. (2024). A Systematic Review on Advances in Management of Oxidative Stress-Associated Cardiovascular Diseases. *Antioxidants, 13*(8), 923.

Jing, L., Zong, S., Li, J., Surhio, M. M., & Ye, M. (2016). Purification, structural features and inhibition activity on α-glucosidase of a novel polysaccharide from Lachnum YM406. *Process Biochemistry, 51*(10), 1706-1713.

Johnson, L. P., Walton, G. E., Psichas, A., Frost, G. S., Gibson, G. R., & Barraclough, T. G. (2015). Prebiotics Modulate the Effects of Antibiotics on Gut Microbial Diversity and Functioning in Vitro. *Nutrients, 7*(6), 4480-4497.

Kaminsky, L. W., Al-Sadi, R., & Ma, T. Y. (2021). IL-1β and the intestinal epithelial tight junction barrier. *Frontiers in immunology, 12*, 767456.

Kang, L., Li, P., Wang, D., Wang, T., Hao, D., & Qu, X. (2021). Alterations in intestinal microbiota diversity, composition, and function in patients with sarcopenia. *Scientific reports, 11*(1), 4628.

Kaoutari, A. E., Armougom, F., Gordon, J. I., Raoult, D., & Henrissat, B. (2013). The abundance and variety of carbohydrate-active enzymes in the human gut microbiota. *Nature Reviews Microbiology, 11*(7), 497-504.

Ke, L. q. (2015). Optimization of ultrasonic extraction of polysaccharides from L entinus Edodes based on enzymatic treatment. *Journal of Food Processing and Preservation, 39*(3), 254-259.

Keung, W.-S., Zhang, W.-H., Luo, H.-Y., Chan, K.-C., Chan, Y.-M., & Xu, J. (2025). Correlation between the structures of natural polysaccharides and their properties in regulating gut microbiota: Current understanding and beyond. *Carbohydrate Polymers, 352*, 123209.

Khan, I., Huang, G., Li, X., Leong, W., Xia, W., & Hsiao, W. L. W. (2018). Mushroom polysaccharides from Ganoderma lucidum and Poria cocos reveal prebiotic functions. *Journal of Functional Foods, 41*, 191-201.

Khaskheli, S. G., Zheng, W., Sheikh, S. A., Khaskheli, A. A., Liu, Y., Soomro, A. H., Feng, X., Sauer, M. B., Wang, Y. F., & Huang, W. (2015). Characterization of Auricularia auricula polysaccharides and its antioxidant properties in fresh and pickled product. *International Journal of Biological Macromolecules, 81*, 387-395.

Kircher, B., Woltemate, S., Gutzki, F., Schlüter, D., Geffers, R., Bähre, H., & Vital, M. (2022). Predicting butyrate- and propionate-forming bacteria of gut microbiota from sequencing data. *Gut Microbes, 14*(1), Article 2149019.

Klindworth, A., Pruesse, E., Schweer, T., Peplies, J., Quast, C., Horn, M., & Glöckner, F. O. (2013). Evaluation of general 16S ribosomal RNA gene PCR primers for classical and

next-generation sequencing-based diversity studies. *Nucleic acids research, 41*(1), Article e1.

Koh, A., De Vadder, F., Kovatcheva-Datchary, P., & Bäckhed, F. (2016). From Dietary Fiber to Host Physiology: Short-Chain Fatty Acids as Key Bacterial Metabolites. *Cell, 165*(6), 1332-1345.

Koh, G. Y., Kane, A. V., Wu, X., & Crott, J. W. (2020). Parabacteroides distasonis attenuates tumorigenesis, modulates inflammatory markers and promotes intestinal barrier integrity in azoxymethane-treated A/J mice. *Carcinogenesis, 41*(7), 909-917.

Lai, H.-C., Lin, T.-L., Chen, T.-W., Kuo, Y.-L., Chang, C.-J., Wu, T.-R., Shu, C.-C., Tsai, Y.-H., Swift, S., & Lu, C.-C. (2022). Gut microbiota modulates COPD pathogenesis: role of anti-inflammatory Parabacteroides goldsteinii lipopolysaccharide. *Gut, 71*(2), 309-321.

Larrañaga-Ordaz, D., Martínez-Maldonado, M. A., Millán-Chiu, B. E., Fernández, F., Castaño-Tostado, E., Gómez-Lim, M. Á., & Loske, A. M. (2022). Effect of shock waves on the growth of Aspergillus niger conidia: Evaluation of germination and preliminary study on gene expression. *Journal of Fungi, 8*(11), 1117.

Lei, H., Guo, S., Han, J., Wang, Q., Zhang, X., & Wu, W. (2012). Hypoglycemic and hypolipidemic activities of MT-α-glucan and its effect on immune function of diabetic mice. *Carbohydrate Polymers, 89*(1), 245-250.

Lenoir, M., Martín, R., Torres-Maravilla, E., Chadi, S., González-Dávila, P., Sokol, H., Langella, P., Chain, F., & Bermúdez-Humarán, L. G. (2020). Butyrate mediates anti-inflammatory effects of Faecalibacterium prausnitzii in intestinal epithelial cells through Dact3. *Gut Microbes, 12*(1), 1-16.

Leung, P., Zhang, Q., & Wu, J. (2006). Mycelium cultivation, chemical composition and antitumour activity of a Tolypocladium sp. fungus isolated from wild Cordyceps sinensis. *Journal of Applied Microbiology, 101*(2), 275-283.

Leung, P. H., Zhang, Q. X., & Wu, J. Y. (2006). Mycelium cultivation, chemical composition and antitumour activity of a Tolypocladium sp. fungus isolated from wild Cordyceps sinensis. *J Appl Microbiol, 101*(2), 275-283.

Ley, R. E., Bäckhed, F., Turnbaugh, P., Lozupone, C. A., Knight, R. D., & Gordon, J. I. (2005). Obesity alters gut microbial ecology. *Proceedings of the national academy of sciences, 102*(31), 11070-11075.

Li, C., & Xu, S. (2022). Edible mushroom industry in China: current state and perspectives. *Applied microbiology and biotechnology, 106*(11), 3949-3955.

Li, J., Fan, L., & Ding, S. (2011). Isolation, purification and structure of a new water-soluble polysaccharide from Zizyphus jujuba cv. Jinsixiaozao. *Carbohydrate Polymers, 83*(2), 477-482.

Li, J. H., Zhu, Y. Y., Gu, F. T., & Wu, J. Y. (2023). Efficient isolation of immunostimulatory polysaccharides from Lentinula edodes by autoclaving-ultrasonication extraction and fractional precipitation. *International Journal of Biological Macromolecules, 237*, 124216.

Li, L.-Q., Song, A.-X., Wong, W.-T., & Wu, J.-Y. (2021). Isolation and assessment of a highly-active anti-inflammatory exopolysaccharide from mycelial fermentation of a medicinal fungus Cs-HK1. *International Journal of Molecular Sciences, 22*(5), Article 2450.

Li, L.-Q., Song, A.-X., Yin, J.-Y., Siu, K.-C., Wong, W.-T., & Wu, J.-Y. (2020). Anti-inflammation activity of exopolysaccharides produced by a medicinal fungus Cordyceps sinensis Cs-HK1 in cell and animal models. *International Journal of Biological Macromolecules, 149*, 1042-1050.

Li, L. Q., Song, A. X., Wong, W. T., & Wu, J. Y. (2021a). Isolation and Assessment of a Highly-Active Anti-Inflammatory Exopolysaccharide from Mycelial Fermentation of a Medicinal Fungus Cs-HK1. *Int J Mol Sci, 22*(5).

Li, L. Q., Song, A. X., Wong, W. T., & Wu, J. Y. (2021b). Modification and enhanced anti-inflammatory activity by Bifidobacterial fermentation of an exopolysaccharide from a medicinal fungus Cs-HK1. *Int J Biol Macromol, 188*, 586-594.

Li, Q.-Y., Dou, Z.-M., Chen, C., Jiang, Y.-M., Yang, B., & Fu, X. (2022). Study on the Effect of Molecular Weight on the Gut Microbiota Fermentation Properties of Blackberry Polysaccharides In Vitro. *Journal of Agricultural and Food Chemistry, 70*(36), 11245-11257.

Li, S., Liu, M., Zhang, C., Tian, C., Wang, X., Song, X., Jing, H., Gao, Z., Ren, Z., Liu, W., Zhang, J., & Jia, L. (2018). Purification, in vitro antioxidant and in vivo anti-aging activities of soluble polysaccharides by enzyme-assisted extraction from Agaricus bisporus. *International Journal of Biological Macromolecules, 109*, 457-466.

Li, W., Cai, Z.-N., Mehmood, S., Liang, L.-L., Liu, Y., Zhang, H.-Y., Chen, Y., & Lu, Y.-M. (2019). Anti-inflammatory effects of Morchella esculenta polysaccharide and its derivatives in fine particulate matter-treated NR8383 cells. *International Journal of Biological Macromolecules, 129*, 904-915.

Li, X., Chen, Q., Liu, G., Xu, H., & Zhang, X. (2021). Chemical elucidation of an arabinogalactan from rhizome of Polygonatum sibiricum with antioxidant activities. *International Journal of Biological Macromolecules, 190*, 730-738.

Li, Y.-M., Zhong, R.-f., Chen, J., & Luo, Z.-G. (2021). Structural characterization, anticancer, hypoglycemia and immune activities of polysaccharides from Russula virescens. *International Journal of Biological Macromolecules, 184*, 380-392.

Liang, J., Rao, Z.-H., Jiang, S.-L., Wang, S., Kuang, H.-X., & Xia, Y.-G. (2023). Structure of an unprecedent glucuronoxylogalactoglucomannan from fruit bodies of Auricularia auricula-judae (black woody ear). *Carbohydrate Polymers, 315*, 120968.

Liang, R., Zhang, Z., & Lin, S. (2017). Effects of pulsed electric field on intracellular antioxidant activity and antioxidant enzyme regulating capacities of pine nut (Pinus koraiensis) peptide QDHCH in HepG2 cells. *Food Chemistry, 237*, 793-802.

Liang, Z., Yin, Z., Liu, X., Ma, C., Wang, J., Zhang, Y., & Kang, W. (2022). A glucomannogalactan from Pleurotus geesteranus: Structural characterization, chain conformation and immunological effect. *Carbohydrate Polymers, 287*, 119346.

Liu, D., Tang, W., Huang, X.-J., Hu, J.-L., Wang, J.-Q., Yin, J.-Y., Nie, S.-P., & Xie, M.-Y. (2022). Structural characteristic of pectin-glucuronoxylan complex from Dolichos lablab L. hull. *Carbohydrate Polymers, 298*, Article 120023.

Liu, H., Liu, X., Xie, J., & Chen, S. (2023). Structure, function and mechanism of edible fungus polysaccharides in human beings chronic diseases. *Food Science and Technology, 43*.

Liu, X., Chen, S., Liu, H., Xie, J., Hasan, K. M. F., Zeng, Q., Wei, S., & Luo, P. (2023). Structural properties and anti-inflammatory activity of purified polysaccharides from Hen-of-the-woods mushrooms (Grifola frondosa). *Front Nutr, 10*, 1078868.

Liu, X., Pang, H., Gao, Z., Zhao, H., Zhang, J., & Jia, L. (2019). Antioxidant and hepatoprotective activities of residue polysaccharides by Pleurotus citrinipileatus. *International Journal of Biological Macromolecules, 131*, 315-322.

Liu, X., Renard, C. M. G. C., Bureau, S., & Le Bourvellec, C. (2021). Revisiting the contribution of ATR-FTIR spectroscopy to characterize plant cell wall polysaccharides. *Carbohydrate Polymers, 262*, Article 117935.

Long, H., Gu, X., Zhou, N., Zhu, Z., Wang, C., Liu, X., & Zhao, M. (2020). Physicochemical characterization and bile acid-binding capacity of water-extract polysaccharides fractionated by stepwise ethanol precipitation from Caulerpa lentillifera. *International Journal of Biological Macromolecules, 150*, 654-661.

Louis, P., Scott, K. P., Duncan, S. H., & Flint, H. J. (2007). Understanding the effects of diet on bacterial metabolism in the large intestine. *Journal of Applied Microbiology, 102*(5), 1197-1208.

Lozupone, C., & Knight, R. (2005). UniFrac: a new phylogenetic method for comparing microbial communities. *Appl Environ Microbiol, 71*(12), 8228-8235.

Lu, A., Yu, M., Fang, Z., Xiao, B., Guo, L., Wang, W., Li, J., Wang, S., & Zhang, Y. (2019). Preparation of the controlled acid hydrolysates from pumpkin polysaccharides and their antioxidant and antidiabetic evaluation. *International Journal of Biological Macromolecules, 121*, 261-269.

Lu, H., Xu, X., Fu, D., Gu, Y., Fan, R., Yi, H., He, X., Wang, C., Ouyang, B., & Zhao, P. (2022). Butyrate-producing Eubacterium rectale suppresses lymphomagenesis by alleviating the TNF-induced TLR4/MyD88/NF-κB axis. *Cell host & microbe, 30*(8), 1139-1150. e1137.

Luissint, A.-C., Parkos, C. A., & Nusrat, A. (2016). Inflammation and the intestinal barrier: leukocyte–epithelial cell interactions, cell junction remodeling, and mucosal repair. *Gastroenterology, 151*(4), 616-632.

Ma, G., Xu, Q., Du, H., Kimatu, B. M., Su, A., Yang, W., Hu, Q., & Xiao, H. (2022). Characterization of polysaccharide from Pleurotus eryngii during simulated gastrointestinal digestion and fermentation. *Food Chemistry, 370*, Article 131303.

Ma, G., Xu, Q., Du, H., Muinde Kimatu, B., Su, A., Yang, W., Hu, Q., & Xiao, H. (2022). Characterization of polysaccharide from Pleurotus eryngii during simulated gastrointestinal digestion and fermentation. *Food Chemistry, 370*, 131303.

Ma, R.-H., Zhang, X.-X., Ni, Z.-J., Thakur, K., Wang, W., Yan, Y.-M., Cao, Y.-L., Zhang, J.-G., Rengasamy, K. R. R., & Wei, Z.-J. (2023). Lycium barbarum (Goji) as functional food: a review of its nutrition, phytochemical structure, biological features, and food industry prospects. *Critical Reviews in Food Science and Nutrition, 63*(30), 10621-10635.

Ma, X., Meng, M., Han, L., Cheng, D., Cao, X., & Wang, C. (2016). Structural characterization and immunomodulatory activity of Grifola frondosa polysaccharide via toll-like receptor 4–mitogen-activated protein kinases–nuclear factor κB pathways. *Food & Function, 7*(6), 2763-2772.

Ma, X. L., Song, F. F., Zhang, H., Huan, X., & Li, S. Y. (2017). Compositional Monosaccharide Analysis of Morus nigra Linn by HPLC and HPCE Quantitative Determination and

Comparison of Polysaccharide from Morus nigra Linn by HPCE and HPLC. *Curr Pharm Anal, 13*(5), 433-437.

Ma, Y., Jiang, S., & Zeng, M. (2021). In vitro simulated digestion and fermentation characteristics of polysaccharide from oyster (Crassostrea gigas), and its effects on the gut microbiota. *Food Research International, 149*, Article 110646.

Magalhães, L. M., Segundo, M. A., Reis, S., & Lima, J. L. (2008). Methodological aspects about in vitro evaluation of antioxidant properties. *Analytica chimica acta, 613*(1), 1-19.

Makarova, E. N., & Shakhmatov, E. G. (2021). Characterization of pectin-xylan-glucan-arabinogalactan proteins complex from Siberian fir Abies sibirica Ledeb. *Carbohydrate Polymers, 260*, Article 117825.

Makarova, E. N., Shakhmatov, E. G., & Belyy, V. A. (2018). Structural studies of water-extractable pectic polysaccharides and arabinogalactan proteins from Picea abies greenery. *Carbohydrate Polymers, 195*, 207-217.

Mancin, L., Wu, G. D., & Paoli, A. (2023). Gut microbiota–bile acid–skeletal muscle axis. *Trends in Microbiology, 31*(3), 254-269.

Mao, Y.-H., Song, A.-X., Li, L.-Q., Siu, K.-C., Yao, Z.-P., & Wu, J.-Y. (2020). Effects of exopolysaccharide fractions with different molecular weights and compositions on fecal microflora during in vitro fermentation. *Int J Biol Macromol, 144*, 76-84.

McDonald, D., Price, M. N., Goodrich, J., Nawrocki, E. P., DeSantis, T. Z., Probst, A., Andersen, G. L., Knight, R., & Hugenholtz, P. (2012). An improved Greengenes taxonomy with explicit ranks for ecological and evolutionary analyses of bacteria and archaea. *The ISME journal, 6*(3), 610-618.

Meng, G., Zhu, H., Yang, S., Wu, F., Zheng, H., Chen, E., & Xu, J. (2011). Attenuating effects of Ganoderma lucidum polysaccharides on myocardial collagen cross-linking relates to advanced glycation end product and antioxidant enzymes in high-fat-diet and streptozotocin-induced diabetic rats. *Carbohydrate Polymers, 84*(1), 180-185.

Miller, G. L. (1959). Use of Dinitrosalicylic Acid Reagent for Determination of Reducing Sugar. *Analytical chemistry, 31*(3), 426-428.

Nakamura, Y. K., & Omaye, S. T. (2012). Metabolic diseases and pro-and prebiotics: mechanistic insights. *Nutrition & metabolism, 9*(1), 1-9.

Nguyen, Q.-V., Vu, T.-T., Tran, M.-T., Ho Thi, P. T., Thu, H., Le Thi, T. H., Chuyen, H. V., & Dinh, M.-H. (2021). Antioxidant activity and hepatoprotective effect of

exopolysaccharides from cultivated ophiocordyceps sinensis against CCl4-induced liver damages. *Natural Product Communications, 16*(2), 1934578X21997670.

Niego, A. G., Rapior, S., Thongklang, N., Raspé, O., Jaidee, W., Lumyong, S., & Hyde, K. D. (2021). Macrofungi as a Nutraceutical Source: Promising Bioactive Compounds and Market Value. *Journal of Fungi, 7*(5), 397.

Ning, X., Liu, Y., Jia, M., Wang, Q., Sun, Z., Ji, L., Mayo, K. H., Zhou, Y., & Sun, L. (2021). Pectic polysaccharides from Radix Sophorae Tonkinensis exhibit significant antioxidant effects. *Carbohydrate Polymers, 262*, 117925.

Nogal, A., Valdes, A. M., & Menni, C. (2021). The role of short-chain fatty acids in the interplay between gut microbiota and diet in cardio-metabolic health. *Gut Microbes, 13*(1), Article 1897212.

Nogal, A., Valdes, A. M., & Menni, C. (2021). The role of short-chain fatty acids in the interplay between gut microbiota and diet in cardio-metabolic health. *Gut Microbes, 13*(1), 1-24.

Nowak, R., Nowacka-Jechalke, N., Juda, M., & Malm, A. (2018). The preliminary study of prebiotic potential of Polish wild mushroom polysaccharides: the stimulation effect on Lactobacillus strains growth. *Eur J Nutr, 57*(4), 1511-1521.

Osińska-Jaroszuk, M., Jarosz-Wilkołazka, A., Jaroszuk-Ściseł, J., Szałapata, K., Nowak, A., Jaszek, M., Ozimek, E., & Majewska, M. (2015). Extracellular polysaccharides from Ascomycota and Basidiomycota: production conditions, biochemical characteristics, and biological properties. *World journal of microbiology and biotechnology, 31*, 1823-1844.

Patterson, E., Ryan, P. M., Cryan, J. F., Dinan, T. G., Ross, R. P., Fitzgerald, G. F., & Stanton, C. (2016). Gut microbiota, obesity and diabetes. *Postgraduate medical journal, 92*(1087), 286-300.

Peng, K., Xiao, S., Xia, S., Li, C., Yu, H., & Yu, Q. (2024). Butyrate Inhibits the HDAC8/NF-κB Pathway to Enhance Slc26a3 Expression and Improve the Intestinal Epithelial Barrier to Relieve Colitis. *Journal of Agricultural and Food Chemistry, 72*(44), 24400-24416.

Pizzino, G., Irrera, N., Cucinotta, M., Pallio, G., Mannino, F., Arcoraci, V., Squadrito, F., Altavilla, D., & Bitto, A. (2017). Oxidative Stress: Harms and Benefits for Human Health. *Oxid Med Cell Longev, 2017*, 8416763.

Porterfield, J. Z., & Zlotnick, A. (2010). A simple and general method for determining the protein and nucleic acid content of viruses by UV absorbance. *Virology, 407*(2), 281-288.

Poznyak, A. V., Litvinova, L., Poggio, P., Sukhorukov, V. N., & Orekhov, A. N. (2022). Effect of glucose levels on cardiovascular risk. *Cells, 11*(19), 3034.

Pramanik, M., Chakraborty, I., Mondal, S., & Islam, S. S. (2007). Structural analysis of a water-soluble glucan (Fr.I) of an edible mushroom, Pleurotus sajor-caju. *carbohydrate research, 342*(17), 2670-2675.

Qian, D., Zhao, Y., Yang, G., & Huang, L. (2017). Systematic review of chemical constituents in the genus Lycium (Solanaceae). *Molecules, 22*(6), Article 911.

Qian, L., Liu, H., Li, T., Liu, Y., Zhang, Z., & Zhang, Y. (2020). Purification, characterization and in vitro antioxidant activity of a polysaccharide AAP–3–1 from Auricularia auricula. *International Journal of Biological Macromolecules, 162*, 1453-1464.

Qu, J., Huang, P., Zhang, L., Qiu, Y., Qi, H., Leng, A., & Shang, D. (2020). Hepatoprotective effect of plant polysaccharides from natural resources: A review of the mechanisms and structure-activity relationship. *International Journal of Biological Macromolecules, 161*, 24-34.

Quigley, E. M. (2017). Microbiota-brain-gut axis and neurodegenerative diseases. *Current neurology and neuroscience reports, 17*, 1-9.

Reddy, S. K., Bågenholm, V., Pudlo, N. A., Bouraoui, H., Koropatkin, N. M., Martens, E. C., & Stålbrand, H. (2016). A β-mannan utilization locus in Bacteroides ovatus involves a GH36 α-galactosidase active on galactomannans. *FEBS Letters, 590*(14), 2106-2118.

Reichardt, N., Duncan, S. H., Young, P., Belenguer, A., McWilliam Leitch, C., Scott, K. P., Flint, H. J., & Louis, P. (2014). Phylogenetic distribution of three pathways for propionate production within the human gut microbiota. *The ISME journal, 8*(6), 1323-1335.

Rinninella, E., Raoul, P., Cintoni, M., Franceschi, F., Miggiano, G. A. D., Gasbarrini, A., & Mele, M. C. (2019). What is the healthy gut microbiota composition? A changing ecosystem across age, environment, diet, and diseases. *Microorganisms, 7*(1), Article 14.

Rodionova, I. A., Li, X., Thiel, V., Stolyar, S., Stanton, K., Fredrickson, J. K., Bryant, D. A., Osterman, A. L., Best, A. A., & Rodionov, D. A. (2013). Comparative genomics and functional analysis of rhamnose catabolic pathways and regulons in bacteria. *Frontiers in microbiology, 4*, 407.

Sajnaga, E., Socała, K., Kalwasińska, A., Wlaź, P., Waśko, A., Jach, M. E., Tomczyk, M., & Wiater, A. (2023). Response of murine gut microbiota to a prebiotic based on oligosaccharides derived via hydrolysis of fungal α-(1→3)-d-glucan: Preclinical trial study on mice. *Food Chemistry, 417*, Article 135928.

Sassaki, G. L., Gorin, P. A., Souza, L. M., Czelusniak, P. A., & Iacomini, M. (2005). Rapid synthesis of partially O-methylated alditol acetate standards for GC–MS: Some relative activities of hydroxyl groups of methyl glycopyranosides on Purdie methylation. *carbohydrate research, 340*(4), 731-739.

Schepetkin, I. A., & Quinn, M. T. (2006). Botanical polysaccharides: macrophage immunomodulation and therapeutic potential. *International immunopharmacology, 6*(3), 317-333.

Schlesier, K., Harwat, M., Böhm, V., & Bitsch, R. (2002). Assessment of antioxidant activity by using different in vitro methods. *Free Radic Res, 36*(2), 177-187.

Sensoy, I. (2021). A review on the food digestion in the digestive tract and the used in vitro models. *Current research in food science, 4*, 308-319.

Shao, S.-y., Si, X.-l., Zhang, Y.-s., Tu, P.-f., & Zhang, Q.-y. (2020). Recent advances in analytical methods for polysaccharides from edible mushroom.

Shi, Q., Li, X., He, J., Ye, D., Tang, H., Xuan, J., Tang, Y., Zhang, Y., & Zhang, Y. (2024). Effects of Auricularia auricula-judae (Bull.) Quél. polysaccharide acid hydrolysate on glucose metabolism in diabetic mice under oxidative stress. *Phytomedicine, 128*, 155485.

Shi, Y., Xiong, Q., Wang, X., Li, X., Yu, C., Wu, J., Yi, J., Zhao, X., Xu, Y., & Cui, H. (2016). Characterization of a novel purified polysaccharide from the flesh of Cipangopaludina chinensis. *Carbohydrate Polymers, 136*, 875-883.

Singh, R. K., Chang, H.-W., Di, Y., Kristina M., L., Derya, U., Kirsten, W., Michael, A., Benjamin, F., Mio, N., Tian, H. Z., Tina, B., & Wilson, L. (2017). Influence of diet on the gut microbiome and implications for human health. *Journal of Translational Medicine, 1*(15), 73-89.

Siu, K.-C., Chen, X., & Wu, J.-Y. (2014). Constituents actually responsible for the antioxidant activities of crude polysaccharides isolated from mushrooms. *Journal of Functional Foods, 11*, 548-556.

Song, A.-X., Mao, Y.-H., Siu, K.-C., Tai, W. C. S., & Wu, J.-Y. (2019). Protective effects of exopolysaccharide of a medicinal fungus on probiotic bacteria during cold storage and

simulated gastrointestinal conditions. *International Journal of Biological Macromolecules, 133*, 957-963.

Song, Q., Wang, Y., Huang, L., Shen, M., Yu, Y., Yu, Q., Chen, Y., & Xie, J. (2021). Review of the relationships among polysaccharides, gut microbiota, and human health. *Food Research International, 140*, Article 109858.

Stoeva, M. K., Garcia-So, J., Justice, N., Myers, J., Tyagi, S., Nemchek, M., McMurdie, P. J., Kolterman, O., & Eid, J. (2021). Butyrate-producing human gut symbiont, Clostridium butyricum, and its role in health and disease. *Gut Microbes, 13*(1), 1907272.

Stoica, R. M., Moscovici, M., Lakatos, E. S., & Cioca, L. I. (2023). Exopolysaccharides of fungal origin: properties and pharmaceutical applications. *Processes, 11*(2), 335.

Stojkovic, K., Szijártó, V., Kaszowska, M., Niedziela, T., Hartl, K., Nagy, G., & Lukasiewicz, J. (2017). Identification of d-Galactan-III as part of the lipopolysaccharide of Klebsiella pneumoniae serotype O1. *Frontiers in microbiology, 8*, 684.

Su, Y., & Li, L. (2020). Structural characterization and antioxidant activity of polysaccharide from four auriculariales. *Carbohydrate Polymers, 229*, 115407.

Sun, H., Yu, X., Li, T., & Zhu, Z. (2021). Structure and hypoglycemic activity of a novel exopolysaccharide of Cordyceps militaris. *International Journal of Biological Macromolecules, 166*, 496-508.

Sun, L., & Miao, M. (2020). Dietary polyphenols modulate starch digestion and glycaemic level: A review. *Critical Reviews in Food Science and Nutrition, 60*(4), 541-555.

Sun, Q., Bu, J., Chen, H., Liu, M., Ning, C., Tan, C., Guo, C., Li, W., & Wang, S. (2025). Preparation, structural characterisation, and biological activities of polysaccharides from Malus American crabapple fruits. *International Journal of Food Science and Technology, 60*(1).

Susilawati, E., Levita, J., Susilawati, Y., & Sumiwi, S. A. (2023). Review of the case reports on metformin, sulfonylurea, and thiazolidinedione therapies in type 2 diabetes mellitus patients. *Medical Sciences, 11*(3), 50.

Tabibzadeh, F., Alvandi, H., Hatamian-Zarmi, A., Kalitukha, L., Aghajani, H., & Ebrahimi-Hosseinzadeh, B. (2024). Antioxidant activity and cytotoxicity of exopolysaccharide from mushroom Hericium coralloides in submerged fermentation. *Biomass Conversion and Biorefinery, 14*(21), 26953-26963.

Tang, H., Wei, W., Wang, W., Zha, Z., Li, T., Zhang, Z., Luo, C., Yin, H., Huang, F., & Wang, Y. (2017). Effects of cultured Cordyceps mycelia polysaccharide A on tumor neurosis

factor-α induced hepatocyte injury with mitochondrial abnormality. *Carbohydrate Polymers, 163*, 43-53.

Tang, H.-L., Chen, C., Wang, S.-K., & Sun, G.-J. (2015). Biochemical analysis and hypoglycemic activity of a polysaccharide isolated from the fruit of Lycium barbarum L. *International Journal of Biological Macromolecules, 77*, 235-242.

Tudu, M., & Samanta, A. (2023). Natural polysaccharides: Chemical properties and application in pharmaceutical formulations. *European Polymer Journal, 184*, Article 111801.

Turnbaugh, P. J., Hamady, M., Yatsunenko, T., Cantarel, B. L., Duncan, A., Ley, R. E., Sogin, M. L., Jones, W. J., Roe, B. A., & Affourtit, J. P. (2009). A core gut microbiome in obese and lean twins. *Nature, 457*(7228), 480-484.

Turner, J. R. (2009). Intestinal mucosal barrier function in health and disease. *Nature reviews immunology, 9*(11), 799-809.

Udchumpisai, W., & Bangyeekhun, E. (2020). Purification, Structural Characterization, and Biological Activity of Polysaccharides from Lentinus velutinus. *Mycobiology, 48*(1), 51-57.

Venkatachalam, G., Arumugam, S., & Doble, M. (2021). Industrial production and applications of α/β linear and branched glucans. *Indian Chemical Engineer, 63*(5), 533-547.

Voorhies, A. A., Mark Ott, C., Mehta, S., Pierson, D. L., Crucian, B. E., Feiveson, A., Oubre, C. M., Torralba, M., Moncera, K., & Zhang, Y. (2019). Study of the impact of long-duration space missions at the International Space Station on the astronaut microbiome. *Scientific reports, 9*(1), 9911.

Wang, J., Hu, S., Nie, S., Yu, Q., & Xie, M. (2016). Reviews on mechanisms of in vitro antioxidant activity of polysaccharides. *Oxidative medicine and cellular longevity, 2016*.

Wang, J., Ke, S., Strappe, P., Ning, M., & Zhou, Z. (2023). Structurally Orientated Rheological and Gut Microbiota Fermentation Property of Mannans Polysaccharides and Oligosaccharides. *Foods, 12*(21), Article 4002.

Wang, J., Nie, S., Cui, S. W., Wang, Z., Phillips, A. O., Phillips, G. O., Li, Y., & Xie, M. (2017). Structural characterization and immunostimulatory activity of a glucan from natural Cordyceps sinensis. *Food Hydrocolloids, 67*, 139-147.

Wang, L., Zhang, Z., Zeng, Z., Lin, Y., Xiong, B., Zheng, B., Zhang, Y., & Pan, L. (2025). Structural characterization of polysaccharide from an edible fungus Dictyophora indusiata and the remodel function of gut microbiota in inflammatory mice. *Carbohydrate Polymers, 351*, 123141.

Wang, M., Chen, G., Chen, D., Ye, H., Sun, Y., Zeng, X., & Liu, Z. (2019). Purified fraction of polysaccharides from Fuzhuan brick tea modulates the composition and metabolism of gut microbiota in anaerobic fermentation in vitro. *International Journal of Biological Macromolecules, 140*, 858-870.

Wang, Y., He, P., He, L., Huang, Q., Cheng, J., Li, W., Liu, Y., & Wei, C. (2019). Structural elucidation, antioxidant and immunomodulatory activities of a novel heteropolysaccharide from cultured Paecilomyces cicadae (Miquel.) Samson. *Carbohydrate Polymers, 216*, 270-281.

Wang, Y., Jia, J., Ren, X., Li, B., & Zhang, Q. (2018). Extraction, preliminary characterization and in vitro antioxidant activity of polysaccharides from Oudemansiella radicata mushroom. *International Journal of Biological Macromolecules, 120*, 1760-1769.

Wang, Y., Zeng, T., Li, H., Wang, Y., Wang, J., & Yuan, H. (2023). Structural Characterization and Hypoglycemic Function of Polysaccharides from Cordyceps cicadae. *Molecules, 28*(2), 526.

Wang, Y.-X., Xin, Y., Yin, J.-Y., Huang, X.-J., Wang, J.-Q., Hu, J.-L., Geng, F., & Nie, S.-P. (2022). Revealing the architecture and solution properties of polysaccharide fractions from Macrolepiota albuminosa (Berk.) Pegler. *Food Chemistry, 368*, 130772.

Wang, Z.-W., Zhang, Z.-H., Qiao, Z.-R., Cai, W.-D., & Yan, J.-K. (2021). Construction and characterization of antioxidative ferulic acid-grafted carboxylic curdlan conjugates and their contributions on β-carotene storage stability. *Food Chemistry, 349*, 129166.

Wardman, J. F., Bains, R. K., Rahfeld, P., & Withers, S. G. (2022). Carbohydrate-active enzymes (CAZymes) in the gut microbiome. *Nature Reviews Microbiology, 20*(9), 542-556.

Wu, D.-T., Guo, H., Lin, S., Lam, S.-C., Zhao, L., Lin, D.-R., & Qin, W. (2018). Review of the structural characterization, quality evaluation, and industrial application of Lycium barbarum polysaccharides. *Trends in Food Science & Technology, 79*, 171-183.

Wu, D.-T., Meng, L.-Z., Wang, L.-Y., Lv, G.-P., Cheong, K.-L., Hu, D.-J., Guan, J., Zhao, J., & Li, S.-P. (2014). Chain conformation and immunomodulatory activity of a hyperbranched polysaccharide from Cordyceps sinensis. *Carbohydrate Polymers, 110*, 405-414.

Wu, D.-T., Nie, X.-R., Gan, R.-Y., Guo, H., Fu, Y., Yuan, Q., Zhang, Q., & Qin, W. (2021). In vitro digestion and fecal fermentation behaviors of a pectic polysaccharide from okra (Abelmoschus esculentus) and its impacts on human gut microbiota. *Food Hydrocolloids, 114*, 106577.

Wu, F., Guo, X., Zhang, J., Zhang, M., Ou, Z., & Peng, Y. (2017). Phascolarctobacterium faecium abundant colonization in human gastrointestinal tract. *Experimental and therapeutic medicine, 14*(4), 3122-3126.

Wu, J., Chen, T., Wan, F., Wang, J., Li, X., Li, W., & Ma, L. (2021). Structural characterization of a polysaccharide from Lycium barbarum and its neuroprotective effect against β-amyloid peptide neurotoxicity. *International Journal of Biological Macromolecules, 176*, 352-363.

Wu, J., Shi, S., Wang, H., & Wang, S. (2016). Mechanisms underlying the effect of polysaccharides in the treatment of type 2 diabetes: A review. *Carbohydrate Polymers, 144*, 474-494.

Wu, M., Feng, H., Song, J., Chen, L., Xu, Z., Xia, W., & Zhang, W. (2020). Structural elucidation and immunomodulatory activity of a neutral polysaccharide from the Kushui Rose (Rosa setate x Rosa rugosa) waste. *Carbohydrate Polymers, 232*, 115804.

Wu, Z.-W., Liu, X.-C., Quan, C.-X., Tao, X.-Y., Yi, L., Zhao, X.-F., Peng, X.-R., & Qiu, M.-H. (2025). Novel galactose-rich polysaccharide from Ganoderma lucidum: structural characterization and immunomodulatory activities. *Carbohydrate Polymers, 362*, 123695.

Xia, F., Fan, J., Zhu, M., & Tong, H. (2011). Antioxidant effects of a water-soluble proteoglycan isolated from the fruiting bodies of Pleurotus ostreatus. *Journal of the Taiwan Institute of Chemical Engineers, 42*(3), 402-407.

Xiang, L., Peng, L., Du, W., & Wei, H. (2016). Protective effects of bifidobacterium on intestinal barrier function in LPS-induced enterocyte barrier injury of Caco-2 monolayers and in a rat NEC model. *PLoS ONE, 11*(8), e0161635.

Xiao, J., Sun, J., Yao, L., Zhao, Q., Wang, L., Wang, X., Yuan, X., & Zhao, B. (2012). Physicochemical characteristics of ultrasonic extracted polysaccharides from cordyceps cephalosporium mycelia. *International Journal of Biological Macromolecules, 51*(1), 64-69.

Xiao, X., Qiao, J., Wang, J., Kang, J., He, L., Li, J., Guo, Q., & Cui, S. W. (2022). Grafted ferulic acid dose-dependently enhanced the apparent viscosity and antioxidant activities of arabinoxylan. *Food Hydrocolloids, 128*, 107557.

Xie, J.-H., Wang, Z.-J., Shen, M.-Y., Nie, S.-P., Gong, B., Li, H.-S., Zhao, Q., Li, W.-J., & Xie, M.-Y. (2016). Sulfated modification, characterization and antioxidant activities of polysaccharide from Cyclocarya paliurus. *Food Hydrocolloids, 53*, 7-15.

Xu, B., Song, S., Yao, L., Wang, H., Sun, M., Zhuang, H., Zhang, X., Liu, Q., Yu, C., & Feng, T. (2024). Digestion under saliva, simulated gastric and small intestinal conditions and fermentation in vitro by human gut microbiota of polysaccharides from Ficus carica Linn. *Food Hydrocolloids, 146*, 109204.

Xu, J., Wang, R., Liu, J., Cheng, H., Peng, D., Xing, L., Shi, S., & Yu, N. (2021). Determination of monosaccharides in Lycium barbarum fruit polysaccharide by an efficient UHPLC-QTRAP-MS/MS method. *Phytochemical Analysis, 32*(5), 785-793.

Xu, X., Xu, P., Ma, C., Tang, J., & Zhang, X. (2013). Gut microbiota, host health, and polysaccharides. *Biotechnology Advances, 31*(2), 318-337.

Yan, J., Shi, S., Wang, H., Liu, R., Li, N., Chen, Y., & Wang, S. (2016). Neutral monosaccharide composition analysis of plant-derived oligo- and polysaccharides by high performance liquid chromatography. *Carbohydrate Polymers, 136*, 1273-1280.

Yan, J.-K., Li, L., Wang, Z.-M., & Wu, J.-Y. (2010). Structural elucidation of an exopolysaccharide from mycelial fermentation of a Tolypocladium sp. fungus isolated from wild Cordyceps sinensis. *Carbohydrate Polymers, 79*(1), 125-130.

Yan, J.-K., Wang, W.-Q., Li, L., & Wu, J.-Y. (2011). Physiochemical properties and antitumor activities of two α-glucans isolated from hot water and alkaline extracts of Cordyceps (Cs-HK1) fungal mycelia. *Carbohydrate Polymers, 85*(4), 753-758.

Yan, J.-K., Wang, W.-Q., & Wu, J.-Y. (2014). Recent advances in Cordyceps sinensis polysaccharides: Mycelial fermentation, isolation, structure, and bioactivities: A review. *Journal of Functional Foods, 6*, 33-47.

Yang, D. R., Wang, M. Y., Zhang, C. L., & Wang, Y. (2024). Endothelial dysfunction in vascular complications of diabetes: a comprehensive review of mechanisms and implications. *Front Endocrinol (Lausanne), 15*, 1359255.

Yang, H., Wang, D., Deng, J., Yang, J., Shi, C., Zhou, F., & Shi, Z. (2018). Activity and structural characteristics of peach gum exudates. *International journal of polymer science, 2018*(1), Article 4593735.

Yang, H.-R., Chen, L.-H., & Zeng, Y.-J. (2021). Structure, Antioxidant Activity and In Vitro Hypoglycemic Activity of a Polysaccharide Purified from Tricholoma matsutake. *Foods, 10*(9), 2184.

Yang, K., Zhang, Y., Cai, M., Guan, R., Neng, J., Pi, X., & Sun, P. (2020). In vitro prebiotic activities of oligosaccharides from the by-products in Ganoderma lucidum spore polysaccharide extraction. *Rsc Advances, 10*(25), 14794-14802.

Yang, X., Zhao, Y., & Lv, Y. (2007). Chemical Composition and Antioxidant Activity of an Acidic Polysaccharide Extracted from Cucurbita moschata Duchesne ex Poiret. *Journal of Agricultural and Food Chemistry, 55*(12), 4684-4690.

Yang, Y., Chang, Y., Wu, Y., Liu, H., Liu, Q., Kang, Z., Wu, M., Yin, H., & Duan, J. (2021). A homogeneous polysaccharide from Lycium barbarum: Structural characterizations, anti-obesity effects and impacts on gut microbiota. *International Journal of Biological Macromolecules, 183*, 2074-2087.

Yang, Y., Chen, J., Lei, L., Li, F., Tang, Y., Yuan, Y., Zhang, Y., Wu, S., Yin, R., & Ming, J. (2019). Acetylation of polysaccharide from Morchella angusticeps peck enhances its immune activation and anti-inflammatory activities in macrophage RAW264. 7 cells. *Food and chemical toxicology, 125*, 38-45.

Yao, C. K., Muir, J. G., & Gibson, P. R. (2016). Review article: insights into colonic protein fermentation, its modulation and potential health implications. *Alimentary pharmacology & therapeutics, 43*(2), 181-196.

Yao, H.-Y.-Y., Wang, J.-Q., Yin, J.-Y., Nie, S.-P., & Xie, M.-Y. (2021). A review of NMR analysis in polysaccharide structure and conformation: Progress, challenge and perspective. *Food Research International, 143*, 110290.

Yao, Y., Liu, J., Miao, Q., Zhu, X., Sun, L., Hua, W., Zhang, N., Huang, G., Ruan, R., Cheng, Y., & Mi, S. (2024). Inhibition and effect of almond hull extract on activities of α-amylase and α-glucosidase, and postprandial glucose in normal SD rats. *Journal of Functional Foods, 123*, 106624.

Yaşar, A., Ryu, H.-J., Esen, E., Sarıoğlan, İ., Deemer, D., Çetin, B., Yoo, S.-H., Lindemann, S. R., Lee, B.-H., & Tunçil, Y. E. (2024). The branching ratio of enzymatically synthesized α-glucans impacts microbiome and metabolic outcomes of in vitro fecal fermentation. *Carbohydrate Polymers, 335*, Article 122087.

Yi, Y., Xu, W., Wang, H.-X., Huang, F., & Wang, L.-M. (2020). Natural polysaccharides experience physiochemical and functional changes during preparation: A review. *Carbohydrate Polymers, 234*, 115896.

Yin, C., Li, C., Ma, K., Fan, X., Yao, F., Shi, D., Wu, W., Qiu, J., Hu, G., & Gao, H. (2023). The physicochemical, antioxidant, hypoglycemic and prebiotic properties of γ-irradiated polysaccharides extracted from Lentinula edodes. *Food Sci Biotechnol, 32*(7), 987-996.

Yu, G., Yue, C., Zang, X., Chen, C., Dong, L., & Liu, Y. (2019). Purification, characterization and in vitro bile salt-binding capacity of polysaccharides from Armillaria mellea mushroom. *Czech Journal of Food Sciences, 37*(1).

Yu, Y., Shen, M., Song, Q., & Xie, J. (2018). Biological activities and pharmaceutical applications of polysaccharide from natural resources: A review. *Carbohydrate Polymers, 183*, 91-101.

Yuan, Q., He, Y., Xiang, P.-Y., Wang, S.-P., Cao, Z.-W., Gou, T., Shen, M.-M., Zhao, L., Qin, W., & Gan, R.-Y. (2020). Effects of simulated saliva-gastrointestinal digestion on the physicochemical properties and bioactivities of okra polysaccharides. *Carbohydrate Polymers, 238*, Article 116183.

Yuan, S., Wang, J., Li, X., Zhu, X., Zhang, Z., & Li, D. (2023). Study on the structure, antioxidant activity and degradation pattern of polysaccharides isolated from lotus seedpod. *Carbohydrate Polymers, 316*, Article 121065.

Ze, X., Duncan, S. H., Louis, P., & Flint, H. J. (2012). Ruminococcus bromii is a keystone species for the degradation of resistant starch in the human colon. *The ISME journal, 6*(8), 1535-1543.

Zeng, X., Li, P., Chen, X., Kang, Y., Xie, Y., Li, X., Xie, T., & Zhang, Y. (2019). Effects of deproteinization methods on primary structure and antioxidant activity of Ganoderma lucidum polysaccharides. *International Journal of Biological Macromolecules, 126*, 867-876.

Zhang, J.-Q., Li, C., Huang, Q., You, L.-J., Chen, C., Fu, X., & Liu, R. H. (2019). Comparative study on the physicochemical properties and bioactivities of polysaccharide fractions extracted from Fructus Mori at different temperatures. *Food & Function, 10*(1), 410-421.

Zhang, L., Hu, Y., Duan, X., Tang, T., Shen, Y., Hu, B., Liu, A., Chen, H., Li, C., & Liu, Y. (2018). Characterization and antioxidant activities of polysaccharides from thirteen boletus mushrooms. *International Journal of Biological Macromolecules, 113*, 1-7.

Zhang, L., & Wang, M. (2016). Polyethylene glycol-based ultrasound-assisted extraction and ultrafiltration separation of polysaccharides from Tremella fuciformis (snow fungus). *Food and Bioproducts Processing, 100*, 464-468.

Zhang, M., Cui, Y., Liu, P., Mo, R., Wang, H., Li, Y., & Wu, Y. (2024). Oat β-(1 → 3, 1 → 4)-d-glucan alleviates food allergy-induced colonic injury in mice by increasing Lachnospiraceae abundance and butyrate production. *Carbohydrate Polymers, 344*, 122535.

Zhang, M., Zhuang, H., Zhang, X., Wang, X., Fu, X., Chen, S., Yao, L., Wang, H., Sun, M., Yu, C., Yue, H., & Feng, T. (2025). Structural characteristics of areca nut seed neutral polysaccharide and its impact on gut microbiota from human feces. *Food Hydrocolloids, 158*, 110492.

Zhang, Q., Xu, Y., Xie, L., Shu, X., Zhang, S., Wang, Y., Wang, H., Dong, Q., & Peng, W. (2024). Chapter Two - The function and application of edible fungal polysaccharides. In G. M. Gadd & S. Sariaslani (Eds.), *Advances in Applied Microbiology* (Vol. 127, pp. 45-142): Academic Press.

Zhang, T., Yang, Y., Liang, Y., Jiao, X., & Zhao, C. (2018). Beneficial Effect of Intestinal Fermentation of Natural Polysaccharides. *Nutrients, 10*(8).

Zhang, X., Liu, Z., Zhong, C., Pu, Y., Yang, Z., & Bao, Y. (2021). Structure characteristics and immunomodulatory activities of a polysaccharide RGRP-1b from radix ginseng Rubra. *International Journal of Biological Macromolecules, 189*, 980-992.

Zhang, Y., Li, S., Wang, X., Zhang, L., & Cheung, P. C. (2011). Advances in lentinan: Isolation, structure, chain conformation and bioactivities. *Food Hydrocolloids, 25*(2), 196-206.

Zhang, Y., Zeng, Y., Cui, Y., Liu, H., Dong, C., & Sun, Y. (2020). Structural characterization, antioxidant and immunomodulatory activities of a neutral polysaccharide from Cordyceps militaris cultivated on hull-less barley. *Carbohydrate Polymers, 235*, 115969.

Zhang, Y., Zhang, M., Guo, X., Bai, X., Zhang, J., Huo, R., & Zhang, Y. (2023). Improving the adsorption characteristics and antioxidant activity of oat bran by superfine grinding. *Food Science & Nutrition, 11*(1), 216-227.

Zhao, C., He, Y., Li, R., & Cui, G. (1996). Chemistry and Pharmacological Activity of Peptidoglycan from Lycium Barbarum L. *Chin Chem Lett*(7), 1009-1010.

Zhao, Y., Wang, Y., Ma, Q., Wang, D., Jiang, Q., Wang, P., Ge, Z., Wang, J., Qin, P., & Zhao, X. (2024). Different microbiota modulation and metabolites generation of five dietary glycans during in vitro gut fermentation are determined by their monosaccharide profiles. *Food Research International, 196*, 115011.

Zheng, L., Ma, Y., Zhang, Y., Meng, Q., Yang, J., Wang, B., Liu, Q., Cai, L., Gong, W., Yang, Y., & Shi, J. (2021). Increased antioxidant activity and improved structural characterization of sulfuric acid-treated stepwise degraded polysaccharides from Pholiota nameko PN-01. *International Journal of Biological Macromolecules, 166*, 1220-1229.

Zheng, Y., Fan, J., Chen, H.-w., & Liu, E.-q. (2019). Trametes orientalis polysaccharide alleviates PM 2.5-induced lung injury in mice through its antioxidant and anti-inflammatory activities. *Food & Function, 10*(12), 8005-8015.

Zhu, Z.-Y., Liu, X.-C., Fang, X.-N., Sun, H.-Q., Yang, X.-Y., & Zhang, Y.-M. (2016). Structural characterization and anti-tumor activity of polysaccharide produced by Hirsutella sinensis. *International Journal of Biological Macromolecules, 82*, 959-966.